



## DEVELOPMENT OF HYDROPHOBIC THERMOPLASTIC STARCH COMPOSITES

Mahyar Fazeli

Tese de Doutorado apresentada ao Programa de Pós-graduação em Engenharia Metalúrgica e de Materiais, COPPE, da Universidade Federal do Rio de Janeiro, como parte dos requisitos necessários à obtenção do título de Doutor em Engenharia Metalúrgica e de Materiais.

Orientadora: Renata Antoun Simão

Rio de Janeiro  
Novembro de 2018

DEVELOPMENT OF HYDROPHOBIC THERMOPLASTIC STARCH  
COMPOSITES

Mahyar Fazeli

TESE SUBMETIDA AO CORPO DOCENTE DO INSTITUTO ALBERTO LUIZ  
COIMBRA DE PÓS-GRADUAÇÃO E PESQUISA DE ENGENHARIA (COPPE) DA  
UNIVERSIDADE FEDERAL DO RIO DE JANEIRO COMO PARTE DOS  
REQUISITOS NECESSÁRIOS PARA A OBTENÇÃO DO GRAU DE DOUTOR EM  
CIÊNCIAS EM ENGENHARIA METALÚRGICA E DE MATERIAIS.

Examinada por:

---

Prof<sup>ª</sup>. Renata Antoun Simão , D.Sc.

---

Prof. Jose Roberto Moraes d'Almeida, D.Sc.

---

Prof<sup>ª</sup>. Veronica Maria de Araujo Calado, D.Sc.

---

Prof<sup>ª</sup>. Rossana Mara da Silva Moreira Thiré, D.Sc.

---

Prof. Marcos Lopes Dias, D.Sc.

RIO DE JANEIRO, RJ - BRASIL

NOVEMBRO DE 2018

Fazeli, Mahyar

Development of hydrophobic thermoplastic starch composites

/ Mahyar Fazeli. – Rio de Janeiro: UFRJ/COPPE, 2018.

XIII, 106 p.: il.; 29,7 cm.

Orientadora: Renata Antoun Simão

Tese (doutorado) – UFRJ/ COPPE/ Programa de Engenharia Metalúrgica e de Materiais, 2018.

Referências Bibliográficas: p. 88-104.

1. Cellulose fibers. 2. Biocomposite. 3. Starch. I. Simão, Renata Antoun. II. Universidade Federal do Rio de Janeiro, COPPE, Programa de Engenharia Metalúrgica e de Materiais. III Título

## Acknowledgement

Firstly, I would like to express my sincere gratitude to my advisor Prof. Renata Antoun Simão for the continuous support of my D.Sc. study and related research, for her patience, motivation, and immense knowledge. Her guidance helped me in all the time of research and writing of this thesis. I could not have imagined having a better advisor and mentor for my D.Sc study.

I thank my fellow labmates in for the stimulating discussions, for the sleepless nights we were working together before deadlines, and for all the fun we have had in the last four years. I would also like to thank CAPES for financing my project during these four years.

Last but not the least, I would like to thank my family: my father Hossein Fazeli, my mother Maryam Sajedi Khanian and to my sister Faegheh Fazeli, not only for all their support in these last years, but for a whole life of teaching, learning, exchanged experiences and encouragement. You have allowed me to follow my passions, find my own way in life and ultimately reach the title of doctor in science. Thank you.

Resumo da Tese apresentada à COPPE/UFRJ como parte dos requisitos necessários para a obtenção do grau de Doutor em Ciências (D.Sc.)

## DESENVOLVIMENTO DE COMPÓSITOS DE AMIDO TERMOPLÁSTICOS HIDROFÓBICOS

Mahyar Fazeli

Novembro/2018

Orientadora: Renata Antoun Simão

Programa: Engenharia Metalúrgica e de Materiais

Este trabalho trata do fornecimento e caracterização de compósitos à base de biopolímero obtidos pela incorporação de fibras de celulose como reforço dentro da matriz plastificada de glicerol formada por biopolímero de amido de milho termoplástico. A função dos polímeros à base de amido é limitada devido a propriedades mecânicas ruins. No entanto, melhora-se com a formação de um biocompósito de amido termoplástico (TPS) como matriz e as fibras de celulose (CF) como reforço. A superfície das fibras de celulose é modificada com sucesso usando o tratamento com plasma de ar com o objetivo de melhorar a adesão matriz / fibra. As fibras modificadas são estudadas por meio de difração de raios X (DRX), microscopia eletrônica de varredura (MEV) e espectroscopia de infravermelho por transformada de Fourier (FTIR). Os compósitos TPS/CF são preparados usando procedimentos de alta fricção e compressão a quente. Resultados de testes de tração e imagens de MEV das superfícies de fratura mostram uma melhora significativa na adesão entre as fibras de celulose tratadas e a matriz de TPS. Por outro lado, as nanopartículas de amido (SNP) foram preparadas pela entrega de etanol como precipitante na solução de pasta de amido, gota a gota. De acordo com a caracterização de nanopartículas de amido com FTIR, DRX e MEV, o SNP amorfo não pode ser gelatinizado em água quente por causa do cross-linking. Os filmes TPS/SNP também foram preparados usando o processo de fundição. MEV e microscopia de força atômica (AFM) revelaram que o SNP foi disperso uniformemente na matriz de amido. Como mostrado na análise térmica mecânica dinâmica (DMA) e TGA, a introdução do SNP poderia melhorar o módulo de armazenamento e a temperatura de transição vítrea dos filmes preparados.

Abstract of Thesis presented to COPPE/UFRJ as a partial fulfillment of the requirements for the degree of Doctor of Science (D.Sc.)

## DEVELOPMENT OF HYDROPHOBIC THERMOPLASTIC STARCH COMPOSITES

Mahyar Fazeli

November / 2018

Advisor: Renata Antoun Simão

Department: Metallurgical and Materials Engineering

This work deals with provision and characterization of the biopolymer-based composites achieved by incorporation of cellulose fibers as the reinforcement within the glycerol plasticized matrix formed by thermoplastic cornstarch biopolymer. The function of starch-based polymers is limited due to poor mechanical properties. However, it is improved with forming a biocomposite of thermoplastic starch (TPS) as matrix and the cellulose fibers (CF) as reinforcement. The surface of cellulose fibers is successfully modified using the air plasma treatment with the aim of improving the matrix/fiber adhesion. The modified fibers are studied using X-ray diffraction (XRD), scanning electron microscopy (SEM) and Fourier transform infrared spectroscopy (FTIR). The TPS/CF composites are prepared using high friction and hot compression procedure. Tensile test results and SEM images of the fracture surfaces show significant improvement of adhesion between treated cellulose fibers and TPS matrix. In another hand, starch nanoparticles (SNP) were prepared by delivering ethanol as the precipitant into starch-paste solution dropwise. According to the characterization of starch nanoparticles with FTIR, XRD and SEM, amorphous SNP could not be gelatinized in hot water because of the cross-linking. The TPS/SNP films were also prepared using casting process. SEM and atomic force microscopy (AFM) revealed that SNP was dispersed evenly in the starch matrix. As shown in the dynamic mechanical thermal analysis (DMA) and TGA, the introduction of SNP could improve the storage modulus and the glass transition temperature of the prepared films.

## TABLE OF CONTENT

<b>1 INTRODUCTION</b> .....	1
<b>2 OBJECTIVES</b> .....	5
2.1 General objective .....	5
2.2 Specific objectives .....	5
<b>3 LITERATURE REVIEW</b> .....	6
3.1 Composite .....	6
3.2 Bio-Composite .....	7
3.3 Starch .....	10
3.4 Thermoplastic starch (TPS): obtaining and main characteristics .....	13
3.5 Natural Fiber .....	17
3.5.1 Disadvantages of natural fiber in composite .....	18
3.6 Cellulose .....	18
3.6.1 Cellulose properties .....	19
3.6.2 Crystalline Structure of Cellulose .....	20
3.6.3 Amorphous Regions .....	22
3.7 Cellulose Nanofillers .....	24
3.8 Microfibrillated Cellulose (MFC) .....	25
3.9 Cellulose Nanocrystals .....	26
3.10 Preparation of nanocellulose .....	26
3.11 Chemically induced restructuring strategy .....	28
3.12 Mechanical properties of cellulose nanoparticles .....	30
3.13 Starch nanoparticles .....	31
3.13.1 Preparation and Characterization of starch nanoparticles .....	31
3.13.1.1 Chemical Method .....	31
3.13.1.1.1 Acid hydrolysis .....	31
3.13.1.1.2 Precipitation in a water-in-oil microemulsion .....	33
3.13.1.1.3 Complex formation with n-butanol .....	33
3.13.1.1.4 Solvent displacement method .....	34
3.13.1.1.5 Alkali Freezing Treatment .....	34
3.13.1.2 Physical Method .....	35
3.13.1.2.1 Milling .....	35
3.13.1.2.2 Reactive Extrusion .....	35
3.13.1.2.3 Ultrasonication .....	35
3.13.1.2.4 Gamma Radiation .....	36
3.13.1.2.5 Nanoprecipitation .....	36
3.13.1.3 Enzymatic Method .....	37

3.13.3 Applications of Starch Nanoparticles .....	38
3.13.3.1 Food uses .....	38
3.13.3.2 Non-Food uses .....	38
3.14 Plasma Treatment .....	40
3.14.1 Plasma surface modification.....	41
3.15. Plasma surface modification.....	43
3.15.1. Cold plasma .....	43
<b>4 MATERIALS AND METHODS</b> .....	49
4.1 Starch.....	49
4.2 Cellulose fibers .....	49
4.3 Thermoplastic starch based composite reinforced by cellulose fibers .....	50
4.3.1 Plasma reactor construction.....	50
4.3.2 Plasma treatment conditions.....	53
4.3.3 Mixer for composite production .....	54
4.3.4 Hydraulic press for compression molding.....	55
4.3.5 Tensile properties .....	56
4.4 Thermoplastic Starch reinforced by starch nanoparticles.....	57
4.4.1 Gelatinization and Casting .....	57
4.4.2 Dynamic mechanical analysis (DMA) .....	59
4.5 Characterization Techniques .....	60
4.5.1 Scanning electron microscope (SEM) .....	60
4.5.2 Fourier transform infrared spectroscopy (FTIR) .....	60
4.5.3 X-ray diffraction (XRD).....	60
4.5.4 Thermogravimetric analysis (TGA) .....	61
4.5.5 Atomic force microscopy (AFM).....	61
4.5.6 Contact angle .....	61
<b>5 RESULTS AND DISCUSSION</b> .....	63
5.1 Thermoplastic starch based composite reinforced by cellulose fibers .....	63
5.1.1 Morphology of cellulose fibers .....	63
5.1.2 Fourier transform infrared spectroscopy (FT-IR).....	64
5.1.3 Thermogravimetric analysis (TGA) .....	65
5.1.4 X-ray diffraction (XRD).....	67
5.1.5 Mechanical properties of the composites .....	70
5.1.6 SEM analysis of composites.....	72
5.2 Thermoplastic Starch reinforced by starch nanoparticles.....	73
5.2.1 Dynamic mechanical analysis (DMA) of SNP films.....	73
5.2.2 Fourier transform infrared spectroscopy (FT-IR) of SNP films.....	76

5.2.3 Crystalline properties of SNP films.....	77
5.2.4 Thermogravimetric analysis (TGA) of SNP films .....	78
5.2.5 Scanning electron microscopy (SEM) of SNP films .....	80
5.2.6 Topography of SNP films.....	81
5.2.7 Water contact angle of SNP films .....	82
<b>6 CONCLUSION .....</b>	<b>85</b>
<b>7 SUGGESTIONS FOR FUTURE WORKS .....</b>	<b>87</b>
<b>8 REFERENCES .....</b>	<b>88</b>
<b>ANNEX 1.....</b>	<b>105</b>

## LIST OF FIGURES

Figure 1. Structure of Amylose and Amylopectin [14].	11
Figure 2. Molecular structure of cellulose [25].	19
Figure 3. (a) Atomic arrangement and hydrogen bonding network in cellulose $I\alpha$ .	21
Figure 4. Schematic of amorphous cellulose and crystalline cellulose [43].	23
Figure 5. Schematic of hierarchical structure of a wood from macroscale to nanoscale [46].	24
Figure 6. Illustration of acid hydrolysis of semicrystalline cellulose fibers [50].	26
Figure 7. Picture of a 2 wt% microfibrillated cellulose aqueous suspension from eucalyptus, enzymatically pretreated [63].	27
Figure 8. Transmission electron micrograph showing MFC obtained after high-pressure mechanical treatment of <i>Opuntia ficus-indica</i> fibers [64].	28
Figure 9. Photograph of an aqueous dispersion of capim dourado cellulose nanocrystals (0.50 wt%) observed between cross-nicols showing the formation of birefringent domains [65].	29
Figure 10. Transmission electron micrographs from a dilute suspension of (a) tunicin, and (b) ramie nanocrystals [69, 70].	30
Figure 11. Inductively coupled plasma.	43
Figure 12. Schematic of Glow discharge plasma system.	45
Figure 13. Photo of inductively coupled plasmas (ICP), SFF – Superfícies e Filmes Finos Laboratory.	46
Figure 14. Schematic of plasma reactor.	50
Figure 15. Plasma reactor, SFF – Superfícies e Filmes Finos Laboratory.	51
Figure 16. Schematics of the fibers movement in the plasma region throughout the reactor rotation (a), the geometry of sample holder (b), and schematic illustration of the plasma penetration in the accumulated fibers (c).	52
Figure 17. Photo of mixer for composite production.	55
Figure 18. Compression molding equipment.	56
Figure 19. Reactor of preparing the gelatinized starch and SNP.	57
Figure 20. Prepared samples of TPS, TPS/UCF, and TPS/PCF for tensile test.	59

Figure 21. SEM of pure cellulose fibers (a, b, c, and d), plasma-treated cellulose fibers (e,f).....	63
Figure 22. FTIR spectrum of plasma treated and untreated cellulose fibers.....	65
Figure 23. TGA curves for TPS, composites containing untreated fibers (TPS/UCF) 6 wt% and composites containing plasma treated fibers (TPS/PCF) 6 wt%.....	66
Figure 24. DTG for TPS, composites containing untreated fibers (TPS/UCF) 6 wt% and composites containing plasma treated fibers (TPS/PCF) 6 wt%.....	66
Figure 25. XRD pattern of (a) TPS, (b) TPS/UCF 2wt%, (c) TPS/UCF 4wt%, (d) TPS/UCF 6wt%, (e) TPS/UCF 8wt%, (f) TPS/UCF 10wt% and (g) TPS/UCF 12wt%.....	69
Figure 26. XRD pattern of (a) TPS, (b) TPS/PCF 2wt%, (c) TPS/PCF 4wt%, (d) TPS/PCF 6wt%, (e) TPS/PCF 8wt%, (f) TPS/PCF 10wt% and (g) TPS/PCF 12wt%.....	69
Figure 27. Tensile strength of TPS, TPS/UCF and TPS/PCF biocomposite films.....	71
Figure 28. Elongation at Break of TPS, TPS/UCF and TPS/PCF biocomposite film.....	71
Figure 29. Young's modulus of TPS, TPS/UCF and TPS/PCF biocomposite films.....	72
Figure 30. Microstructure of fracture surfaces of TPS/UCF 6 wt% (a, c), TPS/PCF 6 wt% (b), and TPS/PCF 12 wt% (d).....	73
Figure 31. Loss factor ( $\tan \delta$ ) – temperature curves of SNP films.....	75
Figure 32. Loss modulus of SNP films.....	75
Figure 33. Loss modulus of SNP films .....	76
Figure 34. FT-IR curves of SNP films.....	77
Figure 35. X-ray diffraction of SNP films.....	78
Figure 36. Thermogravimetric analysis (TGA) curves of SNP films.....	79
Figure 37. Derivative thermogravimetric (DTG) of SNP films.....	79
Figure 38. Scanning electron microscopy (SEM) of (a) SNP1, (b) SNP2, (c) SNP3, and (d) SNP4.....	81
Figure 39. Atomic force microscopy (AFM) of (a) SNP1, (b) SNP2, (c) SNP3, and (d) SNP4.....	82

Figure 40. Contact angle images of (a) SNP1, (b) SNP2, (c) SNP3, and (d) SNP4.....	83
Figure 41. Contact angle measurements of (a) SNP1, (b) SNP2, (c) SNP3, and (d) SNP4.....	84
Figure 42. SEM images of the extracted cellulose nanofibers by plasma and ultrasonic treatments.....	87

## LIST OF TABLES

Table 1. $I\alpha$ fractions in specimens of various origins [34]. .....	20
Table 2. Degree of crystallinity (WC) and lateral dimension (D) of elementary fibrils from several cellulose samples [38-41]. .....	21
Table 3. Range of diameters of microfibril of various cellulose sources [45]. .....	22
Table 4. Preparation conditions of SNP. ....	47
Table 5. Relative crystallinity of thermoplastic starch and its biocomposites with untreated cellulose fibers and plasma treated cellulose fibers. ....	57

## 1 INTRODUCTION

The vast majority of engineered plastic materials which are using today are made from synthetic polymers. Petrochemically based polymers have been progressively used as packaging materials, in part, their availability, low cost, and favorable mechanical properties. The use of conventional petroleum-based polymer products creates potential problems owing to their non-renewable nature and ultimate disposal. More than 40 % of all plastic materials are used in packaging, and their disposal contributes to growing landfills and enhanced greenhouse effects when burned. Environmental concerns arising from the use of nondegradable plastics have resulted in the search for suitable substitutes. In the recent years, the concern is growing in finding new ways to utilize biopolymers such as polysaccharides, proteins, and lipids to create biodegradable composites due to their ready availability, sustainability and contribution to the reduction of environmental pollution and simplified end-of-life disposal issues (KAW, 2005, VISAKH *et al.*, 2013).

Cellulose fiber reinforced polymer composites have received much attention because of their lightweight, nonabrasive, combustible, nontoxic, low cost and biodegradable properties. A lot of research work has been performed all over the world on the use of cellulose fibers as a reinforcing material for the preparation of various types of composites. However, lack of good interfacial adhesion, low melting point, and poor resistance towards moisture make the use of cellulose fiber reinforced composites less attractive. Pre-treatments of the cellulose fibers can clean the fiber surface, chemically modify the surface, stop the moisture absorption process, and increase the surface roughness. The extraction of cellulose fibers and their application in composite materials has gained increasing attention due to their high strength and stiffness combined with low weight, biodegradability, and renewability. Application of cellulose fibers in polymer reinforcement is a relatively new research field. The main reason to utilize cellulose fibers in composite materials is that one can potentially exploit the high stiffness of the cellulose crystal for reinforcement. This can be done by breaking down the hierarchical structure of the plant into individualized fibers of high crystallinity, therefore reducing the amount of amorphous material present by using various methods like as acidic or basic hydrolysis, plasma treatment, mechanical treatment and etc. (DEMIRBAS, 2010).

Miniaturization is a continuing trend in the development of technology. Unfortunately, not many of the most recent developments of this nature are able to satisfy the core concept of sustainability. One way to address issues related to sustainability is to incorporate renewable materials as miniaturized elements of construction materials (WANG & SAIN, 2007). The backbone of a plant or tree is a polymeric carbohydrate with an abundance of tiny structural entities known as “cellulose fibrils”. These fibrils are comprised of different hierarchical microstructures commonly known as nano-sized microfibrils with high structural strength and stiffness (STAMBOULIS *et al.*, 2001). Biopolymers from renewable resources have attracted much attention lately. Renewable sources of polymeric materials offer an answer to maintain sustainable development of economically and ecologically attractive technology. In recent years, scientists and engineers have been working together to use the inherent strength and performance of these nano-fibrils, combined with natural green polymers, to produce a new class material.

The cellulose molecules are always biosynthesized in the form of micro-sized fibrils; up to 100 glucan chains aggregate together to form cellulose microfibrils or nanofibers (HEPWORTH *et al.*, 2000). The mechanical performance of cellulose fibers in terms of the tensile strength and Young’s modulus is comparable to other engineering materials such as glass fiber, carbon fiber, etc. Therefore, the cellulose fibers can be considered to be an important structural element of natural cellulose in a number of applications such as plastic reinforcement, gel-forming and thickening agents (HEPWORTH *et al.*, 2000). Furthermore, a cellulose fiber has more surface area of isolated softwood cellulose and possesses higher water holding capacity, higher crystallinity, higher tensile strength, and a finer web-like network. In combination with a suitable matrix polymer, cellulose fiber networks show considerable potential as an effective reinforcement for high-quality specialty application of bio-based composites. Conventional polymers derived synthetically from petroleum constitute a growing concern in view of problems associated with their disposal. Fully biodegradable synthetic polymers have been commercially available since 1990, such as starch, PVA, PLA, and PHB. In view of better environmental characteristics at the end of service life, biodegradable plastics obtained from plant sources are becoming increasingly attractive. Typical examples of such biopolymers include plastics derived from natural sources like cellulose, soybean, and starch. The fairly new idea of biocomposites, in which the reinforcing material has various

dimensions, is emerging to create the value-added materials with superior performance and extensive applications. The cellulose fiber-reinforced composites can be used in medical devices such as biocompatible drug delivery system, blood bags, cardiac devices, and valves as reinforcing biomaterials. Biological tissues are made from nano-sized materials and given an interest in manufacturing synthetic nanocomposites (ANGLES *et al.*, 2000a). Due to their lightweight and high strength; they also can be utilized as high strength components in the aerospace and automotive sector. The use of cellulose fibers as reinforcement is a new field in technology, and as a result, there are still some disadvantages. Firstly, the separation of reinforcement components from natural materials and the associated processing techniques have been limited to the laboratory scale. Secondly, the fiber isolation process consumes a large amount of energy, water, and chemicals. The production is time-consuming and is still associated with low yields. Thirdly, due to their strong hydrogen bonding between cellulose chains, the fibers obtained after chemo-mechanical treatments are kept in water suspensions. Water is the most widely used carrier to disperse cellulose fibers (NABI SAHEB & JOG, 1999). Therefore the use of fibers has been mostly restricted to water-soluble polymers. Cellulose fibers have not been used extensively in the common thermoplastics, as the poor dispersion of the filler in the matrix of a composite material seriously affects its mechanical properties. But to expand the horizon of bio-based composites for high-end applications, it is necessary to reduce the entanglement of the fibrils and improve their dispersion in the solid phase polymer matrix by surface modification of fibers without deteriorating their reinforcing capability. It has been reported that the surface modifications of cellulose fibers to make them compatible with non-polar solvents/non-polar polymers, such as polyolefin or other commodity polymer has been attempted. The treatment of the fibers may be bleaching, grafting of monomers, acetylation, and so on. Various processing acids/coupling agents such as stearic acid, mineral oil, and maleate ethylene have been used (LAM *et al.*, 2011). The compatibilizer can be polymers with functional groups grafted onto the chain of the polymer for effective stress transfer across the interface. In this way, high-performance composite materials can be processed with a good level of dispersion. Interaction of cellulose with surfactants has been another way to stabilize cellulose suspensions into non-polar systems. In some approaches, corona or plasma discharges have been used in achieving acceptable dispersion levels.

This study consists of two different steps. The first one is the main purpose of this thesis and it is about the preparation and characterization of thermoplastic starch composite reinforced by cellulose fibers which their surface are modified by atmospheric plasma treatment. The second step of the project is to synthesis the starch nanoparticles by the solution casting method based on a novel leading to the surface modification of cellulose fibers by atmospheric plasma treatment.

These steps will be presented separately. In the first step, low-pressure, low-temperature plasma treatments of cellulose fibers are studied. Surface analysis of the fibers and compounding of these with polymeric matrices are also performed, followed by mechanical and other analysis of the composites. The different aspects of surface modification and interaction are explored and discussed in an attempt to shed light on the mechanisms behind fiber-matrix compatibility. The work presented here is an evidence for the versatility and potential of plasma surface treatments to enhance the adhesion of cellulose fibers with the thermoplastic starch polymer. This is a potentially effective and viable technique that, if further developed, can help to improve the overall properties of composites reinforced with natural fibers, making them more attractive and expanding their use of traditional composites and polymers.

In the second step, starch films reinforced by starch nanoparticles will be produced by casting in one step procedure by nanoprecipitation.

As different procedures will be adopted in some of the production and characterization steps, every time a different methodology is applied, information of the procedure will be clearly addressed.

## **2 OBJECTIVES**

### 2.1 General objective

Producing and characterizing the biodegradable thermoplastic starch composites using different reinforcement.

### 2.2 Specific objectives

- Modify the cellulose fibers using plasma treatment employing atmospheric air as working gas, under controlled conditions of pressure, time and power.
- Elaborate starch/cellulose composites by means of the compression molding technique with different content of untreated and plasma-treated cellulose fibers and to investigate the modification of the physical, chemical and thermal properties of the composites.
- Study the effect of plasma treatment on the physical, chemical, thermal, and mechanical properties of composites reinforced by treated and untreated cellulose fibers.
- Evaluate the properties of starch composites produced using starch nanoparticles as reinforcement.

### 3 LITERATURE REVIEW

#### 3.1 Composite

The term of the composite is considered to a structural material which is consists of two or more combined constituents that are combined and are not soluble in each other. One of the constituents is called reinforcing phase and another one in which it is embedded is called the matrix. The reinforcing phase materials are distributed and may be in the form of fibers, particles or flake. The matrix phase materials are generally continuous. Examples of natural composites include wood, where the lignin matrix is reinforced with cellulose fibers as reinforcing phase and bones in which the bone-salt plates made of calcium and phosphate ions reinforce soft collagen. The roles of the matrix in composite materials are to give shape to the composite part, protect the reinforcements to the environment, transfer loads to reinforcements and toughness of the material, together with reinforcements. The aims of reinforcements in composites are to get strength, stiffness and other mechanical properties, dominate other properties as the coefficient of thermal extension, conductivity and thermal transport (KAW, 2005). As a comparison between composites and metals, the composites materials have some advantages as:

- Light weight
- High specific stiffness and strength
- Easy moldable to complex forms
- Easy bondable
- Good dumping
- Low electrical conductivity and thermal expansion
- Good fatigue resistance
- Part consolidation due to lower overall system costs
- Low radar visibility
- Internal energy storage and release

Such as disadvantages of composites are the followings:

- Cost of materials
- Long development time
- Difficulty manufacturing
- Fasteners

- Low ductility
- Temperature limits
- Solvent or moisture attack
- Hidden damages and damage susceptibility

All of these have made those composites to substitute more and more the metals, in specials in aircrafts, automotive, marines, constructions, etc. (VISAKH *et al.*, 2013).

### 3.2 Bio-Composite

The widespread use of petroleum products has created a twin dilemma; discharge of petroleum resources and entrapment of plastics in the food chain and environment. The increasing pollution caused by the use of plastics and emissions during incineration is affecting the food we eat, the water we drink, the air we breathe and threatening the greatest right of human beings, the right to live (DEMIRBAS, 2010). The whole use of petroleum-based resources has started the scramble to develop biodegradable plastics. This is based on the renewable bio-based plant that can compete in the markets currently dominated by petroleum-based products (DEMIRBAS, 2010). The production of 100% bio-based materials as the substitute for petroleum-based products is not an economical solution because of high final cost. A more feasible solution would be to combine petroleum and bio-based resources to develop a cost-effective product having enormous applications (DEMIRBAS, 2010). Biopolymers reinforced with natural or bio-fibers (termed as bio-composites) are a viable alternative to glass fiber composites (JOHN *et al.*, 2008). For these reasons, Scientists are looking at the various possibilities of combining bio-fibers such as sisal, flax, hemp, banana, wood and various grasses with polymer matrices from non-renewable and renewable resources to form composite materials to make the bio-composite revolution a reality. The term “Biocomposites” refers to those composites that can be used in bioengineering. The constituents of the composite retain their identities in the composite (LIMBERT & TAYLOR, 2002). Namely, they do not dissolve or otherwise merge completely into each other. In composites, properties such as the elastic modulus can be significantly different from those of the constituents alone but are considerably modified by the constituent structures and contents. From a structural point of view, composites are anisotropic in nature. Bio-composites are composite materials, that is, materials formed by a matrix and a

reinforcement of natural fibers (usually derived from plants or cellulose) (MOHANTY *et al.*, 2002). Bio-composites are the combination of natural fibers (bio-fibers) such as wood fibers (hardwood and softwood) or non - wood fibers (e.g., wheat, kenaf, hemp, and flax) with polymer matrices from both of the renewable and nonrenewable resources. Actually, bio-fibers are one of the major components of Bio-composites. The fine fibers or particles derived from the tree, plant, or shrub sources are defined as bio-fiber. Bio-composites often imitate the structures of the living materials involved in the process, in addition to the strengthening properties of the matrix that was used, but still providing bio-compatibility, e.g. in bio-composites made of cellulose or in creating scaffolds in bone tissue engineering. The degree of biodegradability in bio-based polymers depends on their structure and their service environment. Natural/Bio-fiber composites are emerging as a viable alternative to glass fiber composites, particularly in automotive, packaging, building, and consumer product industries, and becoming one of the fastest growing additives for thermoplastics. Further, research into biological inorganic interfaces focuses on the design, synthesis, and characterization of novel amalgams that incorporate biological and inorganic materials (KOHJIYA & IKEDA, 2014). The integration of soft biological and organic molecular assemblies with hard inorganic nano-architectures is the special interest because of the opportunity to combine normally disparate chemical and physical properties within a single system. Broadly defined, bio-composites are composite materials made from natural/bio-fiber and petroleum-derived non-biodegradable, for example, polymers (PP, PE) or biodegradable, for example, polymers (PLA, PHA). The subsequent category i.e. bio-composites derived from plant-derived fiber (natural/bio-fiber) and crop/bio-derived plastic (biopolymer/bioplastic) are likely to be more eco-friendly and such composites are termed as green composites. The best known renewable resources capable of making biodegradable plastics are starch and cellulose which are used in this research. Starch is one of the least expensive biodegradable materials available on the world market today (MOHANTY *et al.*, 2005). It is a versatile polymer with immense potential for use in non-food industries. Cellulose from trees and cotton plants is a substitute for petroleum feedstocks to make cellulose plastics (JOHN & THOMAS, 2012). Another aspect that has gained global attention is the development of biodegradable plastics from vegetable oils like soybean oil, peanut oil, walnut oil and sunflower oil. Green composites from soy protein-based bio-plastics and natural fibers show potential for rigid packing and housing and transportation applications. One of the major applications for bio-composites that recently have also

gained a lot of attention in North America is in building materials (THAKUR *et al.*, 2014). Nowadays, bio-composites are being used to fabricate products such as decking, fencing, siding, window, door, and so on. Use of bio-composites in building materials offers several advantages such as they are cheap, lightweight, environmentally friendly, bio-renewable, and more durable. In addition to these advantages, on another hand, they have some disadvantages as well, such as moisture absorption and photochemical degradation because of the UV radiations.

The poor fiber-matrix interaction is one of the main issues concerning the fabrication and use of natural fibers reinforced polymers. The most used thermoplastic matrices are hydrophobic while lignocellulosic fibers are hydrophilic, causing poor wettability, low interfacial shear stress and load transfer, and sometimes agglomeration of fibers during processing (FARUK *et al.*, 2012, GURUNATHAN *et al.*, 2015). Even when the matrix is also hydrophilic, there is evidence that the interaction between matrix and the fibers is not ideal and can still be greatly improved (ROSA *et al.*, 2009, SATYANARAYANA *et al.*, 2009, VILASECA *et al.*, 2007). Currently there are many different strategies being researched to improve fiber-matrix adhesion in composites reinforced with natural fibers. Parallels can be drawn between the present situation of natural fibers composites and the beginning of development of glass fibers composites, when the interaction between glass fibers and polymers was also poor until the full development of the silane-based coupling agents, used up to this day to coat glass fibers for use with both thermoset and thermoplastic matrices (MUÑOZ-VÉLEZ *et al.*, 2017). However, given the great variability of chemical, structural and superficial characteristics of natural fibers, with its many different plant origins, development of a single strategy to improve adhesion is much more complicated in this case. Two broad categories can be defined when discussing methods to improve fiber-matrix interface: Modification of the matrix chemical character and overall modification of the fibers surfaces, including both physical and chemical modification.

Modification of the natural fiber surface is one of the most investigated methods to improve the fiber-matrix adhesion and thus the composite properties. Because of the many different approaches researchers use to perform the surface modification, this field is usually classified in one of four broad categories, as discussed by GURUNATHAN *et al.* (GURUNATHAN *et al.*, 2015): chemical (including silane treatment, acetylation and mercerization, also known as alkaline treatment), physicochemical (solvent extraction), mechanical (rolling, swaging, etc.) and physical (plasma, corona, etc.).

Chemical modification is the most common surface treatment, thanks to its relative simplicity. In most cases the fibers are put into a bath of chemical solutions that remove or add components to the surface. Mercerization or alkaline treatment for removal of lignin is the most commonly used (RAY *et al.*, 2001). Replacement of hydroxyl groups from the lignocellulosic fibers by different functional groups is also used to reduce the surface polarity and hydrophilic character. This can be achieved by silanization, esterification, benzoylation, among others (MEZEY *et al.*, 2003). However, chemical modifications present two main problems: Extensive fiber modification beyond the surface, reducing the mechanical properties of the fiber as a whole; and generation of large volumes of wastes, which can't be easily discarded since they are often toxic, harmful to human health and to the environment (FELEKOGU *et al.*, 2009, FORNES *et al.*, 2013). This also increases the cost of these processes due to the necessary steps to neutralize or treat the waste generated.

Among the physical surface modifications technique, plasma discharges are the most explored (FORNES *et al.*, 2013). In this technique, fibers are exposed to a plasma environment (ionized gas), at low or atmospheric pressure, which causes surface reactions and modifications ranging from etching to incorporation of functional groups and changes in surface energy. Plasma treatments are considered the most “eco-friendly” and are able to modify surface chemical composition and physical structure without altering bulk properties (GURUNATHAN *et al.*, 2015, KUSANO *et al.*, 2011, MAHLBERG *et al.*, 1999). Furthermore, when low pressure is used, the process gas consumption is minimized and the treatment creates little to no process waste (FARUK *et al.*, 2012, LI *et al.*, 1997, SINHA & PANIGRAHI, 2009, ZHOU *et al.*, 2011).

### 3.3 Starch

During the last decades, synthetic polymer materials and composites made of them have been widely used in every field of human activity as well-known (VERT *et al.*, 2002). These artificial and synthetic macromolecular substances are usually emanating from petroleum and most of the conventional ones are considered as nondegradable (VERT *et al.*, 2002, WRÓBLEWSKA-KREPSZTUL *et al.*, 2018). However, the petroleum resources are limited and the blooming use of nonbiodegradable polymers has caused serious environmental problems. In addition, the nonbiodegradable polymers are not suitable for temporary use such as sutures. Therefore, the polymer materials and

composites which are degradable and biodegradable have been paid more attention since the 1970s. Both synthetic polymers and natural polymers that contain hydrolytically or enzymatically unstable bonds or groups are degradable. The advantages of synthetic polymers are clear, including predictable properties, batch-to-batch uniformity and can be tailored easily. Without being affected by the particular factor mentioned, they are quite expensive. This reminds us to focus on natural polymers, which are intrinsically biodegradable and can be promising candidates to meet different requirements. Among the natural polymers, starch is one of the most interesting polymers. It is refined from carbon dioxide and water by photosynthesis in plants. Owing to its complete biodegradability, low cost, and renewability, starch is considered as a promising candidate for developing sustainable materials. In this point of view, starch has been receiving growing attention since the 1970s. Many efforts have been applied to develop starch-based polymers for protecting the petrochemical resources, reducing environmental impact and searching more applications. Structure and properties of starch mainly consist of two homopolymers of D glucose: amylose, a mostly linear  $\alpha$ -D (1, 4'')-glucan and branched amylopectin, having the same backbone structure as amylose but with many  $\alpha$ -1, 6''-linked branch points (PARETA & EDIRISINGHE, 2006). (figure 1)

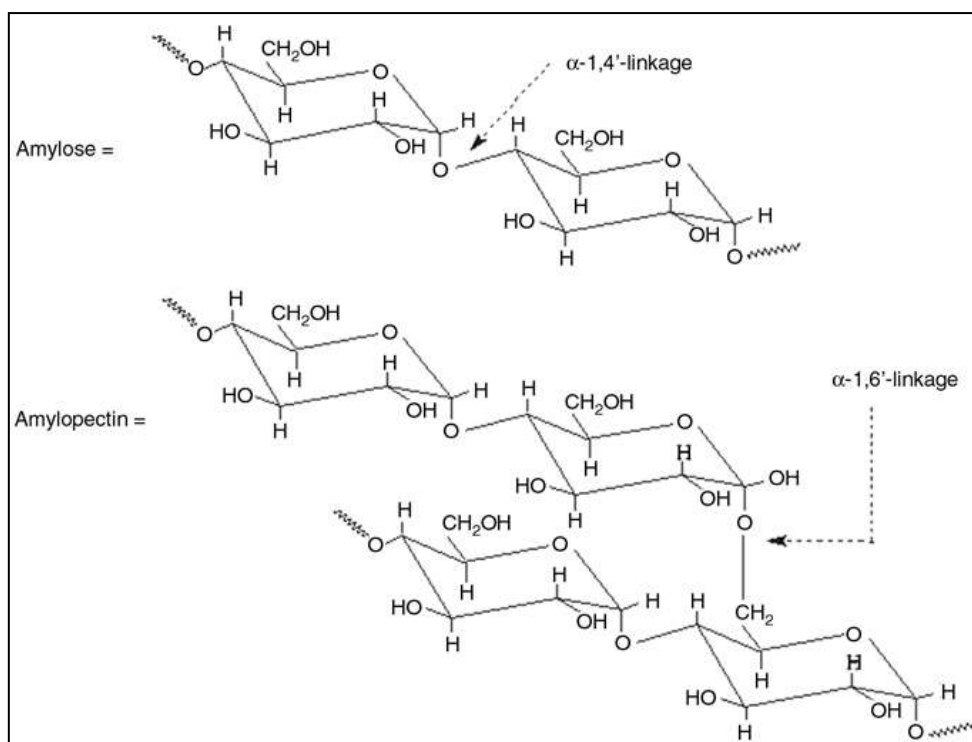


Figure 1. Structure of Amylose and Amylopectin (PARETA & EDIRISINGHE, 2006).

In the structure of starch, there are many hydroxyl groups, two secondary hydroxyl groups at C-2 and C-3 of each glucose residue, as well as one primary hydroxyl group at C-6 when it is not linked (MASINA *et al.*, 2017). As we know, starch is hydrophilic. The available hydroxyl groups on the starch chains potentially exhibit reactivity specific for alcohols. In other words, they can be oxidized and reduced and may participate in the formation of hydrogen bonds, ethers, and esters. Naturally, Starch has different proportions of amylose and amylopectin ranging from about 10–20% amylose and 80–90% amylopectin depending on the source (RAMESH *et al.*, 1999). Amylose forms a spiral structure and it is soluble in water. Starch forms naturally as separate granules since the short branched amylopectin chains are able to form helical structures which crystallize (WALLACE RA, SANDER GP, 1991). Starch granules represent hydrophilic properties and strong inter-molecular assembly via hydrogen bonding formed by the hydroxyl groups on the granule surface. Due to its hydrophilicity, the internal interaction and morphology of starch will be readily modified by water molecules, and thereby its glass transition temperature (T<sub>g</sub>), the dimension and mechanical properties depend on the water content. T<sub>g</sub> of native starch can be as low as 60 to 80°C when the weight fraction of water is in the range 0.12 to 0.14, which allows starch to be successfully injection molded to gain thermoplastic starch polymers in the presence of water. On the other hand, the hydrophilicity of starch can be used to ameliorate the degradation rate of some degradable hydrophobic polymers. Starch is completely biodegradable in a wide variety of environments (BASTIOLI *et al.*, 2012). It can be hydrolyzed into glucose by microorganism or enzymes and then metabolized into carbon dioxide and water. In another hand, carbon dioxide will recycle into starch again by plants and sunshine. Starch is poor in processability, also poor in the dimensional stability and mechanical properties for its end products. Therefore, native starch is not used directly.

In the last decade, food packaging and edible films are two major applications of the starch-based biodegradable polymers in the food industry. The requirements for food packaging include reducing the food losses, keeping food fresh, enhancing organoleptic characteristics of food such as appearance, odor, and flavor, and providing food safety. Common food packaging materials such as low-density polyethylene have the problem of environmental pollution and disposal problems. The starch-based biodegradable polymers can be a possible alternative for food packaging to vanquish these disadvantages and to keep the advantages of traditional packaging materials. However, the components in the conventional starch-based polymer packaging materials are not completely inert.

The migration of additional substances into the food possibly happens, and the component which migrates into the food may cause harm to the human health. For this reason, new starch-based packaging materials are being developed.

For instance, a starch/cellulose nanocomposite food packaging material is developed, which can offer better mechanical properties and lower migration of polymer and additives. Starch-based edible films are odorless, without any taste, non-toxic and biodegradable. They display very low penetrance to oxygen at low relative humidity and are suggested for food product protection to improve quality and shelf life without noxious consumer acceptability. In addition, starch can be transformed into a foamed material by using water steam to replace the polystyrene foam as a packaging material. It can be pressed into plates or disposable dishes, which are able to dissolve in water and leave a non-toxic solution, then can be consumed by the microbic environment. Evidently, the starch-based biodegradable polymers are attractive for the food industry and will make great progress in the future (BASTIOLI *et al.*, 2012).

#### 3.4 Thermoplastic starch (TPS): obtaining and main characteristics

The term “thermoplastic” indicates that these materials melt on heating and may be processed by a variety of molding and extrusion techniques. The most common thermoplastics are polyethylene, polystyrene and polymer chloride together with a number of more specialized engineering polymers. If one of the reacting substances in a step polymerization possesses more than two functional groups, then the reaction will lead naturally to branched structures. As these intercom bines, random three-dimensional networks are developed. Ultimately the network extends throughout the mass of polymerized material, which therefore in effect constitutes a single giant molecule. Such structures are by their very nature incapable of melting or of truly dissolving. Important examples are the phenolic and amino resins. Similar thermoset network structures may be formed by crosslinking linear chains in a second post-polymerization or 'curing' reaction, which may be free radical initiated.

The production of TPS (also known as plasticized starch, PS) basically involves three essential components, namely: starch, plasticizer and thermo-mechanical energy. The thermo-plasticization of starch entails the collapse of starch crystallinity (which in general is about 15-45% of the granule molecular order) through the formation of hydrogen bonds

between the plasticizer and starch in the presence of some energy, invariably severing the hydrogen bonds between the hydroxyl groups of the starch molecules to form TPS (LI *et al.*, 2014). Therefore, the crystallinity observed in TPS is due to the hydrogen bonds formed between starch and the plasticizer molecules and according to (YEH & YOUNG, 1998), this degree of crystallinity is expected to be rather low. It is important to mention that there must be sufficient amount of plasticizer (30% wt for glycerol-PS) for the formation of a homogeneous (continuous) phase to occur, otherwise some starch granules will remain intact in the TPS, a condition that can make the TPS fracture under tension at very low strains. Plasticizers impart flexibility by modifying the free volume of the matrix such that starch chains enjoy more mobility (DESMORAT, 2009). The use of starch alone is not encouraged because of its lack of melt-processability and humidity-resistance which in turn militates against its suitability for extrusion or injection molding (MATHEW *et al.*, 2006).

The most common plasticizers used are water and glycerol, which often times are used together. The TPS thus produced exhibits two major drawbacks, namely, poor mechanical properties and water resistance. To this end, four areas of consideration are being explored; these include plasticizers, starch forms (in relation to chemical modification and amylose/amylopectin ratio), reinforcements (organic and inorganic), polymer orientation and blends with other synthetic polymers. Accordingly, materials such as ethylene bisformamide, urea (WANG & SAIN, 2007), formamide (STAMBOULIS *et al.*, 2001), sorbitol (HEPWORTH *et al.*, 2000) and xylitol (ANGLES *et al.*, 2000a) have been investigated for their plasticizing abilities. Using cornstarch (NABI SAHEB & JOG, 1999), reported that extruded ethylene bisformamide-PS showed better water resistance than glycerol-PS but rather lower corresponding tensile strengths at plasticizer contents measured, with both decreasing in strength with increase in contents. The glass transition of the ethylene bisformamide-PS was found higher than that of glycerol-PS (63.3 °C against 38.3 °C) since ethylene bisformamide form stronger hydrogen bonds with starch than glycerol. Thunwall *et al.* (2006) reported that glycerol plasticized potato starch produced using hydroxypropylation/oxidation modified starch exhibited a modestly higher resistance than that of native starch. However, an increase in glycerol content reduced the moisture resistance of the TPS regardless of the type of starch used. Modified native potato starch and high amylose starch offered reduced viscosity levels (measured at 140 °C) for starch melts containing 30% (dry mass) glycerol. In comparison with high polyethylene Thunwall *et al.* (2006) further noted that polyethylene melt at 180 °C had a

lower viscosity than native potato PS and hydroxypropylation/oxidation-modified high amylose PS but higher than that of hydroxypropylation/oxidation modified native potato PS, all at 140 °C. They also discovered that starch melt drawability, a crucial property in film production, generally increased with glycerol and chemical modification but decreased with temperature, but in comparison with PE melt, PS melt was very much lower in extensibility. It is important to mention that it is rather difficult to make thin blown films with granular starches as fillers in polymer composites due to their big particle size range (5-100 µm). Hence the preference for TPS (PHILIP *et al.*, 2007) approached the issue slightly differently by blending cassava starch (74.70±1.76%) plasticized with water and glycerol, and another with water and Buriti oil, all in ratio 50:15:35 (mass/vol/vol) with polystyrene in different ratios by mass. It was observed that blends with TPS plasticized by buriti oil were apparently more thermally stable than those by glycerol. A reduction of up to 60% in the water uptake of TPS could be achieved by replacing glycerol with sugar/water mixture as plasticizer though with a concomitant reduction in the TPS crystallinity (OLAYIDE OYEYEMI FABUNMI *et al.*, 2007). One property peculiar to TPSs plasticized with polyols (such as glycerol, sorbitol, glycol and sugars) is their retrogradation (recrystallization due to the reformation of hydrogen bonds between starch molecules) propensities as they age, a condition that leads to embrittlement. This phenomenon could be inhibited using formamide as the plasticizer (since it could form stronger or more stable hydrogen bonds with starch –OH groups) but with a reduction in tensile strength and modulus against a simultaneous increase in elongation at break and energy break vis-a-vis glycerol plasticized starch (TANG *et al.*, 2012). Amides generally form stronger hydrogen bonds with starch -OH groups than polyols in the following order: urea > formamide > acetamide > polyols (JIUGAO *et al.*, 2005). Though with a compromise on tensile stress, similar result of inhibited retrogradation coupled with reduced shear viscosity (improved fluidity) of TPS, improved elongation, thermal stability and water resistance at high relative humidities was achieved by Jiugao et. al. (JIUGAO *et al.*, 2005) when glycerol plasticized TPS was modified with citric acid in comparison with the unmodified glycerol TPS. Pickering (PICKERING, 2008), explored some natural fibers reinforcing potentials for thermoplastic starch in their work published recently. Three material variables were considered, namely: starch (sweet potato, corn and potato starches), plasticizer (ethylene glycol, glycerol, chitosan, water, and propylene glycol) and fiber (jute, sisal and cabuya with fiber lengths of 5±1 mm). All these factors coupled with processes (compression molding) conditions such as time and

temperature were found to affect the tensile strength of the TPS. Individual assessments (done keeping other variables constant) shows that potato starch, sisal, and ethylene glycol gave the highest tensile strength results whereas water and cabuya fiber give the highest impact strength.

Besides discrete macro fibers as reinforcements for TPS, cellulosic nanofibers, such as cellulose microfibrils (SU *et al.*, 2015) and tunicin whiskers (MURANO & TOFFANIN, 2017) have also been investigated. Two types of wood pulps (bleached Kraft pulp from Eucalyptus Euro grand and unbleached thermomechanical pulp of Eucalyptus grand) were evaluated by De Carvalho *et. al.* (CARVALHO *et al.*, 2016) in reinforcing TPS produced with cornstarch (28% amylose) and glycerol. It was found that though an increase in glycerol (above 30%) decreased both the tensile strength and modulus, increase in fiber (pulp) contents (from 5-15% of matrix mass) remarkably increased both the tensile strength and modulus in all cases. On the other hand, the tensile strains of the composites decreased with the addition of fiber or glycerol to the raw matrix. Interestingly, regardless of glycerol amounts, fiber breakage as against debonding was observed on all fracture surfaces, an indication of a strong fiber-matrix interfacial bonding.

In agreement with similar work, the equilibrium water absorption of the TPS matrix increased with glycerol and was found higher than those of TPS-fiber composites (thus, implying improved moisture resistance by fiber inclusion), which were similar irrespective of the formulation. Besides organic materials like natural fibers, the potentials of inorganic minerals such as hydroxyapatite (CARROW & GAHARWAR, 2015) as reinforcement materials for TPS have been reported. The reinforcing potentials of clay were examined by Mitra (MITRA, 2014), whereby TPS/clay nano-composites produced from native potato starch and natural montmorillonite (clay) were found to possess higher tensile strength and thermal stability and lower water vapor transmission rate than ordinary TPS. In addition, their recent study of the effectiveness of fly ash in reinforcing corn PS prepared with glycerol and formamide-urea combination as plasticizers observed a considerable increase in the tensile stress, Young's modulus, and water resistance, though with a corresponding decrease in ductility. Fly ash was also found to inhibit retrogradation.

Lastly, Ortega-Torto *et. al.* (2017), exploited the polymer orientation technique in improving extruded corn TPS sheet. The orientation was achieved by drawing at different speeds TPS sheet extrudates from the die under positive tension by a three-roller system

in front of the die after which the mechanical properties were measured along and across the extrusion direction. Unlike elongation, both tensile modulus and yield strength improved in both directions. However, the effect of orientation was influenced by amylose/amylopectin ratio, such that differences in modulus and yield stress in the two directions widened with the increase in amylose while differences in elongation became pronounced at higher amylopectin contents. These directional differences in tensile properties are much higher in conventional polymers and for instance, may be in the order of 10 times in polypropylene. On a broader view, amylose contents have actually been found to proportionately influence mechanical properties such as tensile modulus, tensile strength and elongation of TPS (MERINO *et al.*, 2018, DEBIAGI *et al.*, 2017).

### 3.5 Natural Fiber

Researchers are trying to ameliorate the mechanical properties of polymers by using natural fibers and fabricating new cheap and useful bio-composites. So natural fibers, as reinforcement, have recently attracted the attention of scientists because of their advantages over other established materials (LI *et al.*, 2000). They are environmentally friendly (eco-friendly), fully biodegradable, abundantly available, renewable and cheap and have low density (NOSONOVSKY & BHUSHAN, 2012). Plant fibers are light compared to other fibers like as glass, carbon and aramid fibers. The biodegradability of plant fibers can contribute to a healthy ecosystem while their low cost and high performance fulfill the economic interest of the industry. When plastics reinforced by natural are subjected, at the end of their life cycle, to combustion process or landfill, the released amount of CO<sub>2</sub> of the fibers is neutral with respect to the assimilated amount during their growth. Regard to technical process and recycling process of the composite materials in general, the abrasive nature of fiber is much lower which leads to advantages in regard to technical process and recycling process of the composite materials in general. Natural fiber-reinforced plastics, by using biodegradable polymers as matrices, are the most environmental friendly materials, which can be composed at the end of their life cycle. Natural fiber composites are used in place of glass mostly in non-structural applications (PICKERING *et al.*, 2016). A number of automotive components previously made with glass fiber composites are now being produced using environmentally friendly composites. However natural fibers and their composites are environmental friendly and

renewable (unlike traditional sources of energy, i.e., coal, oil, and gas), these have several impasses. Some of them are poor wettability, incompatibility with some polymeric matrices and the high moisture absorption. Composite materials made with the use of unmodified plant fibers frequently exhibit unsatisfactory mechanical properties. To overcome this, in many cases, a surface treatment like as plasma treatment or compatibilizing agents need to be used prior to composite fabrication. The properties can be improved both by physical treatments (cold plasma treatment, corona treatment) and chemical treatments. Mechanical properties of natural fibers are much lower than those of glass fibers but their specific properties, especially stiffness, are comparable to the glass fibers(PICKERING *et al.*, 2016).

### 3.5.1 Disadvantages of natural fiber in composite

Although the natural fibers have many advantages, there are some disadvantages which limit their applications. The performance of biocomposites depends on the properties of the natural fibers which used in their structure (GEJO *et al.*, 2010). However, using natural fibers in building materials has also some disadvantages such as low modulus elasticity, high moisture absorption, decomposition in alkaline environments or in the biological attack, and variability in mechanical and physical properties. To understand these problems, it is necessary to study fibers precisely. Generally, cell wall polymers and their matrices are the reason for the chemical and physical properties of natural fibers. For instance, dimensional stability, flammability, biodegradability, and degradation are attributed to acids bases and UV radiation that alters the biocomposites back into their basic building blocks (carbon dioxide and water). However, the properties of natural fibers that result from the chemistry of the cell wall components make some main problems in biocomposites. Therefore, to address these problems, improving the natural fiber properties by modifying the basic chemistry of the cell wall polymers has been recommended (GUPTA & KUMAR, 2012).

### 3.6 Cellulose

Cellulose is a biopolymer which is renewable, biodegradable and is considered to be the most abundant renewable polymer on earth (DUFRESNE, 2006). It can be gained from

various sources such as trees, algae, fungi, and bacteria. Cellulose is a polydispersed linear polymer consisting of  $\beta$ -D-glucopyranose units linked by a glucoside bond between their C-1 and C-4 hydroxyl groups. Figure 2 shows the structure of cellulose in its chair configuration.

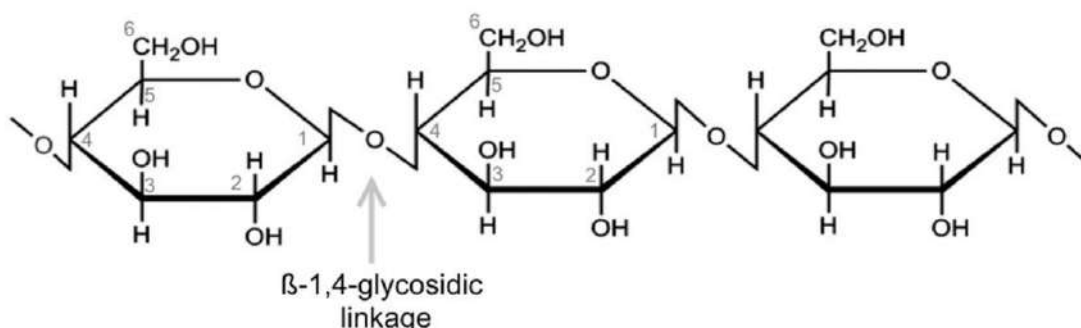


Figure 2. Molecular structure of cellulose (GURUNATHAN *et al.*, 2015).

Cellulose can be deliberated as a syndiotactic polyacetal of glucose. The C-1 hydroxyl at one end of the molecule is an aldehyde hydrate group with enhanced activity. In another hand, the C-4 hydroxyl on the other end of the chain is non-reducing (KRÄSSIG, 1995). The chemical character of the cellulose molecule is specified by the  $\beta$ -glucosidic linkage between the glucose repeating units, to hydrolytic attack, and by the presence of three reactive hydroxyl groups, one primary and two secondaries, in each of the base units (KRÄSSIG, 1995, GURUNATHAN *et al.*, 2015).

### 3.6.1 Cellulose properties

Cellulose is not soluble in water and most of the organic solvents due to its extensive hydrogen bonding and tendency to form crystalline structures. It has no taste and it is odorless. However, it is soluble in more exotic solvents, such as CdO/ethylenediamine (cadoxen), aqueous N-methyl morpholine-N-oxide (NMNO), LiCl/N,N'-dimethyl acetamide, near supercritical water and in some ionic liquids (KO *et al.*, 2015). Chain length or degree of polymerization (DP) is an important attribute of a polymer. Many properties of cellulose are related to its chain length. Chain lengths of cellulose are different depending on the sources. The degree of polymerization of native wood is about 10,000 and it is approximately 15,000 in cotton (BJORKMAN & SALMEN, 2000). Different parts of the plant have the different Chain length from the same source. Shorter

chain lengths may also result from chemical and mechanical degradation during the purification and analysis processes (AZIZI SAMIR *et al.*, 2005). These smaller molecules are referred to as cellodextrins, which are usually soluble in water and most organic solvents. High concentrations of hydroxyl groups result in strong intra- and inter-molecule forces, which have the great effect on the properties of cellulose (GEORGE & SABAPATHI, 2015). For example, the hydrophilic and swelling properties are strongly influenced by hydrogen bonding. Cellulose is a very hydrophilic material which swells when exposed to high humidity environments. The swelling is reversible to some extent (SUGIYAMA *et al.*, 1991), though, the desorption curves of cellulose have higher moisture contents than the adsorption curves. This hysteresis effect was clarified as the inaccessibility of hydroxyl groups of cellulose in the dry state. In other words, hydroxyl groups satisfy each other, because of this reason hydroxyl groups are more difficult to access at dry state, while at high moisture level the hydroxyl groups are easier to access as the adsorbed water breaks up the hydrogen bonding between the polymer chains (SUGIYAMA *et al.*, 1991).

### 3.6.2 Crystalline Structure of Cellulose

Cellulose is familiar to be in several crystalline forms. Cellulose I is the dominant form in nature (GAUTAM *et al.*, 2010). It consists of a microfibrillar crystalline array of linear  $\beta$ -1, 4-glucan chains, all of which are oriented parallel to one another with the same polarity (IMAI & SUGIYAMA, 1998). The cellulose I allomorph is the thermodynamically metastable form of cellulose. There are two known suballomorphs of cellulose I which discovered using NMR and later confirmed by using electron diffraction (cellulose  $I\alpha$  and cellulose  $I\beta$ ). The cellulose  $I\beta$  has doublets at C-1, C4 and C-6. Cellulose  $I\beta$  is thermodynamically more stable between these two forms. The two forms of cellulose in which  $I\alpha$  is dominant in celluloses from lower plants on the other hand  $I\beta$  is dominant in celluloses from higher plants where the major component is secondary wall (GAUTAM *et al.*, 2010, IMAI & SUGIYAMA, 1998). Table 1 summarizes the  $I\alpha$  fractions in specimens of various origins (WADA *et al.*, 2004). It was reported that tunicin, the cellulose from tunicate (a sea animal), consists of nearly pure (around 90%)  $I\beta$  phase. On the contrary, freshwater alga *Glaucozystis* sp. consists of nearly pure (around 90%)  $I\alpha$  cellulose.

Table 1.  $I_\alpha$  fractions in specimens of various origins (WADA *et al.*, 2004).

Sample	$I_\alpha$
Cladophora	0.76
Glaucocystis sp	0.90
Western yellow pine	0.62
Eucalyptus	0.68

Cellulose  $I_\alpha$  has a triclinic one-chain unit cell where parallel cellulose chains stack, via van der Waals interactions, with progressive shear parallel to the chain axis. Cellulose  $I_\beta$  has a monoclinic two-chain unit cell, which means parallel cellulose chains are stacked with alternating shear (DE SOUZA LIMA & BORSALI, 2004). Furthermore, it has been shown that cellulose  $I_\alpha$  transforms into cellulose  $I_\beta$  without losing its crystallinity, by hydrothermal treatment or by treatments with various solvents. In these two lattices, *i.e.*,  $I_\alpha$  and  $I_\beta$ , the conformation of the polysaccharide chains is similar although the hydrogen-bonding pattern is different (ŠTURCOVA *et al.*, 2004). Both phases show hydrogen bonding only between polymer chains inside a layer of chains. Figure 3a and 3b show the atomic arrangement and hydrogen bonding network in cellulose  $I_\alpha$  and cellulose  $I_\beta$  (NAM *et al.*, 2016).

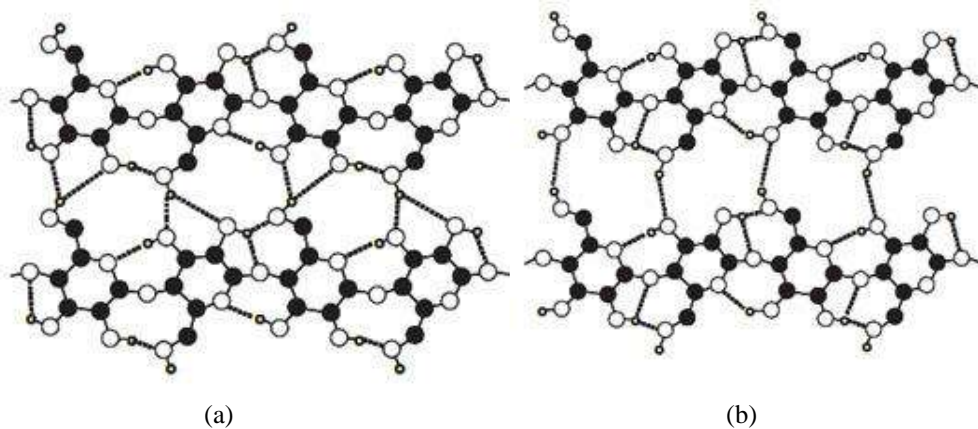


Figure 3. (a) Atomic arrangement and (b) hydrogen bonding network in cellulose  $I_\alpha$ .

Cellulose I is responsible for mechanical properties of reinforced composites due to its high modulus of elasticity and crystallinity. Table 2 summarizes the degree of crystallinity and the lateral dimension of elementary fibrils from several cellulose samples

measured by X-ray diffraction (XRD) (IOELOVICH, 2009, WOLLBOLDT *et al.*, 2010, LI *et al.*, 2009).

Table 2. Degree of crystallinity (WC) and lateral dimension (D) of elementary fibrils from several cellulose samples (IOELOVICH, 2009, WOLLBOLDT *et al.*, 2010, LI *et al.*, 2009).

Sample	WC, %	D, nm
Natural softwood/hardwood	60-62	3-4
Isolated sulfite cellulose	62-63	5-6
Isolated Kraft cellulose	64-65	6-7
Natural cotton cellulose	68-69	5-6
Isolated cotton cellulose	70-72	7-8
Natural flax or ramie cellulose	65-66	4-5
Isolated flax or ramie cellulose	67-68	6-7
Bacterial cellulose	75-80	7-8
Algae cellulose	75-80	10-15

### 3.6.3 Amorphous Regions

Cellulose also has bundles of amorphous regions. Amorphous cellulose is also located between cellulose microfibrils. In the amorphous regions, the cellulose chains are randomly oriented in a spaghetti-like arrangement leading to a lower density in these domains (BHATTACHARYA *et al.*, 2008). This makes the amorphous regions susceptible to attack by acids. Wide-angle X-ray scattering had been used to study possible structures for amorphous cellulose. Diffraction studies showed light and dark areas along a cellulose microfibril, which had been attributed to crystalline and amorphous cellulose, respectively. Cellulose from cotton has a high amount of crystalline cellulose and a small amount of amorphous cellulose. On the other hand, regenerated cellulose has the relatively higher amount of amorphous cellulose. The high amorphous fraction in cellulose means high accessibility of chemicals to cellulose structure. A schematic of amorphous cellulose and crystalline cellulose is shown in figure 4. Disordered domain (DD) represents amorphous cellulose and ordered region is crystalline cellulose. In the amorphous or less ordered regions the cellulose chains are not so tightly packed and thus they are more available for hydrogen bonding to other molecules such as water (CHODAK, 2004).

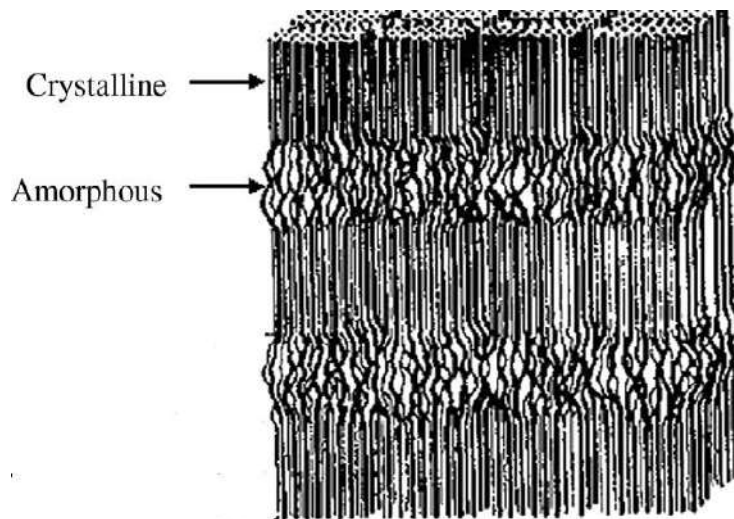


Figure 4. Schematic of amorphous cellulose and crystalline cellulose (KUMAR *et al.*, 2014).

Naturally, cellulose chains form microfibrils due to hydrogen bonding between hydroxyl groups of adjacent molecules, within which highly ordered crystalline regions alternate with less ordered amorphous regions. The molecular arrangement of these fibrillar bundles is called microfibrils, within which highly ordered crystalline regions alternate with less ordered amorphous regions (CÉLINO *et al.*, 2014). The microfibrils are about 10-30 nm wide and contain cellulose molecules of a degree of polymerization from  $2 \times 10^3$  to  $6 \times 10^3$  (CÉLINO *et al.*, 2014). The range of microfibril diameter of various cellulose samples is listed in Table 3. Figure 5 shows a schematic of the hierarchical structure of wood.

Table 3. Range of diameters of microfibril of various cellulose sources (MOON *et al.*, 2011).

Sample	Microfibril diameter (nm)
Bacterial cellulose	4-7
Cotton linters	7-9
Ramie	10-15
Dissolving pulp	10-30
Valonia cellulose	10-35

Since the cell walls differ in their composition and in the orientation of the microfibrils, the mechanical properties of cellulose fibers depend on the cellulose content and the spiral angle of the fibril. The modulus of elasticity of the perfect crystal of cellulose has been calculated by several authors and it has been estimated to lie between 130 to 250 GPa, while the tensile strength is assessed to be approximately 0.8 to 10 GPa (MOON *et al.*, 2011).

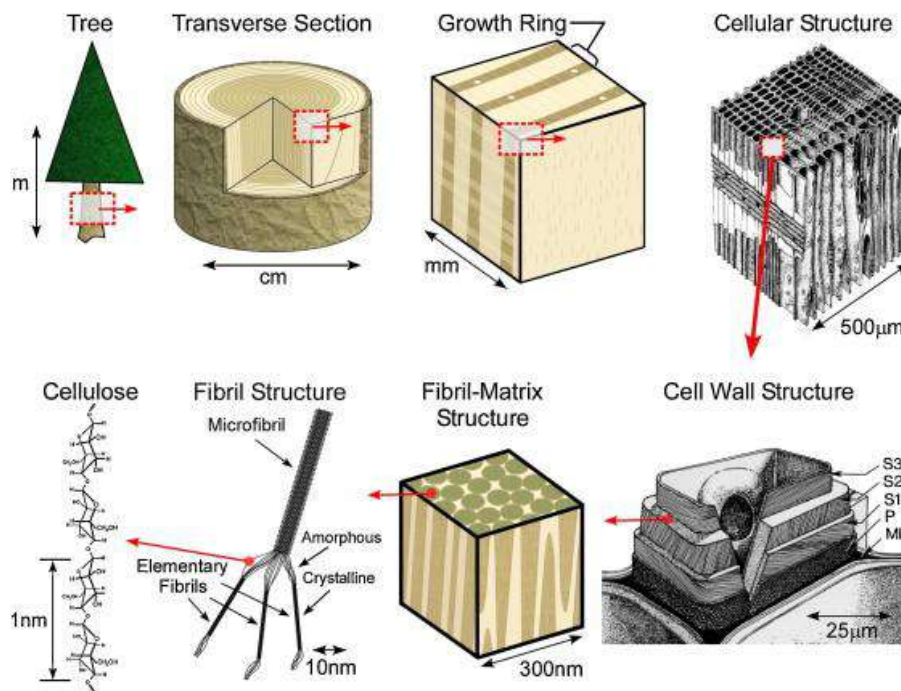


Figure 5. Schematic of hierarchical structure of a wood from macroscale to nanoscale (HABIBI *et al.*, 2010).

### 3.7 Cellulose Nanofillers

Regular fillers are usually in the micrometer or millimeter scale and are required at relatively high loading (10-40%) in order to significantly influence the final properties of a polymer matrix composite. In recent decades, as nanotechnology has grown exceedingly, nanofillers have become more and more promising. Nanofillers are defined as at least one dimension of the filler being in the nano-scale (1~100 nm). It was believed that nanofillers can greatly reinforce the properties of material due to their significantly large surface-area-to-volume ratio. The most researched example to date is nanoclay. In the early 1990s, a research team at Toyota, Japan, found that a small amount (less than 5%, by weight) of an organically modified montmorillonite can enhance the stiffness, strength and increase the heat distortion temperature of Nylon 6 dramatically. After Toyota's study, more and more works on nanoclay have been reported. Fiber-shaped fillers such as carbon nanotubes have also been studied. Due to the depletion of oil reserves as well as environmental concerns, natural fibers (i.e. cellulose) have received widespread interest. Its renewable nature, low density, abundant availability, high specific strength and low cost make cellulose a very favourable candidate for the production of

nanofillers. There are basically two classes of cellulosic nanofillers: cellulose nanocrystal (CN) and microfibrillated cellulose (MFC). Different terminologies are also used in different articles leading to confusion in the research field. For example, cellulose nanocrystals are also referred to in papers as nanocrystalline cellulose (NCC) or cellulose whiskers. The two classes of cellulosic nanofillers are distinguished by the main steps involved in their preparation, namely CNs are prepared chemically by acid hydrolysis while MFC was mainly prepared by mechanical homogenization (SIAUEIRA *et al.*, 2009).

### 3.8 Microfibrillated Cellulose (MFC)

MFC can be considered as cellulosic materials gained by mechanical homogenization process. After the mechanical treatment, the cellulose is moderately degraded, and the volume and surface area is highly expanded. MFCs are long and flexible fibrils with widths ranging from 10~100 nm and length generally in micrometer scale. As there is no chemical reaction involved in the preparation process, MFC maintains the cellulose structure, i.e. consisting of alternating crystalline and amorphous regions. Another difference from cellulose nanocrystal (CN) is that, MFC has web-like structure, while CNs is rod-like whiskers. Two common types of equipment can be used for the mechanical treatment to obtain MFC. The first one is a Gaulin homogenizer, at a pressure of 500 bar and at a temperature of 90~95°C. A gel-like MFC suspension will be obtained after 15 passes of homogenization. A microfluidizer is the most commonly used alternative to produce MFC. A cellulose suspension is fed through a thin channel under high pressure. The pressure can reach as high as 30,000 psi. The high pressure pushes the suspension at an extremely high velocity, leading to high shear at the channel wall and hence, resulting in deformation of the product stream (RÅNBY, 1951). However, high shear also causes heat generation. A heat exchanger is required to cool the product stream down to the room temperature. Both types of equipment are operated at high pressure and require repeated passes to achieve a high degree of homogenization. As a result, high power consumption is the main disadvantage of those processes. Pre-treatments, such as mild acid hydrolysis, enzymatic hydrolysis can be combined with mechanical treatment to reduce the number of passes and hence energy consumption (RÅNBY, 1951).

### 3.9 Cellulose Nanocrystals

Cellulose nanocrystals illustrate the crystalline regions extracted from cellulose, mainly by acid hydrolysis. The origin of acid hydrolysis of cellulose can be dated back to 1950s. Ranby first reported the production of stable suspensions of cellulose crystals by sulphuric acid hydrolysis of wood and cotton(SIQUEIRA *et al.*, 2010b, RÅNBY, 1951). The amorphous regions of cellulose are more accessible to acid attack compared to crystalline regions and therefore, under controlled conditions, the amorphous regions are assumed to be removed whereas the crystalline regions remain, as illustrated in Figure 6. This assumption has been proven by X-ray diffraction, which has shown that the acid treated rod-like particles have the same crystal structure as original cellulose (TING *et al.*, 2010).

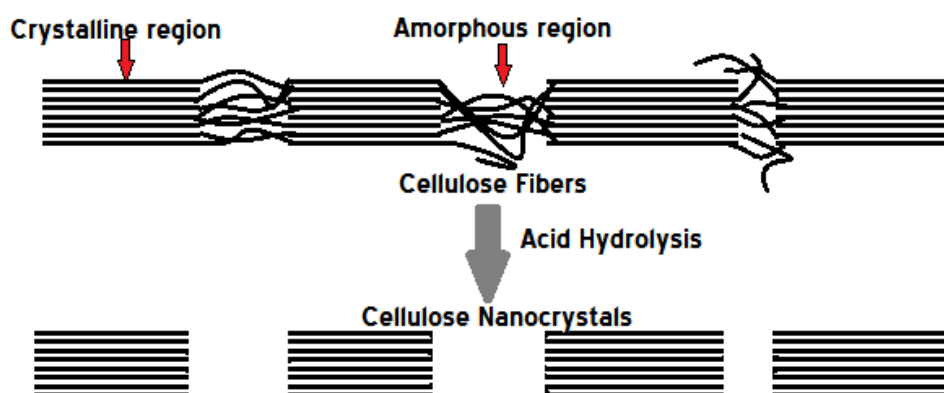


Figure 6. Illustration of acid hydrolysis of semicrystalline cellulose fibers (TING *et al.*, 2010).

### 3.10 Preparation of nanocellulose

Although there are many ways in variety articles to prepare nanocellulose, the final percentage of nanocrystals are very important. Some mechanical shearing actions applied to cellulosic fibers release more or fewer individual microfibrils. This material is usually called microfibrillated cellulose (MFC). Different mechanical treatment procedures have been reported to prepare MFC. They mainly consist of high-pressure homogenization and/or grinding (BARARI *et al.*, 2016). However, this production route is normally associated with high energy consumption for fiber delamination(WANG *et al.*, 2018). Therefore, different pretreatments have been proposed to facilitate this process, for

example, mechanical cutting (AYRILMIS & ASHORI, 2014), acid hydrolysis (HENRIKSSON *et al.*, 2007), enzymatic pretreatment (WÅGGERG *et al.*, 2008), and the introduction of charged groups through carboxymethylation (ISOGAI *et al.*, 2011) or 2,2,6,6-tetramethylpiperidine-1-oxyl (TEMPO)-mediated oxidation (SIQUEIRA *et al.*, 2010b).

After disintegration, MFC is typically obtained as a suspension in liquid, usually water. During homogenization, the suspension changes from a low viscosity to a high viscosity medium. Normally a 2 wt% fiber suspension is used for the preparation of MFC. At higher concentrations, the increased viscosity during processing becomes too high, such that the suspension cannot be moved forward by the pumping system. The MFC aqueous suspensions display a gel-like behavior as shown in Figure. 7.



Figure 7. Picture of a 2 wt% microfibrillated cellulose aqueous suspension from eucalyptus, enzymatically pretreated (MALAININE *et al.*, 2003).

The production of MFC from wood pulp and various non-wood sources has been reported. The morphology of constitutive nanoparticles is generally characterized using microscopic techniques. Figure 8 shows MFC obtained from *Opuntia ficus-indica*. MFC consists of both individual and aggregated nanofibrils made of alternating crystalline and amorphous cellulose domains. Although image analysis can provide information on fibril width, it is more difficult to determine the length because of entanglement and difficulties in identifying both ends of individual nanoparticles. Indeed, the observation scale for length and diameter is quite different. The width is generally in the range 3–100 nm

depending on the source of cellulose, defibrillation process and pretreatment and the length is considered to be higher than 1  $\mu\text{m}$  (NAKAGAITO & YANO, 2004).



Figure 8. Transmission electron micrograph showing MFC obtained after high-pressure mechanical treatment of *Opuntia ficus-indica* fibers (SIQUEIRA *et al.*, 2010a).

### 3.11 Chemically induced restructuring strategy

A controlled strong acid hydrolysis treatment can be applied to cellulosic fibers allowing dissolution of amorphous domains and therefore longitudinal cutting of the microfibrils. The ensuing nanoparticles are generally called cellulose nanocrystals (CNCs) and are obtained as an aqueous suspension. Lee *et al.* observed between crossed-Nicols the CNC dispersion shows the formation of birefringent domains (Figure 9). During the acid hydrolysis process, the hydronium ions penetrate the cellulose chains in the amorphous regions promoting the hydrolytic cleavage of the glycosidic bonds and releasing individual crystallites after mechanical treatment (sonication). Different strong acids have been shown to successfully degrade cellulose fibers, but hydrochloric and sulfuric acids have been extensively used. However, phosphoric (LEE *et al.*, 2009), hydrobromic (FILPPONEN & ARGYROPOULOS, 2010), and nitric acids (ROMAN & WINTER, 2004) have also been reported for the preparation of crystalline cellulosic nanoparticles. One of the main reasons for using sulfuric acid as hydrolyzing agent is its reaction with the surface hydroxyl groups via an esterification process allowing the grafting of anionic sulfate ester groups. The presence of these negatively charged groups induces the formation of a negative electrostatic layer covering the nanocrystals and promotes their dispersion in water. However, it compromises the thermostability of the nanoparticles (PAPADIMITRIOU & BIKIARIS, 2009). To increase the thermal stability of  $\text{H}_2\text{SO}_4$ -

prepared nanocrystals, neutralization of the nanoparticles by sodium hydroxide (NaOH) can be carried out (FAHMA *et al.*, 2016).



Figure 9. Photograph of an aqueous dispersion of capim dourado cellulose nanocrystals (0.50 wt%) observed between cross-nicols showing the formation of birefringent domains (LEE *et al.*, 2009).

These nanoparticles occur as high aspect ratio rod-like nanocrystals, or whiskers. Their geometrical dimensions depend on the origin of the cellulose substrate and hydrolysis conditions. Figure 10 shows CNCs obtained from two different cellulosic sources. Each rod can be considered as a cellulose crystal with no apparent defect. CNCs generally present a relatively broad distribution in length because of the diffusion-controlled nature of the acid hydrolysis. The average length is generally of the order of a few hundred nanometers and the width is of the order of a few nanometers. An important parameter for CNCs is the aspect ratio, which is defined as the ratio of the length to the width. It varies between 10 for cotton (SIQUEIRA *et al.*, 2011), and 67 for tunicin (EBELING *et al.*, 1999) or capim dourado (golden grass)(ZHOU *et al.*, 2012).

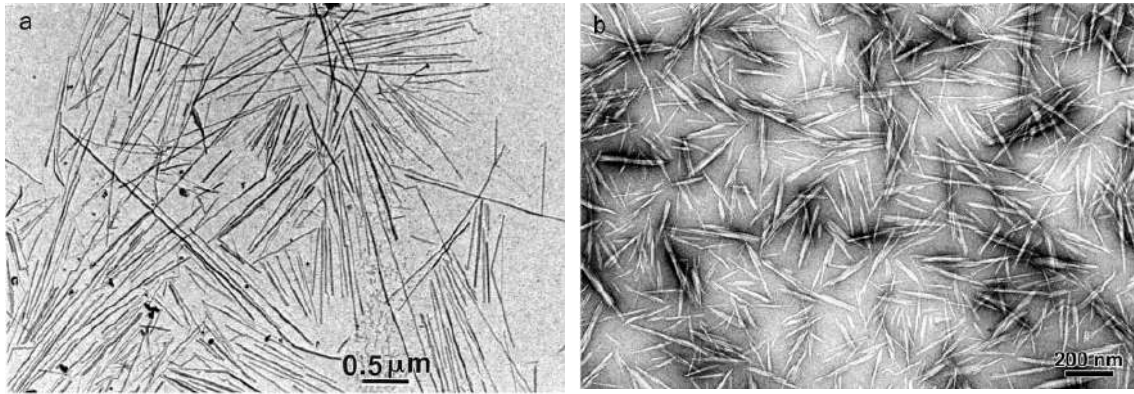


Figure 10. Transmission electron micrographs from a dilute suspension of (a) tunicin, and (b) ramie nanocrystals (EBELING *et al.*, 1999, ANGLES *et al.*, 2000b).

Acid hydrolysis is the classical way of preparing CNCs. However, other processes allowing the release of crystalline domains from cellulosic fibers have more recently been reported, including enzymatic hydrolysis treatment (HIROTA *et al.*, 2010), TEMPO oxidation (DUFRESNE, 2013), hydrolysis with gaseous acid (MAN *et al.*, 2011), and treatment with ionic liquids (ALAIN *et al.*, 2000).

### 3.12 Mechanical properties of cellulose nanoparticles

Cellulose has been used by our society as an engineering material for thousands of years. However, even if cellulose confers its mechanical properties to higher plant cells, the mechanical properties of natural fibers are strongly influenced by many factors, particularly chemical composition and location in plants. Other factors that may affect the fiber properties are maturity, separating processes, microscopic and molecular defects such as pits and nods, type of soil and weather conditions under which they were grown. Further improved fibers and composites can be obtained by disintegrating the natural grown fibers, and separating the almost defect free highly crystalline fibrils (HIRAI *et al.*, 2009).

The mechanical properties of cellulose microfibrils should be higher and less dispersed than those of lignocellulosic fibers from which they are released from because of a more homogeneous nature. Different strategies, both theoretical and experimental, have been used to determine the longitudinal modulus of cellulose microfibrils (or bundles).

However, the average value is around 100 GPa, that is, much higher than for cellulose fibers (PREWO *et al.*, 1986).

The modulus of cellulose microfibrils is expected to result from a mixing rule between the modulus of the crystalline domains and the amorphous fraction. Therefore, it should be higher for more crystalline CNCs. Again a broad range of values was reported (LIU *et al.*, 2018). However, the average value is around 130 GPa, that is, much higher than for cellulose microfibrils as expected.

These impressive mechanical properties make cellulose nanoparticles ideal candidates for the processing of reinforced polymer composites. The Young's modulus of nanocellulose with a density for crystalline cellulose of around 1.5–1.6 g cm<sup>-3</sup> is much higher than the one of glass fibers, around 70 GPa (YOUNG *et al.*, 1988) with a density around 2.6 g cm<sup>-3</sup>, which are classically used in composite applications. It is similar to Kevlar (60–125 GPa, density around 1.45 g cm<sup>-3</sup>) (DESMORAT, 2009) and potentially stronger than steel (200–220 GPa, density around 8 g cm<sup>-3</sup>) (SANCHEZ-GARCIA & LAGARON, 2010). Indeed, the specific Young's modulus, which is the ratio between the Young's modulus and the density, of nanocellulose is around 65 J g<sup>-1</sup> for microfibrils and 85 J g<sup>-1</sup> for nanocrystals whereas it is around 25 J g<sup>-1</sup> for steel.

### 3.13 Starch nanoparticles

Nano-scale starch particles prepared from starch granules have unique physical properties. Starch nanoparticles are suggested as one of the promising biomaterials for novel utilization in foods, cosmetics, medicines as well as various composites due to its environmental friendly nature (H.-Y. *et al.*, 2015).

#### 3.13.1 Preparation and Characterization of starch nanoparticles

##### 3.13.1.1 Chemical Method

###### 3.13.1.1.1 Acid hydrolysis

Kim *et al* (2012) studied various starches of different origins such as waxy maize, normal maize, high amylose maize, potato, and mungbean starches. They were hydrolyzed using

a H<sub>2</sub>SO<sub>4</sub> solution (3.16 M) at 40°C for 7 days, and isolated from hydrolysates by centrifugation. The hydrolysis rate varied from 61.4 to 90.9% depending on the starch type.

XRD results revealed that the starch particles with B-crystalline type exhibited a decrease in peak intensity. While in DSC analysis, the crystals remaining in the B-type starch particles were readily disrupted in the water dispersion so that no melting endotherm appeared. It was confirmed by electron microscopy that the starch particles had round or oval shapes with diameters ranging from 40-70 nm, which possibly represented the starch blocklets in granules.

Miao *et al* (2011) investigated the molecular structure of acid-treated waxy maize starch residues and assessed in vitro digestibility with 2.2 N HCl at 35°C for different time periods. The granular appearance of waxy maize starch was destroyed and small fractions formed aggregates. With the degradation of shortest A chains and long B chains in amylopectin, the change in chain-length occurred. The results demonstrated that the amorphous regions of starch granules, including the shortest A chains and long B chains, were preferentially hydrolyzed and affect the slow digestion and resistance properties of waxy maize starch.

Starch nanoparticles preparation using cold acid hydrolysis and ultrasonication was documented by Kim *et al* (2013). Waxy maize starch was hydrolyzed in an aqueous sulphuric acid solution for 2-6 days, either isothermally at 40°C or 4°C, or at cycled temperatures of 4 and 40°C. The obtained starch hydrolyzates were re-dispersed in water and treated by an ultrasonic treatment (60% amplitude, 3min). The prepared starch nanoparticles had globular shapes with diameters ranging from 50-90nm.

Angellier *et al* (2006) obtained waxy maize starch nanocrystals by hydrolysis of native granules and used as reinforcing agent in a thermoplastic waxy maize starch matrix plasticized with glycerol. The influence of the glycerol content, filler content and ageing on reinforcing properties of waxy maize starch nanocrystals and crystalline structure (X-ray diffraction) were studied. Due to the hydrogen bonding, the reinforcing effect of starch nanocrystals can be attributed to strong filler/ filler and filler/ matrix interactions. The presence of starch nanocrystals leads to a slowing down of the recrystallization of the matrix during ageing in humid atmosphere.

Goncalves *et al* (2014) examined the preparation of starch nanoparticles from *Araucaria angustifolia* by acid hydrolysis and ultrasound. Starch treatment by acid hydrolysis was performed with a solution prepared with 1.1 g starch diluted in 500 mL of 2 mL/100 mL

HCl, maintained for up to 50 days at 22 °C and stirring daily. After the stipulated time, samples were washed 5 times with distilled water at 4–5 °C. The material obtained was subjected to spray drying,

Ding and Kan (2016) prepared Nanoscale retrograded starch (RS III) particles using high-intensity ultrasonication combined with water-in-oil (w/o) miniemulsion cross-linking technique. Results showed that ultrasonication effectively fragmented RS III to nanoparticles 600–700 nm in size. Scanning electron microscopy images showed that ultrasonic treatment produced notches and grooves on the surface of nanoscale RS III. X-ray diffraction analysis indicated that ultrasonication destroyed the crystalline structure of the clustered amylopectin and apparently led to amorphous, or low-crystallinity nanoscale RS III. Differential scanning calorimetry results showed that nanoscale RS III exhibited lower  $\Delta H$  values, which indicated the lower stability of the crystals. Fourier transform infrared spectra showed two new peaks at 1532.30 and 1450.40  $\text{cm}^{-1}$ .

#### 3.13.1.1.2 Precipitation in a water-in-oil microemulsion

Controllable particle sizes of starch nanoparticles were synthesised by Chin *et al* (2014) via a precipitation in a water-in-oil microemulsion approach. The method offered the advantages of ultraflow interfacial tension, large interfacial area, and being thermodynamically stable and affords monodispersed nanoparticles. The mean particle size of starch nanoparticles was found to be affected by the synthesis parameters such as stirring rates, ratios of oil/ cosurfactant, oil phases, cosurfactants, and ratios of water/oil. Starch nanoparticles with mean particle sizes of 109 nm were synthesized by direct nanoprecipitation method, where by using precipitation in microemulsion approach; starch nanoparticles with smaller mean particles sizes of 83nm were obtained.

The preparation of starch-based nanoparticles through high- pressure homogenization combined with water-in-oil microemulsion crosslinking technique was used to prepare sodium trimetaphosphate cross-linked starch nanoparticles (SHI *et al.*, 2011). Dynamic light scattering and transmission electron microscopy revealed that the starch nanoparticles had narrow size distribution, good dispersibility and spherical shape.

#### 3.13.1.1.3 Complex formation with n-butanol

The preparation of starch nanoparticles by complex formation with *n*-butanol was described by Kim *et al* (2009). High amylose corn starch was dissolved in an aqueous dimethyl sulfoxide solution and allowed to form complexes by migrating gravimetrically into *n*-butanol layer through a membrane filter at 70 °C. The starch-butanol complex yielded V61-type crystals with broad reflections at d-spacings of 0.657 and 0.446nm under an X-ray diffractogram. The average Mw of amylose was 2.69 x 10<sup>5</sup> as determined by size-exclusion column chromatography. It contributed mostly to the complex formation. The average chain length of starch residing in the crystalline complex was DP 9, indicating that single crystalline units consisted of approximately 1.5 helical turn of anhydroglucose chains.

#### 3.13.1.1.4 Solvent displacement method

Hebeish *et al* (2014) synthesized starch nanoparticles using native maize starch (NS). The synthesis was carried out as per the solvent displacement method after being modified. Modification involved the use of aqueous alkaline medium as the solvent and ethanol as the organic non-solvent. This was done with a view to assure easier and more reproducible St-NPs preparation without consuming more solvent. The modified method for preparation of St-NPs was evaluated; investigation into factors affecting it was made in order to discover the optimum conditions for such preparation. Factors studied included concentration of starch as well as concentration of surface-active agent, namely, Tween® 80, which was added before precipitation.

#### 3.13.1.1.5 Alkali Freezing Treatment

Zhang *et al* (2013) presented a facile way of producing starch-based nanoparticles (SNPs) with high yields and predictable size by an alkali-freezing treatment. A new mix solvent, sodium hydroxide–urea aqueous solution has been developed to disperse corn starch. After refreezing, thawing, stirring at room temperature and dialysis, resultant aqueous suspensions of SNPs are obtained and characterized using a scanning electron microscope (SEM) and dynamic light scattering (DLS) to learn the particle morphology, mean size and size distribution. By adjusting parameters such as the sodium hydroxide: urea ratio and temperature, the size of particles can be controlled from micro- to nanometer.

### 3.13.1.2 Physical Method

#### 3.13.1.2.1 Milling

The structure and some physicochemical properties of potato and cassava starch particles of size between 50-100 nm were evaluated by Szymonska *et al* (2009), which were obtained by mechanical treatment (starch ethanol suspensions were ground in vibration mill) of native starch. The particles were characterized as amylopectin-type short branched species bundled into larger blocklets released from the granules crumbled in the process. The starch particles were to be utilized in applications, e.g. as drug carriers and/or chemical delivery systems due to their susceptibility to chemical reagents and properties qualitatively different from those of native starch granules.

#### 3.13.1.2.2 Reactive Extrusion

Song *et al* (2011) investigated the mechanism of formation of starch nanoparticles by reactive extrusion method. The effects of extrusion conditions, including temperature (50–100 °C), screw speed, torque, starch water content and crosslinker addition, on particle size were studied. The results indicated that starch nanoparticles with an average size about 160 nm could be obtained with the addition of appropriate crosslinkers. The characterization of morphology, crystalline property, and rheological properties of starch nanoparticles was also done.

#### 3.13.1.2.3 Ultrasonication

Haaj *et al* (2013) were prepared Nano-sized starch particles (NSP) from starch granules using a purely physical method of high-intensity ultrasonication. The results revealed that ultrasound treatment of the starch suspension in water and at low temperature for 75 min results in the formation of starch nanoparticles between 30 and 100 nm in size. Compared to acid hydrolysis, which is the most commonly adopted process, this approach had the advantage of being quite rapid, presenting a higher yield and not requiring any chemical treatment.

Starch nanoparticles preparation using cold acid hydrolysis and ultrasonication was documented by Kim *et al* (2013). Waxy maize starch was hydrolyzed in an aqueous

sulphuric acid solution for 2-6 days, either isothermally at 40 °C or 4 °C, or at cycled temperatures of 4 and 40 °C. The obtained starch hydrolyzates were re-dispersed in water and treated by an ultrasonic treatment (60% amplitude, 3 min). The prepared starch nanoparticles had globular shapes with diameters ranging from 50-90 nm.

#### 3.13.1.2.4 Gamma Radiation

Gamma radiation arises as an advantageous alternative to obtain starch nanoparticles given its low cost, simple methodology and scalability (LAMANNA *et al.*, 2013). Starch nanoparticles with sizes around 20 and 30 nm were obtained by applying a dose of 20 kGy from cassava and waxy maize starch, respectively. They showed the same thermal degradation behaviour and their maximum mass loss zone was similar to the nanoparticles prepared from acid hydrolysis. The nanoparticles from cassava and waxy maize were used as fillers in cassava matrix.

Starch nanoparticles (SNPs) were fabricated via short glucan chains self-assembly at 50 °C and their characteristics were evaluated by transmission electron microscopy, dynamic light scattering, molecular weight distributions, X-ray diffraction, differential scanning calorimetry, and Fourier transforms infrared spectroscopy (LIU *et al.*, 2016). The results showed that SNPs exhibited spherical particles with a diameter of approximately 30-40 nm. The molecular weight of the SNPs mainly distributed at degree of polymerization (DP) 12 and DP 30. The gelatinization temperature of the SNPs increased dramatically compared to that of native waxy maize starch. The crystallinity of the samples increased as the assembling time increased and showed the same A-type in the X-ray diffraction pattern as native starch. This newly proposed SNPs approach has potential application in starch nanocomposite films due to their high gelatinization temperature.

#### 3.13.1.2.5 Nanoprecipitation

Chin *et al* (2014) examined the preparation of Curcumin loaded starch nanoparticles by using in situ nanoprecipitation method and water-in-oil microemulsion system. Curcumin loaded starch nanoparticles exhibited enhanced solubility in aqueous solution as compared to free curcumin. Effects of formulation parameters such as types of reaction medium, types of surfactant, surfactant concentrations, oil/ethanol ratios, loading time, and initial curcumin concentration were found to affect the particle size and loading

efficiency (LF) of the curcumin loaded starch nanoparticles. Under optimum conditions, curcumin loaded starch nanoparticles with mean particles size of 87 nm and maximum loading efficiency of 78% were achieved.

### 3.13.1.3 Enzymatic Method

Hong *et al* (2015) investigated the feasibility of reducing viscosity of high concentration starch slurry by adding pullulanase at lower temperatures and evaluated the hydrophilic properties of pullulanase debranched starch. The crystalline structure was changed from double-helical A-type crystalline to a mixture of B-type and single-helical V-type crystalline, after the pullulanase hydrolysis. The modified starch was partially soluble in cold water, and possessed good water holding capacity. The results of rheological properties showed swollen starches were able to form gel structure after pullulanase modification.

Fine-granule starches were used as mimetics for generating fatty mouthfeel by Ma *et al* (2006). Bacterial  $\alpha$ -amylase,  $\beta$ -amylase, glucoamylase, and dextrozyme were the four hydrolytic enzymes used to hydrolyze corn starch. Dextrose was found to be the most effective in breaking down of corn starch into fine particles. X-ray diffraction and Scanning electron microscopy were used to analyze the hydrolyzed corn starch and results showed that the size of starch particles was in the range of 2-4  $\mu\text{m}$ . The starch was found to be suitable as a fat mimetic when used in mayonnaise.

Duncan *et al* (2011) documented several applications of nanomaterials in food packaging and food safety including, polymer/clay nanocomposites as high barrier packaging materials, silver nanoparticles as potent antimicrobial agents, and nanosensors and nanomaterial- based assays for the detection of food relevant analytes (gasses, small organic molecules and food-borne pathogens).

O'Brien *et al* (2000) evaluated the performance of microencapsulated high fat powders in bread in comparison to commercial partially hydrated vegetable fat. Breads with no added fat were used as control. Powders with different encapsulating agents (caseinates or whey proteins), sugars (sucrose or lactose) and fat [milkfat (AFM, Anhydrous Milk Fat) or vegetable fat blend] were produced under various processing conditions. Various parameters such as specific volume, volume yield, bake loss, colour and crumb structure were all determined on the baked breads. The results revealed that the effects on specific volume bake loss, crust color and textural properties varied significantly.

### 3.13.3 Applications of Starch Nanoparticles

#### 3.13.3.1 Food uses

Li *et al* (2012) studied the capability of starch nanocrystals to stabilize an emulsion. The starch nanocrystals made use of in this study were prepared by sulfuric acid hydrolysis of wx maize starch. The stable oil-in-water emulsions of 50 vol% paraffin liquid were prepared by using starch nanocrystals as emulsifier when the weight percentage concentration of starch nanocrystal relative to water was above 0.02 wt%. The size of the droplets decreased with the raising of the concentration of starch nanocrystal. These emulsions were very stable to coalescence over months and the creaming of emulsions decreased with the increasing of starch nanocrystal concentration.

Winarti *et al* (2014) documented the research which was aimed to find out the characteristics of arrowroot starch nanoparticles produced by butanol-complex precipitation of lintnerized starch and its application as an encapsulation matrix for herb extract. The amylose content and solubility increased but enzymatic digestibility decreased to below than 60%. The lower particle size and enzymatic digestibility with high porosity made arrowroot starch nanoparticles suitable as controlled release matrix for bioactive compound. Application of starch nanoparticles as an encapsulation matrix for andrographolide extract showed smooth and sphere morphology with the average size about 200 nm.

Several studies reported a decrease in water vapour permeability when maize starch nanoparticles were incorporated. Kristo and Biliaderis reported that adding 30-40% waxy maize SNPs led to significant decrease in water vapour permeability of sorbitol plasticized pullulan film (KRISTO & BILIADERIS, 2007). However, in another study it was reported a decrease in the permeability by 40% for a cassava starch film by reinforcing with 2.5% SNPs (GARCIA *et al.*, 2009).

#### 3.13.3.2 Non-Food uses

Yu *et al* (2007) prepared dialdehyde starch nanoparticles (DASNP) by the redox reaction of NaIO<sub>4</sub> and starch in water-in-oil microemulsion. The cell experiment showed that the drug-carrier particle (DOX-DASNP) can release DOX for a long time and strengthened

the effect of the anticancer drug. This work demonstrates that the DASNP, which has good thermal stability, small particle size, low biological toxicity, and slowly anticancer drug-releasing to strengthen drug effect, is a potentially useful carrier for anticancer drug. Chin *et al* (2014) evaluated the preparation and characterization of starch nanoparticles for controlled release of curcumin. Curcumin was loaded onto starch nanoparticles by using *in situ* nanoprecipitation method and water-in-oil microemulsion system. Curcumin loaded starch nanoparticles exhibited enhanced solubility in aqueous solution as compared to free curcumin. Under optimum conditions, curcumin loaded starch nanoparticles with mean particles size of 87 nm and maximum loading efficiency of 78% were achieved. Curcumin was observed to release out from starch nanoparticles in a sustained way under physiological pH over a period of 10 days.

Garcia *et al* (2009) evaluated physic-mechanical properties of biodegradable starch nanocomposites. Nanocomposites of cassava starch reinforced with waxy starch nanocrystals were prepared. They showed a 380% increase of the rubbery storage modulus (at 50 °C) and a 40% decrease in the water vapor permeability. X-ray spectra show that the composite was more amorphous than the neat matrix, which was attributed to higher equilibrium water content in the composites. The reinforcing effect of starch nanocrystals was attributed to strong filler/matrix interactions due to the hydrogen bonding. The decrease of the permeability suggests that the nanocrystals were well dispersed, with few filler/filler interactions.

Bloembergen *et al* (2008) reported an improvement of the performance as a binder for paper by using SNPs instead of cooked starches. With an addition of SNPs, the viscosity of the paste can be substantially reduced, whereas the binding capability can be increased.

Alila *et al* (2009) used chemically modified starch nanocrystals as adsorbents for the removal of aromatic organic compounds from water. The nanocrystals were chemically modified by grafting with stearate moieties which enhanced the adsorption capacity of the nanometric substrate. Their adsorption capacity ranged between 150 and 900  $\mu\text{mol g}^{-1}$  of modified nanoparticles and the adsorption isotherms could be described accurately by the Langmuir model. The adsorption kinetics followed a two-step process with first pure adsorption of the aromatic compounds onto the surface of the nanoparticles followed by a diffusion of the compounds into the layer of surface chains grafted onto the nanoparticles.

(ATICHOKUDOMCHAI & VARAVINIT, 2003) investigated the characterization and utilization of acid-modified cross-linked Tapioca starch in pharmaceutical tablets.

Tapioca starch was cross-linked in the presence of alkaline sodium trimetaphosphate solution. The cross-linked tapioca starch was hydrolyzed by 6% (w/v) HCl solution at room temperature for 192 h. The final product was dried by centrifugal spray dryer to obtain agglomerated acid-modified cross-linked tapioca starch. Spray-dried native tapioca starch, cross-linked tapioca starch and acid-modified tapioca starch were also studied parallel with that of acid-modified cross-linked tapioca starch. It was found that cross-linking didn't increase the relative crystallinity or the melting enthalpy of tapioca starch. Compression of both native and cross-linked tapioca starches gave tablets with a very low crushing strength. Acid hydrolysis introduced to remove the amorphous regions in order to increase the crystallinity of both types of starches, resulting in tablets with a higher crushing strength. In this respect tablets prepared from acid-modified cross-linked tapioca starch were better than those prepared from acid-modified tapioca starch.

### 3.14 Plasma Treatment

In plasma treatment the surface of a substrate is exposed to plasma. Plasma is generated by electrical discharge in a gas feed, always including high energy photons, electrons, ions, radicals and other excited species (LEFEBVRE & GRAY, 2005, LUO *et al.*, 1998). It is generally described as an ionized gas or as an electrically neutral medium of positive and negative particles. "Ionized" refers to the presence of free electrons which are not bound to an atom or molecule. Plasma is considered to be the 4th state of matter after solid, liquid and gas. The state of matter can be changed by adding enough energy. Plasmas can carry electrical current and generate magnetic fields and the most common method to produce plasma is to apply an electrical field to a gas in order to accelerate the free electrons. There are different kinds of processes of plasma treatment such as corona treatment, gas atmosphere plasma, flame plasma, atmospheric plasma, low pressure plasma, vacuum plasma, glow-discharge plasma, cold plasma and etching plasma all relying on the properties of the plasma. Each of the methods mentioned have differences and are chosen based on the desired surface effects and the qualities of the material (GURNETT & BHATTACHARJEE, 2005).

When the surface of a substrate is exposed to plasma, initiated in a gas e.g. N<sub>2</sub>, it may increase the adhesion between the specimen and matrix of a composite. Chemical bonds

in the surface are broken and reactive groups and positions are generated. These could react either with each other creating crosslinking, or the N<sub>2</sub> could integrate into the surface creating new functional groups.

Plasma surface modification technology offers innovative solutions to adhesion and wetting problems in many industries. Component preparation using plasma is an important step prior to printing, bonding, painting, varnishing and coating processes. Plasma surface modification provides an economical solution for the cleaning and activation of component surfaces before further processing.

Plasma treatment only affects surface properties, typically less than 50 Å and the important parameters are:

- Power
- Pressure
- Gas flow
- Reactor geometry
- Positioning of the sample

Influence of plasma on polymers:

- Crosslinking – Chain scissioning
- Etching – Removal of surface contaminants
- Functionalisation – Increase of surface energy

The equipment needed for plasma treatment is commercially available, and consists of a vacuum system, energy supply, gas supply, measurement and control equipment to adjust parameters. The advantage of the process is that no thermal or mechanical strains are introduced into the specimen.

### 3.14.1 Plasma surface modification

Plasma is one of the four fundamental states of matter and is an ionized gas with free electrons and ions. This can be created by heating gasses to extremely high temperatures like as the reaction in surface of sun or by subjecting it to strong electromagnetic fields.

Both these processes are able to reject electrons from the atoms and molecules, and these electrons have enough kinetic energy to remove further electrons from atoms and molecules. These collisions create a cascading ionization process, creating new ions and electrons, which are balanced by the recombination of these two specimens until the plasma reaches equilibrium. Like gas, plasma does not have a definite shape or a definite volume unless enclosed in a container. Unlike gas, under the influence of a magnetic field, it may form structures such as filaments, beams and double layers. When molecules are present in the plasma, their bonds may also be broken by collisions with electrons or ions, generating new unstable molecules and monatomic specimens, both of which are highly reactive (MUKHOPADHYAY & FANGUEIRO, 2009).

Plasma is an electrically neutral medium of unbound positive and negative particles and the overall charge of plasma is roughly zero. Plasma that is not in any local thermodynamic equilibrium is called cold plasma. In this plasma, thermodynamic equilibrium is not reached between electrons and heavy particles even at a local scale in low-pressure discharges. The temperature of the electrons is much higher than that of the heavy particles and the electrons can reach temperatures of  $10^4$ - $10^5$  K, while the temperature of the gas can be as low as room temperature. Because ions, atoms and molecules cannot interchange heat with electrons and electrons travel much faster than them, these species are kept almost at room temperature. As a consequence this plasma might present temperatures similar to room temperature (BRACCO & HOLST, 2013).

13.56 MHz radiofrequency is mostly used as the source to generate electrical field in the plasma system, and electrodes can be either placed inside or outside part of the plasma reactor. Inner electrodes are for the case of metallic reactor and outer electrodes are for the Pyrex and quartz reactors. The electrodeless (outer electrodes) is proffered when treating powder materials to avoid the direct contact of powders with electrodes, such as a copper coil inductively coupled or outer electrodes capacitively couples to the generator. A matching box is needed in all of cases in order to effectively generate plasma and minimize the reflected power. Worth to note that any surface inside the plasma is covered by an electron sheet to develop a negative bias, and the plasma bulk will definitely has a higher potential than the surface. Therefore the positive energetic ions will accelerate to the surface to produce etching or surface ablation effect. Position of sample is also important factor to be taken into consideration. Samples can be either placed in the plasma bulk zone, where the plasma generated, in which plasma shows a strong ion bombardment effect, or placed remote to the plasma generation region, in

which bombardment effect reduced a lot and less severe treatment (MUKHOPADHYAY & FANGUEIRO, 2009, BRACCO & HOLST, 2013).

Cold plasma will achieve easily and quickly at pressures below the atmospheric, so this is the reason why most plasma treatments are made in vacuum, typically between 0.1 to 100 Pa, depending on the application and specific technique used (BRACCO & HOLST, 2013).

The plasma system which will be used in this project is inductively coupled plasmas (ICP) that no electrode is present inside the vacuum chamber. Instead of electrodes, a coil is placed outside the chamber with a dielectric material, usually glass, acting as the reactor wall. A radiofrequency (typically 13.56 MHz) current is applied to a coil as the one shown in Figure 11. This high frequency current induces an alternating magnetic field along the tube, which in turn induces a rotating electric field inside and around the tube. This induced electric field is responsible of accelerating the free charges in the chamber and consequently of inducing the gas ionization. Discharge balance between ionizing collisions and recombination happen in an analogous way as in the glow discharge plasma. However, the distribution of electron densities and temperatures, as well as the degree of ionization and energy of collisions follow different patterns than in the glow discharge, and direct comparison between the deposition parameters in different plasma chambers is complex.



Figure 11. Inductively coupled plasma.

### 3.15. Plasma surface modification

#### 3.15.1. Cold plasma

Plasma is an ionized gas where free electrons and ions coexist. This can be achieved by heating gasses to extremely high temperatures or by subjecting it to strong electromagnetic fields. Both these processes are able to remove electrons from the atoms and molecules, and these electrons have enough kinetic energy to, in case of a collision, remove further electrons from atoms and molecules. These collisions create a cascading ionization process, creating new ions and electrons, which are balanced by the recombination of these two specimens until the plasma reaches equilibrium. When molecules are present in the plasma, their bonds may also be broken by collisions with electrons or ions, generating new unstable molecules and monatomic specimens, both of which are highly reactive (CHEN, 1984, SUN *et al.*, 2014). Laboratory or industrial plasmas, also called “technological plasmas”, are generated by electric or electromagnetic fields and usually have low temperature, which can be as low as room temperature, to avoid damage to the materials being treated. Although high temperatures are needed to maintain ionization, it is possible to keep the perceived temperature of the plasma low with a low degree of ionization. This means that only a fraction (e.g. less than 1% for low temperature plasmas) of all the molecules and atoms in the gas are ionized at any given moment. As a consequence, the average kinetic energy of the molecules, atoms and ions is low, while electrons are accelerated to high velocities thanks to their much lower mass. The result is a so-called “cold plasma”, which is out of thermal equilibrium, i.e. with “hot” electrons and “cold” heavy particles, i.e. atoms, molecules and ions (GURNETT & BHATTACHARJEE, 2005, MULINARI *et al.*, 2011).

Cold plasma is easier to achieve at pressures below the atmospheric, which is the reason why most plasma treatments are made in vacuum, typically between 0.1 to 100 Pa, depending on the application and specific technique used. However, due to simpler operation conditions, atmospheric pressure plasma processes have gained popularity recently, although they have their own drawbacks, like higher consumption of process gas, lower control of the reactions occurring and higher temperatures, due to the higher degree of ionization needed to maintain a plasma discharge at atmospheric pressures (MUKHOPADHYAY & FANGUEIRO, 2009).

For the creation of plasma discharges with electric or electromagnetic fields, many different designs and power sources exist. Interesting for the discussion of this work are two kinds: Glow discharge plasma and radiofrequency (RF) inductively coupled plasma (ICP).



This induced electric field is responsible for accelerating the free charges in the chamber and consequently of inducing the gas ionization. Discharge balance between ionizing collisions and recombination happen in an analogous way as in the glow discharge plasma. However, the distribution of electron densities and temperatures, as well as the degree of ionization and energy of collisions follow different patterns than in the glow discharge, and direct comparison between the deposition parameters in different plasma chambers is complex (JOHANSSON *et al.*, 1999, OKUMURA, 2010).

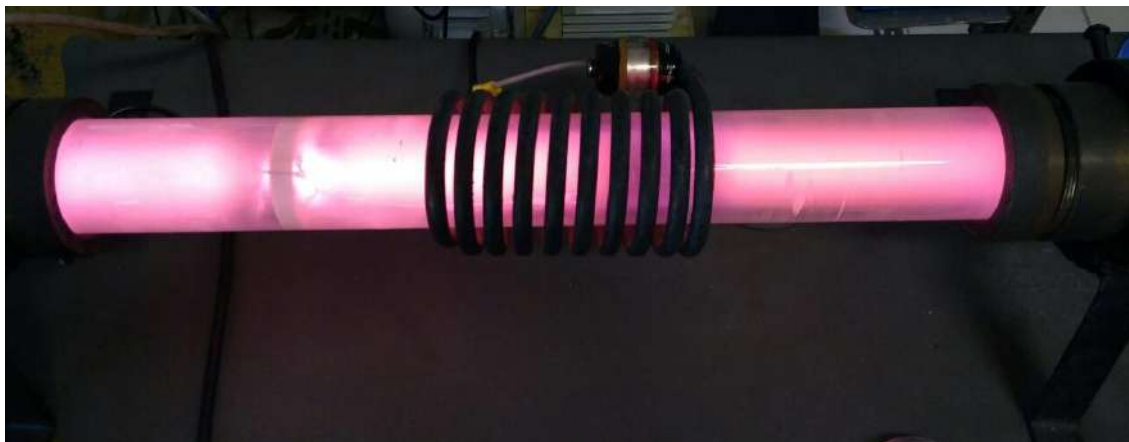


Figure 13. Photo of inductively coupled plasmas (ICP), SFF – Superfícies e Filmes Finos Laboratory.

### 3.15.2. Plasma modification of natural fibers

When plasma of a gas is created, it may react with the fibers (or any substrate) in ways that the neutral gas never could, or at rates much higher than could be achieved by heating, for example. This happens due to the many different specimens created in the plasma, which depend on many factors, including gas composition, intensity of electric field, electron temperatures, among others (GURNETT & BHATTACHARJEE, 2005). Electrons and ions are just a small part of the plasma environment, which may also include, among others (BOGDANOWICZ, 2008, PAPPAS *et al.*, 2006):

- a) Molecules or atoms with excited electrons – still bound but at higher energy levels than the ground state, therefore more prone to reaction.
- b) Neutral, excited or ionized fragments of molecules.
- c) Neutral, excited or ionized atoms which were broken apart from molecules (e.g. Figure 12).
- d) New metastable molecules formed from specimens in the plasma medium, for example,  $C_2$  in  $H_2/CH_4$  plasmas (BOGDANOWICZ, 2008).
- e) UV and visible radiation.

The interaction of the plasma medium with the surface of natural fibers is complex, and many chemical reactions and physical effects can take place simultaneously. As discussed by (MUKHOPADHYAY & FANGUEIRO, 2009) and (RAFFAELE-ADDAMO *et al.*, 2006), processes associated to plasma modification of natural fibers include, but are not limited to:

- a) Cleaning - by sputtering or chemical etching of the surface impurities.
- b) Ablation - removal of fiber material by physical or chemical means, like erosion, etching, vaporization, sputtering, etc. This usually results in rougher surfaces that can promote higher mechanical interlocking with the matrix.
- c) Plasma polymerization – formation of a surface coating from reactions of the gases used, when these have a tendency for polymerization (e.g. methane, ethane, etc.).
- d) Surface chemical modification – Incorporation of atoms or functional groups on the surface material itself, usually replacing atoms or fragments of the material removed by the plasma. This can be due to direct reaction or by formation of free radicals followed by reaction with species in the plasma (neutrals or ions) or after exposure to the atmosphere.

The conditions of plasma treatments found in the literature vary greatly due to different techniques, plasma reactor assembly and geometries, gasses used, fibers treated, matrices with which these will be combined and so forth. Throughout the literature, the expected result reported is always an increase in adhesion between the fibers and the matrix, aiming at better mechanical properties of the resulting composite. Many works have reported improvement in composites tensile strength, elastic modulus or both, as well as in composite flexural and compression strengths (BLEDZKI *et al.*, 2015, GURUNATHAN *et al.*, 2015, LI *et al.*, 2007, SINHA & PANIGRAHI, 2009, FORNES *et al.*, 2013).

An example of the potential for plasma treatments to promote better interaction between fiber and matrix is the work of (LI *et al.*, 2016) which used a helium atmospheric pressure plasma system to treat ramie fibers, some of which were pre-soaked in ethanol for 10 minutes. The fibers were then embedded in a polypropylene matrix. It was reported that plasma treatment alone resulted in only a 4% increase in interfacial shear strength (IFSS) due only to roughening of the surface, while fibers soaked in ethanol and then plasma treated had a 50% increase in IFSS, mainly due to the increased hydrophobicity of the fibers, which presented a greater C–C bond concentration and 40% higher contact angle with water.

Of great interest to this thesis are modifications which can turn the natural fibers surfaces hydrophobic. According to (BASTOS *et al.*, 2013) and (SANTOS *et al.*, 2009), low pressure SF<sub>6</sub> plasma treatment has led to incorporation of fluorine containing groups on starch, a polysaccharide chemically similar to cellulose. This has changed the starch surface from hydrophilic to hydrophobic, with water contact angle increasing from 45° to almost 120°. (SUANPOOT *et al.*, 2008) also reported on the potential of SF<sub>6</sub> plasma to increase the hydrophobicity of silk fibers for use in the textile industry. For this reason, SF<sub>6</sub> was chosen as one of the gasses studied in this thesis.

Other works in the literature are discussed in the following sections, which specify the matrices and fibers combinations used in the work presented in this thesis.

## 4 MATERIALS AND METHODS

The project which is presented in this thesis is performed at Surfaces and Thin Films Laboratory (SFF – Superfícies e Filmes Finos) in Department of Metallurgical and Materials Engineering (DMM – Departamento de Engenharia Metalúrgica e de Materiais) of the Federal University of Rio de Janeiro (UFRJ – Universidade Federal do Rio de Janeiro). This section is about materials and methods which are used in the project by the author.

### 4.1 Starch

The starch which is used in project is provided by Ingredion Company (Sao Paulo). “Amido de Milho AMIDEX 3001” is used as main substance to fabricate the mentioned composite and starch nanoparticles. Actually, it is the main component of bio-polymer that is mentioned in literature review section. The humidity of the starch is 14% and its pH is between 4.5 and 5.5.

### 4.2 Cellulose fibers

The raw material which is used as base of reinforcement phase in matrix is cellulose fibers. Cellulose fibers (Arbocel BC 1000) are provided of KREMER Company (Germany). These fibers are environment friendly products, gained from replenishable raw materials. Among other things, they are used as thickeners, for fiber reinforcement, as an absorbent and diluent or as a carrier and filler in most manifold application fields. The cellulose content of this production is approximately 99.5%, average fiber length is 700  $\mu\text{m}$ , average fiber thickness is 20  $\mu\text{m}$ , bulk density is 35-50 g/l and its pH is 6. According to these data, the fibers are appropriate to being part of reinforcement phase in composite and it is suitable for extracting cellulose nanofibers because it is pure and it does not need any additional process to extracting the cellulose from natural fibers. Actually, in some projects, researcher use natural fibers. So, they should purify and extract the cellulose from these natural fibers like as sisal, hemp, kenaf and so on.

### 4.3 Thermoplastic starch based composite reinforced by cellulose fibers

#### 4.3.1 Plasma reactor construction

Figure 14 demonstrates the plasma reactor which is used in this study. The main components of the reactor include an RF solenoid (A) which is located around the external glass tube (B) and the coil can move throughout the external tube freely. The atmosphere and pressure of inside the tube can be controlled by the gas inlet valve (C) and the vacuum pump (D) which is connected to another side of the reactor. Inside the external tube, there is the internal glass tube (E) which both sides of that are open and the fibers can be located inside of that. Also, it can be rotated by an internal step motor (F) which is connected to the internal tube. Owing to the fact that the low power and low pressure of the mentioned process, it is noteworthy that the plasma does not bring excessive heat to the surfaces of the fibers and the glass tube is only lukewarm to touch during the process.

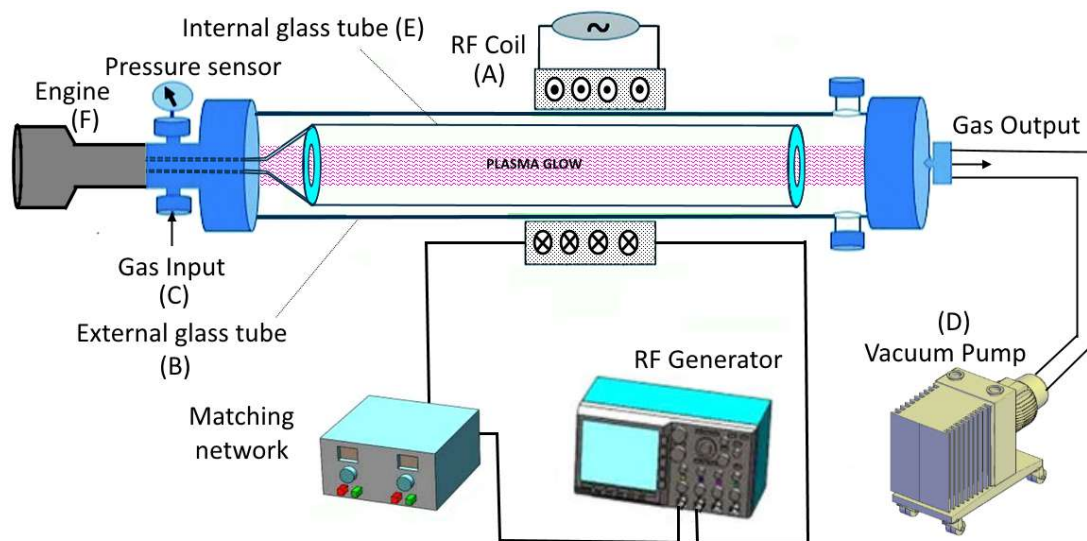


Figure 14. Schematic of plasma reactor.

The selected gas for the mentioned process is pure air and it is expected that this plasma causes surface ablation of the fibers. First, the vacuum pump should be turned on and after a while, the pressure will be decreased. After reaching  $4.0 \times 10^{-2}$  mbar, the gas inlet will be opened slowly until the internal pressure reaches at  $2.0 \times 10^{-1}$  mbar. The working gas pressure is kept at  $2.0 \times 10^{-1}$  mbar during the plasma treatments by opening the gas inlet. Then, the engine will be turned on which can be kept rotating the internal glass tube containing the fibers. Duration of the process is 1 hour and the engine should be kept

working at 50 RPM during the process. Power of the plasma is supplied by a 13.56 MHz RF-generator R301 Meivac (USA), and the impedance circuit is fabricated in-house with diverse capacitors. Figure 15 shows the plasma reactor during the process.

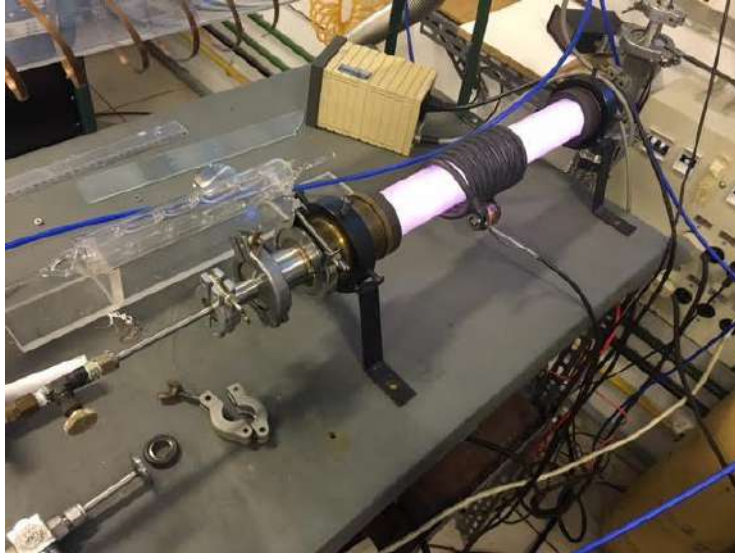


Figure 15. Plasma reactor, SFF – Superfícies e Filmes Finos Laboratory.

By using such a system it is possible to expose all surfaces of a batch (approximately 8 g of fibers). As can be seen in Figure 16a, the rotation of the sample holder causes the high rate penetration of the plasma among the fibers, while, in a static sample holder, only one face of the fibers will face with plasma environment. According to the similarity of the rotational movement of the sample holder with the ball mill which is widely used in the mineral industry, the simplified simulation can be extracted from many works (AGRAWALA *et al.*, 1997, MALEKI-MOGHADDAM *et al.*, 2013).

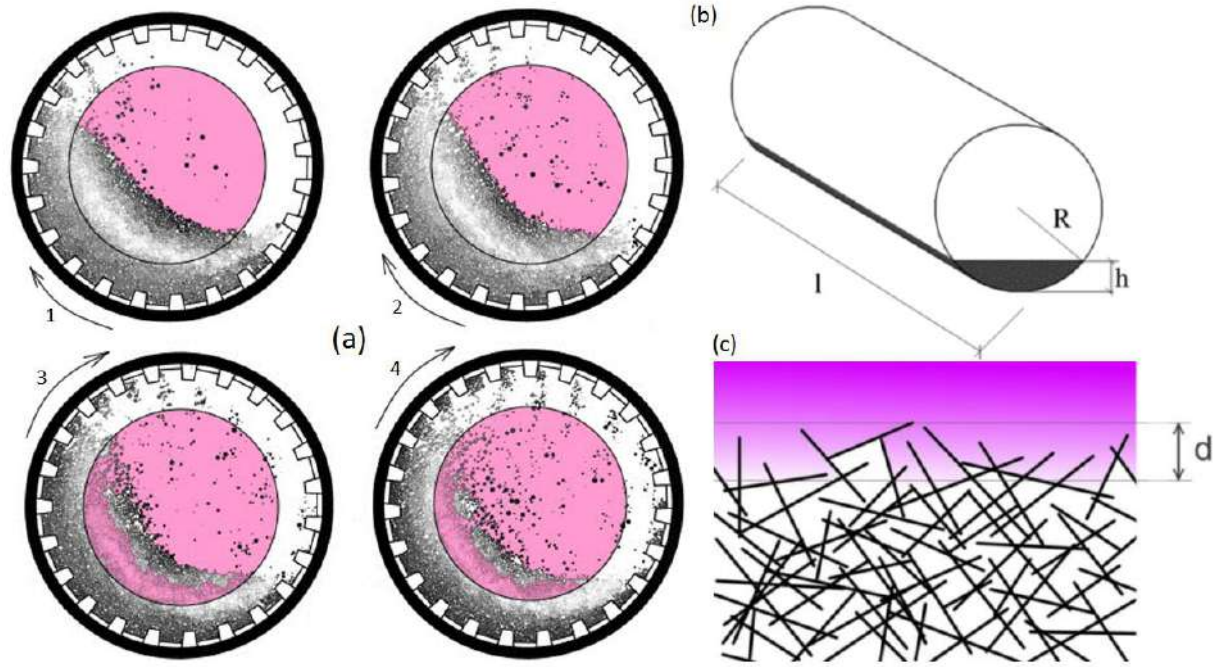


Figure 16. Schematics of the fibers movement in the plasma region throughout the reactor rotation (a), the geometry of sample holder (b), and schematic illustration of the plasma penetration in the accumulated fibers (c).

Eq. 1 presents the simplified model, which introduces the exposed fiber volume ratio at a certain moment over the total volume of fibers. It is essential to note that the velocity in the reactor is fast enough to permit the fibers to rise and then fall in a rotational motion, however, the geometry remains frequently like that schematically displayed in Figure 16b. The total volume of fibers in the sample holder and the exposed fibers volume can be measured by using Eq. 2 and 3 (AGRAWALA *et al.*, 1997, MISHRA & RAJAMANI, 1992).

$$\frac{V_{exposed}}{V_{total}} = \frac{2.d.\sqrt{h(2R-h)}}{R^2 \cos^{-1}\left(\frac{R-h}{R}\right) - (R-h).\sqrt{h(2R-h)}} \quad (\text{Eq. 1})$$

$$V_{total} = l \left( R^2 \cos^{-1}\left(\frac{R-h}{R}\right) - (R-h).\sqrt{h(2R-h)} \right) \quad (\text{Eq. 2})$$

$$V_{exposed} = 2.d.l.\sqrt{h(2R-h)} \quad (\text{Eq. 3})$$

Where  $R$  is cylinder radius,  $l$  is length of internal glass tube (sample holder),  $h$  is height of the fibers and  $d$  is penetration depth (Figure 16c).

Regarding the continuous rotation and considering that the treatment time is long enough to provide the homogeneous mixing, it can be assumed that a single fiber would have occupied all permissible positions inside the moving cylinder. Consequently, the effective

time ( $t_{eff}$ ) for each fiber in a sample holder is given by Eq. 4, which in this study ( $d=0.1$  mm,  $h=4$  mm,  $l=180$  mm, and  $R=18$  mm) is almost 3.6% of the total treatment time.

$$t_{eff} \cong t_{total} \times \frac{V_{exposed}}{V_{total}} \quad (\text{Eq. 4})$$

#### 4.3.2 Plasma treatment conditions

First, the inside of the reactor glass tube and the sample holder are cleaned with a compressed air pistol and later isopropyl alcohol to avoid any cross-contamination of the vacuum and plasma. Then, approximately 5 grams of fibers are weighted and then added to the sample holder (internal glass tube). This is inserted in the reactor and attached to the engine axis, so it could be rotated later. The reactor is closed and then pumped using a rotary vacuum pump. The pump is connected to the reactor chamber by a diaphragm valve, which is opened slowly at first to stop the fibers from being sucked by the strong pressure drop. Once the pressure dropped below 10 Pa ( $10^{-1}$  mbar), the engine is started, causing the sample holder to rotate and the fibers to fall in a tumbling movement. This caused a temporary rise in pressure due to release of trapped gas. The chosen process gas (air) is inserted in the chamber by a needle valve or mass flow controller, rising the pressure to nearly  $10^2$  Pa (1 mbar) while still pumping. This pressure is maintained for 2 minutes, and then the gas input is closed. After 2 to 5 minutes of further pumping, this procedure is repeated. This helped the pressure to drop faster, carrying the humidity which constantly desorbs from the fibers at first, and ensured that leftover gasses would contain mainly the desired gas. The system is then pumped to a base pressure near  $10^{-1}$  Pa. Once base pressure is reached, the desired gas is inserted in the system by the valve, while still pumping, up to a pressure of 10 Pa ( $10^{-1}$  mbar) for air. The gas flow is kept for 5 minutes to guarantee its stability and the purity of the atmosphere in the reactor. The plasma source is turned on and the matching network is adjusted for minimum reflected power. The value of “load power”, as displayed in the power source, is controlled and used as the parameter for plasma treatment. Once the desired time is elapsed, the power source is turned off. Gas flow is maintained for another 5 minutes, to carry away any undesired reaction products. Then, the gas flow is closed and shortly after the vacuum pump valve is also closed. The vacuum is broken slowly with a needle valve, to avoid blowing the

fibers out of the sample holder. Once atmospheric pressure is reached, the reactor is opened, the sample holder removed and the treated fibers are collected.

#### 4.3.3 Mixer for composite production

It needs both friction between particles and high temperature at the same time to manufacture the mentioned polymer which consist of glycerol and starch. To achieve this goal, the MH mixer made in Brazil (MH-50H, M.H. Equipamentos, Brazil) is used in this project. Figure 17 shows this instrument which can work in two different speeds. The first speed, which is necessary for starting the process, works under  $1 \times 10^3$  rpm. In this speed, starch particles and glycerol can mix together perfectly to make the mixture uniform and without changing the nature of particles. The mixture is processed for 10 seconds at this speed. After that, current drops significantly, showing that the matrix is fused. The second speed is then needed, for 5 seconds, to make high friction and high temperature (almost 120 °C) and consolidate the mixture. The time for each step is very important in this process. The times are dependent on the materials which are used. There are three buttons in this device. The first one which is obvious with green color (the left one) in Figure 17 is for starting the process and it starts the first step with low speed. The red button will stop the process and will finish it. It also will be used to change between step 1 and 2. The last green button is for high-speed condition.

This is necessary to know that raw materials have a limit to use. Using under the minimum volume will not result in the polymer because the friction will not happen. In another hand, using upper than maximum volume is very dangerous because the door will be forced and might be opened. So, to start the process, materials should enter the chamber which can be seen in Figure 17 and the door should be closed exactly.

Thermoplastic starch (TPS) films were produced using 25 w.t% glycerol and 75% starch. Films were also produced adding 2, 4, 6, 8 and 12 w.t.% of plasma-treated (PCF) and untreated (UCF) cellulose fibers to starch.



Figure 17. Photo of mixer for composite production.

#### 4.3.4 Hydraulic press for compression molding

After fabricating the polymer or the composite by mixer, the polymer should be in a shape which other tests can be done with that. So, there is a hydraulic press which can change the shape of polymer. MH hydraulic press made in Brazil is connected to the automatic compressor which can feed the force of the press. Figure 18 demonstrates this hydraulic press. As can be seen, the temperature can be changed by this device. So, it can be used in widespread range of temperature. For starch composites, 8 tons and 70°C were used. So, after mixing process, the polymer will put between two steel sheets and a copper ring to make a polymer disc. Thickness of the disc depends on thickness of the ring. In this project, the thickness is 2 mm.

First of all, lower jaw has to go down. Then, the sheets of steel which polymer is between them, will put on top of lower jaw. Then, with pressing the upper button, lower jaw will lift up and the press will start on polymer. After reaching the pressure needed, polymer should stay under the pressure for a while which is depend on polymer. The mentioned time for starch is 3 minutes and this time is needed to transfer the heat of the jaws to the polymer. Then, lower jaw will go down and the polymer disc will be obtained. The radius of the obtained polymer disc is 15 cm.



Figure 18. Compression molding equipment.

#### 4.3.5 Tensile properties

The tensile specimen of neat TPS and TPS/CF composites are cut by an automatic hydraulic press machine (HP-40S). Five samples are tested for each specimen at 23°C and humidity of 70% at a testing speed of 4 mm/min and the average results of the tensile properties are recorded. The Young's modulus, tensile strength, and the elongation at the breakpoint of all the formed samples are gained using INSTRON model 3369, with 100 N load cell, based on ASTM D 882.

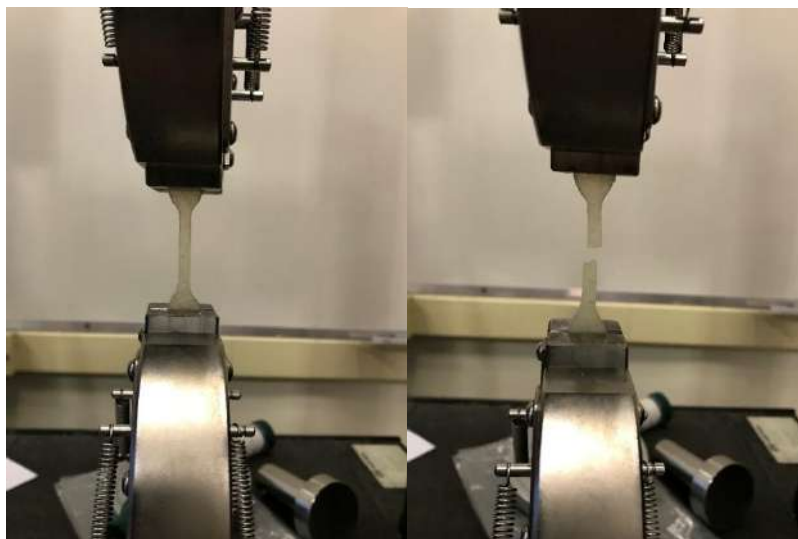


Figure 19. Prepared samples of TPS, TPS/UCF, and TPS/PCF for tensile test.

#### 4.4 Thermoplastic Starch reinforced by starch nanoparticles

##### 4.4.1 Gelatinization and Casting

Corn starch (10.7 g) was added into 200 mL of distilled water. The mixture was heated at 90 °C for 1 h for the complete gelatinization of corn starch with constant stirring with the speed of 240 RPM. The temperature of the solution is controlled by oil bath which is located under the reactor and the reactor is sunk on the oil for the heat exchange. Then

200 mL of ethanol were added dropwise to the solution of gelatinized starch solution with constant stirring. When the resulting nanoparticle suspensions were cooled at the room temperature, another 200 mL of ethanol were added dropwise for about 50 min with constant stirring. The obtained mixture was ground and dried in a furnace for 24 hours at 50 °C. Four types of solution are prepared with this method. The difference among these types of the preparation is summarized below in table. As can be seen, 6.2 gr of glycerol is added to the SNP2, SNP3 and SNP4 in initial solution, but, glycerol does not exist in SNP1. Duration of gelatinization for SNP3 (30 min) is different compared to other films. The step of adding alcohol for SNP4 is different in comparison of other solution. In Table 4, hot solution means 90 °C and cold solution means room temperature. The obtained films were transparent and there were not any cracks on them.

Table 4. Preparation conditions of SNP.

<b>Film</b>	<b>Content of Glycerol</b>	<b>Duration of Gelatinization</b>	<b>Addition of Alcohol</b>
SNP1	0	60 min	In hot and cold solution
SNP2	6.2 gr	60 min	In hot and cold solution
SNP3	6.2 gr	30 min	In hot and cold solution
SNP4	6.2 gr	60 min	Just in cold solution (room temperature)



Figure 20. Reactor of preparing the gelatinized starch and SNP.

#### 4.4.2 Dynamic mechanical analysis (DMA)

The dynamic mechanical properties (storage modulus  $E'$  and  $\tan \delta$ ) of the SNP films are measured on a TA Instruments (New Castle, DE) Dynamic-Mechanical Analyzer. The experiments are performed in the temperature range of  $-80$  to  $200$  °C at a frequency of  $1$  Hz, with a heating rate of  $3$  °C / min. The tests are conducted using a tension film clamp in deformation mode with controlled force of  $0.01$  N. The glass transition temperature,  $T_g$ , is defined as the peak temperature of  $\tan \delta$ . The dimensions of the specimen are approximately  $16.5 \times 6.5 \times 2.0$  mm.

## 4.5 Characterization Techniques

### 4.5.1 Scanning electron microscope (SEM)

To evaluate the changes of the surface morphology of the fibers after plasma treatment, these were observed by scanning electron microscopy (SEM). The fibers were placed over a conducting adhesive tape and coated with a thin film of gold, to make the fibers surface conductive. The microscope used was a JSM-6460LV from JEOL, USA. Secondary electron imaging was used with electron acceleration of 20kV or 15kV, according to the fibers sensitivity to damage by the electron beam. The fracture surfaces of the tensile samples and the microstructure of untreated and treated cellulose fibers are studied by SEM (TESCAN VEGA3) with an acceleration voltage of 15 KV. To study the morphology of TPS/CF composite films, the fracture surfaces of the specimens are studied by SEM. The fracture surfaces of all the specimens are coated with gold by using a plasma sputter (Ted Pella Inc.)

Also, the distribution of nanoparticles of SNP films is studied by SEM (TESCAN VEGA3) with an acceleration voltage of 15 KV. Three samples of each kind of films were prepared for SEM.

### 4.5.2 Fourier transform infrared spectroscopy (FTIR)

FTIR analysis is performed to study the effect of modification on the structures of fibers by THERMO NICOLET 6700. Three kinds of fibers are studied by FTIR, pure cellulose fibers, air plasma treated fibers for 30 minutes and 1 hour. Ten samples are prepared for each of these three kinds. So, FTIR analysis is performed for these samples. Finally, ten figures combined together and one figure is the conclusion of the results for each type of samples, something like the average of the figures. This average is done by FTIR software automatically.

Also, FTIR analysis is studied for comparing the chemical structure of SNP films which were prepared by different methods.

### 4.5.3 X-ray diffraction (XRD)

X-ray Diffraction (XRD) patterns of pure cellulose, air plasma treated cellulose for 30 min and 1 hour were obtained on a BURKER D8 DISCOVER equipped with X'celerator using Cu K $\alpha$  radiation. The patterns were recorded on the prepared films at 45 kV and 40 mA. The pattern was taken over a range of  $2\theta$  from  $10^\circ$  to  $70^\circ$  with a step size of  $0.01^\circ$ . The crystallinity of TPS/CF composites and TPS biopolymer are obtained by X-ray diffractometer in the diffraction angles range  $2\theta = 5^\circ$  and  $60^\circ$ , using Cu K $\alpha$  radiation wavelength of  $1.540\text{\AA}$  with 99 seconds time per step and step size of  $0.025^\circ$ . The specimens are located in the sample holder, and analysis is performed in a static mode. Also, XRD is used to study the crystalline structure of SNP films and to have a comparison among the prepared films. Furthermore, the effect of produced nanoparticles is studied by XRD.

#### 4.5.4 Thermogravimetric analysis (TGA)

Thermogravimetric analysis is carried out to evaluate the degradation characteristics of the TPS and TPS/CF composites. The thermal stability of each specimen is specified by using a thermogravimetric analyzer (TA instruments TGA 2950), in a nitrogen environment with a heating rate of  $10^\circ\text{C}/\text{min}$  from ambient temperature to  $600^\circ\text{C}$ .

To evaluate the thermal properties of SNP films, TGA analysis is done in a nitrogen environment with a heating rate of  $10^\circ\text{C}/\text{min}$  from ambient temperature to  $600^\circ\text{C}$  for SNP films as well. The obtained results is gathered on a figure for precise comparison.

#### 4.5.5 Atomic force microscopy (AFM)

The surface topography of the prepared SNP films are studied by AFM. An Atomic Force Microscope (1M Plus, JPK Instruments, Germany) was used to image the samples. Images were obtained in dynamic mode using a Micromasch NSC 14/AIBS cantilever with nominal spring constant of  $1.75\text{ N/m}$ .

#### 4.5.6 Contact angle

As it is clear, neat thermoplastic starch film is hydrophilic. The hydrophilicity nature of starch limits its application in the industry specifically in food packaging. One of the main objective of the SNP production is to improve the hydrophobicity of TPS. Hence, the

water contact angle of the prepared SNP films were measured by the sessile drop method [55] in a NRL A-100-00 RAME-HART Goniometer. The contact angle value was measured in both sides of the drop profile for 10 seconds, acquiring 100 points which were then averaged. This was repeated at least 5 times for each sample.

## 5 RESULTS AND DISCUSSION

### 5.1 Thermoplastic starch based composite reinforced by cellulose fibers

#### 5.1.1 Morphology of cellulose fibers

SEM micrograph of untreated cellulose fibers is demonstrated in Figure 21 a-d. As it might be seen, the surface of untreated cellulose fibers is without any significant damage. It can be observed in Figure 21e and f that the surface of fibers after air plasma treatment becomes rougher and there are many micro-holes on the surface of the fibers. Actually, the smooth surface of the fibers is modified to the porous surface. This etching can be related to the preferential etching of the hemicellulose in relation to the etching of crystalline cellulose as already observed before by (JAMALI & EVANS, 2011) when treating natural fibers. Hence, this is the main reason for improving the adhesion between fibers and matrix which dues to the improvement of mechanical properties of TPS/CF composite compared to TPS polymer.

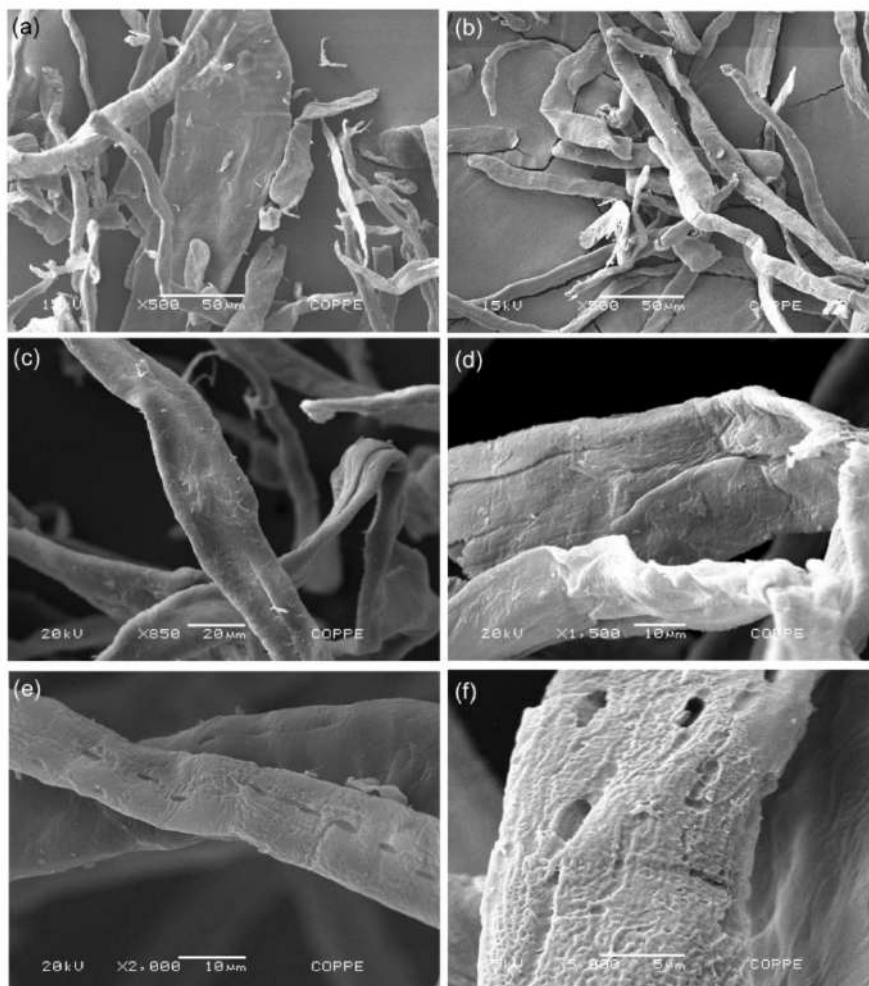


Figure 21. SEM of pure cellulose fibers (a, b, c, d), plasma-treated cellulose fibers (e, f).

### 5.1.2 Fourier transform infrared spectroscopy (FT-IR)

The FTIR spectrum of the cellulose fibers before and after air plasma treatment is demonstrated in Figure 22. Both spectra are very much similar, indicating that no major fiber modification is accomplished by plasma. The peaks in the range of 2820–2900  $\text{cm}^{-1}$  are corresponding to symmetric vibration and antisymmetric of  $\text{CH}_2$  groups. The prevailing spectral band at 1040 and 3340  $\text{cm}^{-1}$  are results of stretching vibrations of C-O ether and OH groups. The region of 1639–1648  $\text{cm}^{-1}$  is due to O-H bending of adsorbed water. The other peaks perceived in the range of 890–895  $\text{cm}^{-1}$  with enhanced sharpness is related to cellulosic-glycosidic linkages,  $\sim 1048 \text{ cm}^{-1}$  associates to C-O-C pyranose ring stretching vibration in cellulose,  $\sim 1317 \text{ cm}^{-1}$  presents  $\text{CH}_2$  wagging, 1367–1374  $\text{cm}^{-1}$  represents C-H bending and 1405–1418  $\text{cm}^{-1}$  is owing to  $\text{CH}_2$  scissoring motion in cellulose. Correspondingly, peaks at 1155–1160  $\text{cm}^{-1}$  demonstrates C-C ring stretching band. Furthermore, a new peak at 1,540  $\text{cm}^{-1}$  which illustrated  $\text{COO}^-$  stretching vibrations, owing to plasma surface oxidation, is perceived in Figure 22. Moreover, a shoulder at 1716  $\text{cm}^{-1}$  (related to the ester groups) (HEREDIA-GUERRERO *et al.*, 2014) is observed after air plasma treatment on cellulose fibers. It is illustrated that bombardment of air plasma on the cellulose fibers provides the starting of chemical reactions and results in a change of chemical composition of the cellulose, i.e. enhance of hydrophilic groups like  $\text{COO}^-$ , OH and C=O and that can improve hydrophilicity of the fibers (SHUJUN *et al.*, 2006, TAO *et al.*, 2007, SAHARI & SAPUAN % \_ REV, 2011, MARTINS *et al.*, 2009).

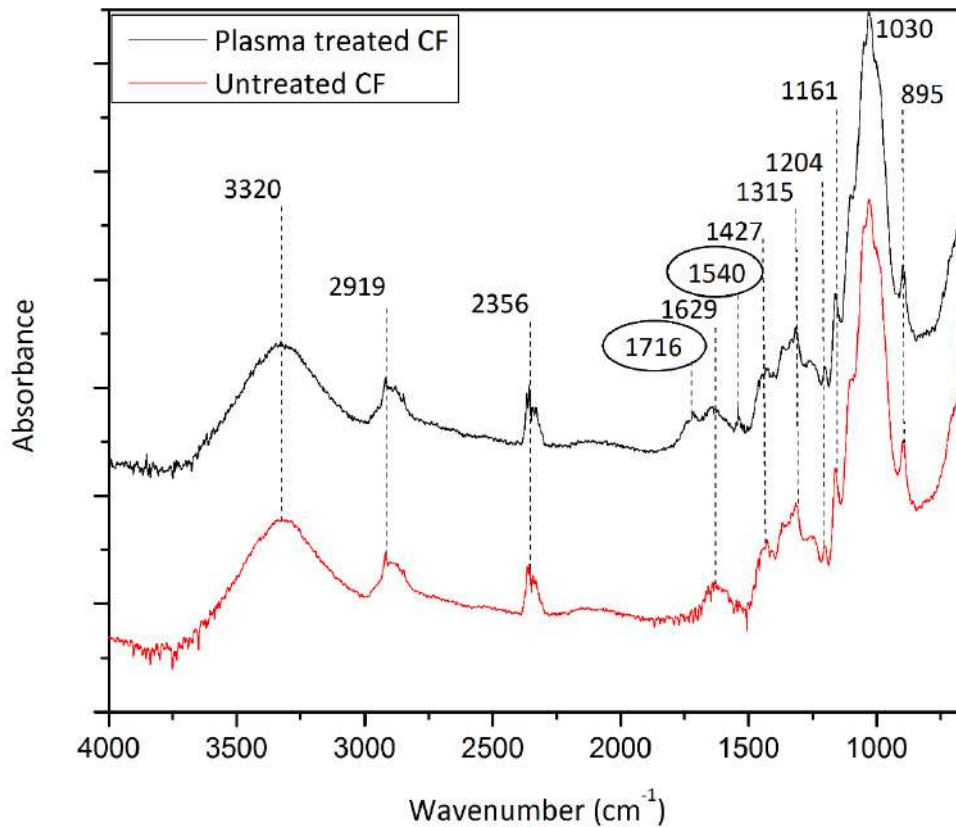


Figure 22. FTIR spectrum of plasma treated and untreated cellulose fibers.

### 5.1.3 Thermogravimetric analysis (TGA)

Figure 23a demonstrates thermogravimetric analysis curves of the neat TPS, TPS/UCF 6 wt% and TPS/PCF 6 wt%. The matrix and cellulose reinforced composites illustrate the identical decomposition trends at different stages of treatment. Also, Figure 24 shows the first derivative thermogravimetric (DTG) curves of the same samples as well. The first steps of analysis of the specimens happened at temperatures below 100 °C, which indicates the loss of compounds with low molecular weights and also water. The most important decomposition happened at nearly 250-350 °C, indicating the decomposition of glycerol and cellulose. The similar outcomes are also reported by Kargarzadeh et al. (2017), who said that glycerol and cellulose nanocrystals started to decompose at temperatures above 190 °C. The thermal consistency of the composite reinforced by PCFs is enhanced as compared to that of the neat thermoplastic starch and the TPS/UCF. The decomposition temperature of the TPS/PCF modified to a higher temperature compared to the TPS and TPS/UCF. According to Figure 24, the principal decomposition temperature of the neat TPS is almost 260 °C, inasmuch as the decomposition temperature

obtained by the TPS/PCF 6 wt% raised to approximately 284 °C. Also, the recorded decomposition temperature of the TPS and TPS/UCF 6 wt% are each almost 245 °C. The achieved outcomes are ascribed to this fact that the PCF compounded into the thermoplastic starch matrix interfaced strongly, making decomposition of the biocomposite arduous. Hence, better thermal stability is attained with PCF as the reinforcement.

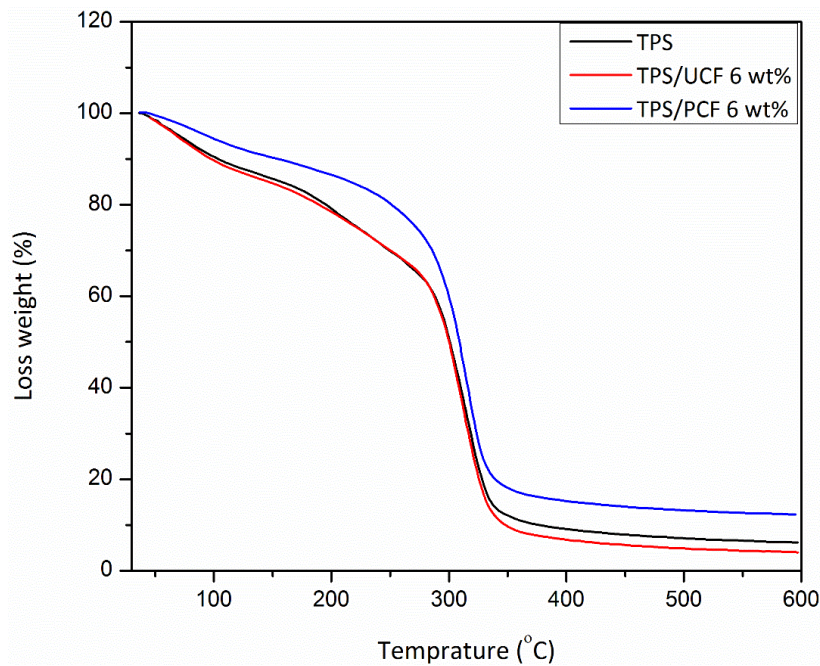


Figure 23. TGA curves for TPS, composites containing untreated fibers (TPS/UCF) 6 wt% and composites containing plasma treated fibers (TPS/PCF) 6 wt%.

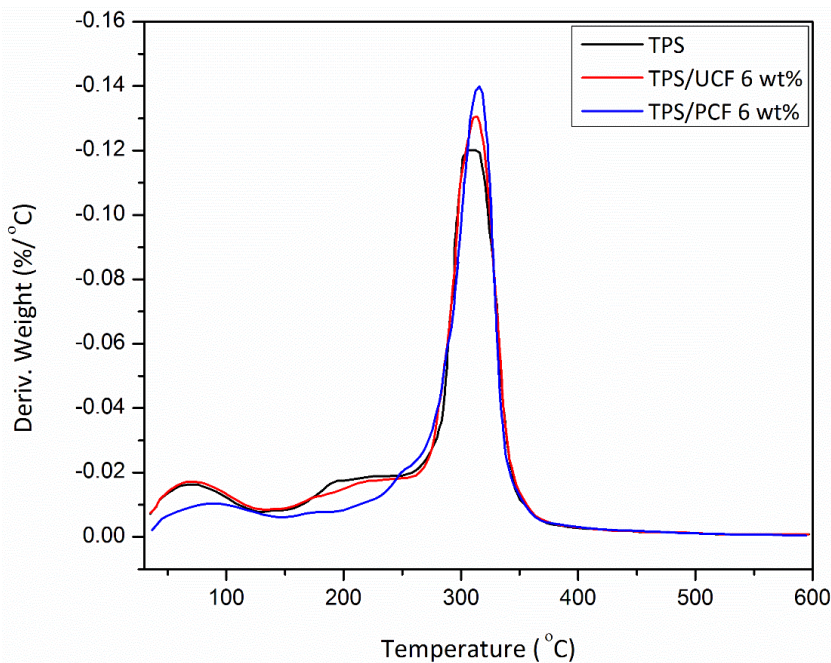


Figure 24. DTG for TPS, composites containing untreated fibers (TPS/UCF) 6 wt% and composites containing plasma treated fibers (TPS/PCF) 6 wt%.

#### 5.1.4 X-ray diffraction (XRD)

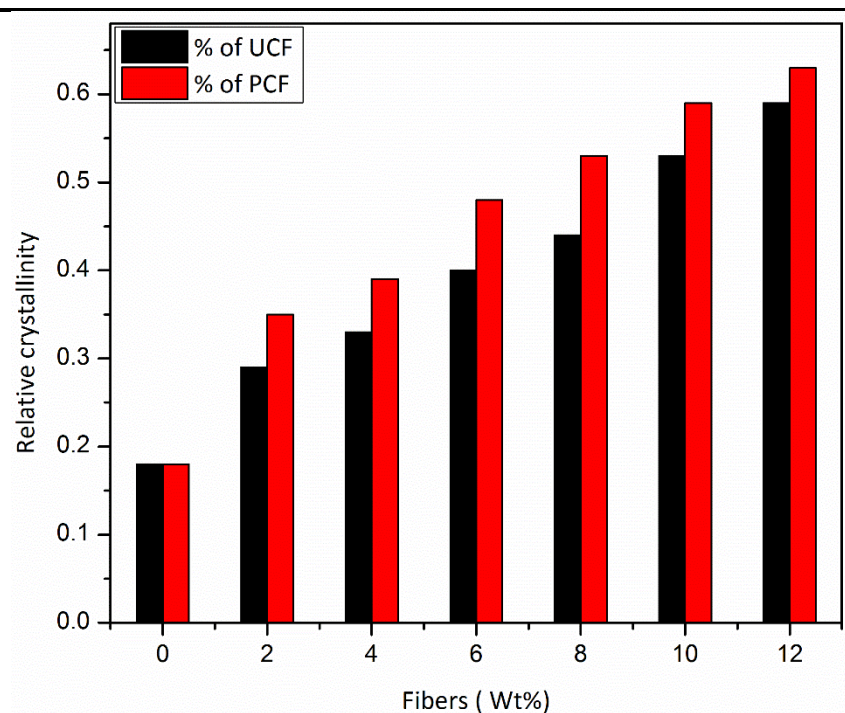
XRD profile of neat TPS and TPS/UCF composites are shown in Figure 25. The starch granules include crystalline lamellae and intermittent amorphous in which two principal ingredients, amylopectin, and amylose are embedded. The amylose, which is the linear polymer, separates of the granule and crystallizes into various single helical molecular structures when starch granules are broken by heat and shear force during hot compression and high friction processes. A broad peak centered on  $19^\circ$  demonstrates that TPS film is fully amorphous (KAUSHIK *et al.*, 2010). This fact proves that the crystalline regions of the starch granules have vanished during the fabrication processes. The intensity of the peaks at  $16.8^\circ$  and  $22.5^\circ$  enhances with the increase of the cellulose fibers quantity before plasma treatment. This affirms the crystalline structure of the cellulose fibers and also the crystallinity of starch during the fabrication processes.

TPS and TPS/PCF composites gave distinct diffractograms in XRD diagram which are shown in Figure 26. TPS has a semi-crystalline structure with the prevalent peaks of A-type crystals ( $2\theta \sim 15^\circ, 17.0\text{--}18^\circ, 20^\circ$  and  $24^\circ$ ) (VAN SOEST *et al.*, 1996). The crystallinity is disappeared during the high friction and hot compression processes leading to diffractograms representing a broad amorphous peak with no significant remaining A-type crystallinity. The outcomes illustrate that the granule structure is destroyed by the processes of high friction and hot compression. Some small peaks are detected around  $2\theta \sim 12.0^\circ, 17.5^\circ$ , and  $20^\circ$ , which are characteristic for the crystallographic parameters of  $V_H$ -type crystals for restructured starch (VAN SOEST *et al.*, 1996). For the TPS/PCF samples, a typical cellulose type 1 profile (KLEMM *et al.*, 2005) is gained, demonstrating that the crystallinity of the gelatinized starch overlaps with the cellulose fibers. The distinct peaks at  $2\theta = 14.7^\circ, 16.3^\circ, 22.6^\circ$  and  $34.7^\circ$  in Figure 26 for composites correspond to the planes of (101),  $(10\bar{1})$ , (002) and (040). The high percentage of crystallinity in plasma treated cellulose fibers is obvious in Figure 26. As can be seen, the percentage of crystallinity in TPS/PCF increases by increasing the percentage of PCF in composite film and the increase is slightly higher for composites produced with plasma treated fibers. Table 1 shows the relative crystallinity of all samples prepared for this project. As can be seen, the crystallinity percentage of composites reinforced by untreated cellulose fibers and plasma treated cellulose fibers increased from 18% to 53% and, to 63% respectively. The obtained results are comparable to other works. Müller *et al.* reported 53% of crystallinity for maximum loading of cellulose fibers

in TPS as well (MÜLLER *et al.*, 2009). The crystallinity percent of the prepared composites is calculated by Origin 2016.

Table 5. Relative crystallinity of thermoplastic starch and its biocomposites with untreated cellulose fibers and plasma treated cellulose fibers.

Fibers (wt%)	Relative crystallinity
TPS	0.18±0.05
TPS/UCF 2wt%	0.29±0.05
TPS/UCF 4wt%	0.33±0.05
TPS/UCF 6wt%	0.40±0.05
TPS/UCF 8wt%	0.44±0.05
TPS/UCF 10wt%	0.53±0.05
TPS/UCF 12wt%	0.59±0.05
TPS/PCF 2wt%	0.35±0.05
TPS/PCF 4wt%	0.39±0.05
TPS/PCF 6wt%	0.48±0.05
TPS/PCF 8wt%	0.53±0.05
TPS/PCF 10wt%	0.59±0.05
TPS/PCF 12wt%	0.63±0.05



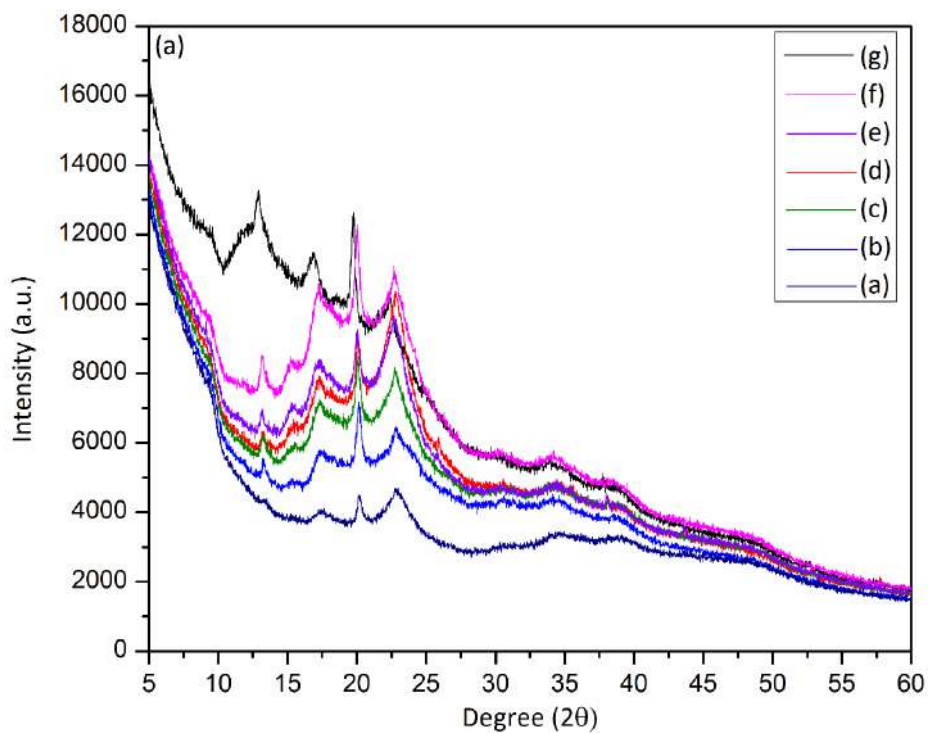


Figure 25. XRD pattern of (a) TPS, (b) TPS/UCF 2wt%, (c) TPS/UCF 4wt%, (d) TPS/UCF 6wt%, (e) TPS/UCF 8wt%, (f) TPS/UCF 10wt% and (g) TPS/UCF 12wt%.

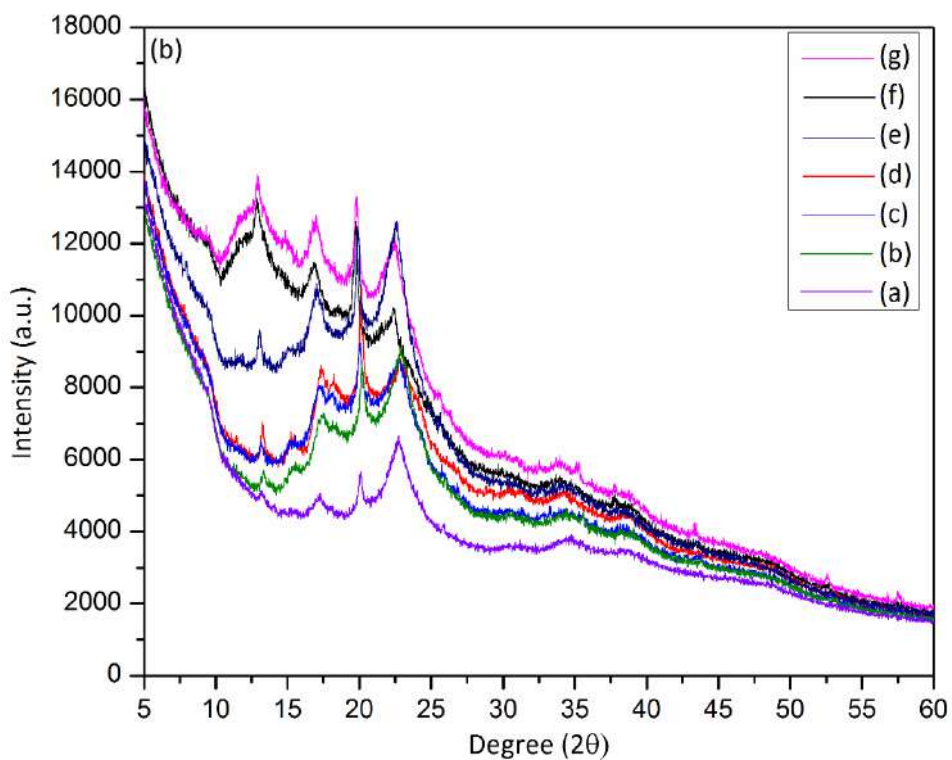


Figure 26. XRD pattern of (a) TPS, (b) TPS/PCF 2wt%, (c) TPS/PCF 4wt%, (d) TPS/PCF 6wt%, (e) TPS/PCF 8wt%, (f) TPS/PCF 10wt% and (g) TPS/PCF 12wt%.

### 5.1.5 Mechanical properties of the composites

Stress-strain diagrams are gained for TPS/UCF (untreated cellulose fibers), TPS/PCF (plasma treated cellulose fibers) and thermoplastic starch samples. Young's modulus, elongation at break and tensile strength have been calculated from the obtained diagrams. As can be seen in Figure 27, the tensile strength result achieved for neat TPS sample is 1.24 MPa and addition of CF, either untreated CF or plasma treated CF, enhances the tensile strength of the samples. Tensile strength increases with enhancement of untreated and plasma treated CF volume up to 6 wt%. The betterment of that for TPS/UCF is almost 63% and for TPS/PCF is approximately 78%. Furthermore, the tensile strength of TPS/CF 8 wt% and 12 wt% (2.19 MPa and 2.09 MPa for UCF and 4.79 MPa and 3.71 MPa for PCF, respectively) are decreased in comparison with TPS/CF 6 wt%. In addition, in Figure 28, elongation at break point reduces for TPS/UCF and TPS/PCF 6 wt% of fibers. Moreover, the elongation at break rises for TPS/UCF and TPS/PCF 8 wt% and 12 wt%. Figure 29 demonstrates Young's modulus values of the above-mentioned samples. As it is obvious in the diagram, Young's modulus result of TPS is 19.93 MPa. Young's modulus of the samples improves by adding UCF and PCF. It increases by raising of UCF and PCF volume up to 6 wt%. The enhancement of Young's modulus for the mentioned samples is approximately 56% for TPS/UCF and 66% for TPS/PCF as well. Contrarily, Young's modulus of TPS/UCF and TPS/PCF 8 wt% and 12 wt% are reduced in comparison with TPS/UCF and TPS/PCF 6 wt%. The mechanical properties of all samples affirmed that ideal concentration of cellulose fibers is 6% and the surplus of CF quantity induces particles agglomeration or phase separation of cellulose fibers in the starch matrices. Above this volume of reinforcement phase, it results deterioration of the mechanical properties of the biocomposites. Actually, cellulose fibers as reinforcement phase improve the Young modulus of the matrices with no significant gain in tensile strength. It is important to note that the quantity of the reinforcement plays a significant role in the fabrication of the biocomposite films. Müller et al. (MÜLLER *et al.*, 2009) studied the effect of cellulose fibers as reinforcement on the mechanical properties of TPS films as well. The maximum Young's modulus and tensile strength of the composite films in mentioned work are 52.6 and 2.5 MPa, respectively. In addition, the minimum elongation at break measured in above-mentioned work is approximately 26%. As discussed above, the values for Young's modulus, tensile strength, and elongation at break afforded by this study, are 58.05 MPa, 5.62 MPa, and 9.2%.

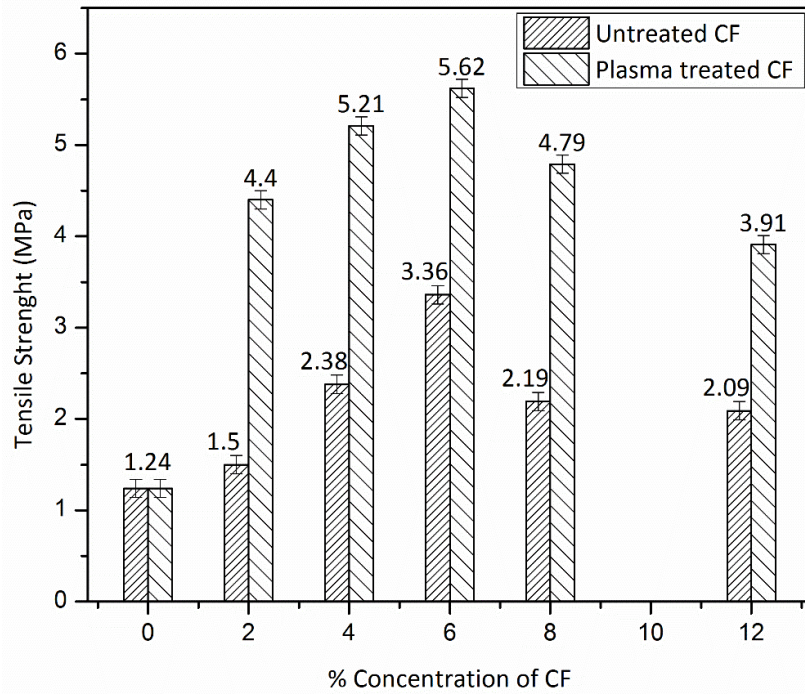


Figure 27. Tensile strength of TPS, TPS/UCF and TPS/PCF biocomposite films.

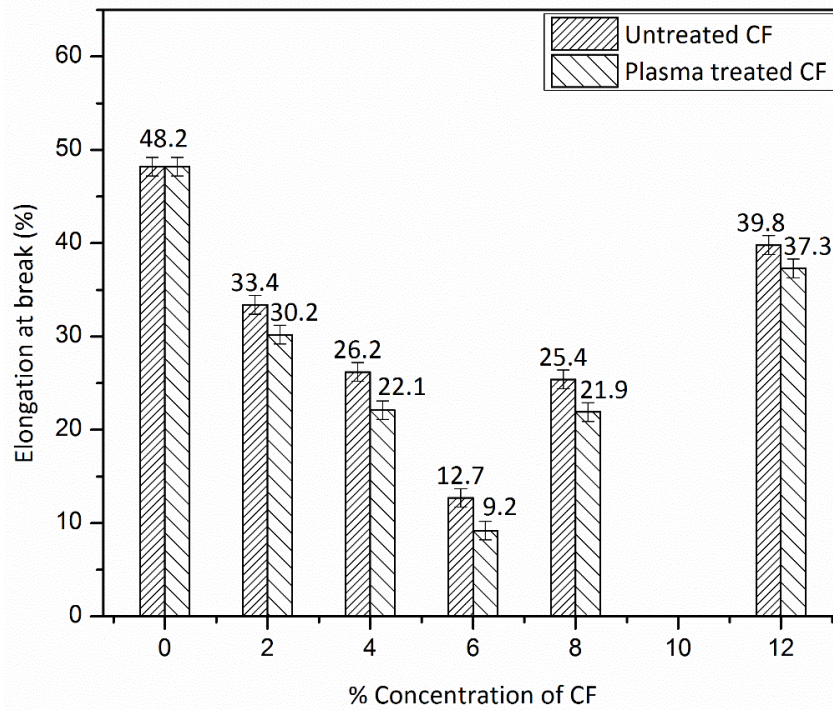


Figure 28. Elongation at Break of TPS, TPS/UCF and TPS/PCF biocomposite films.

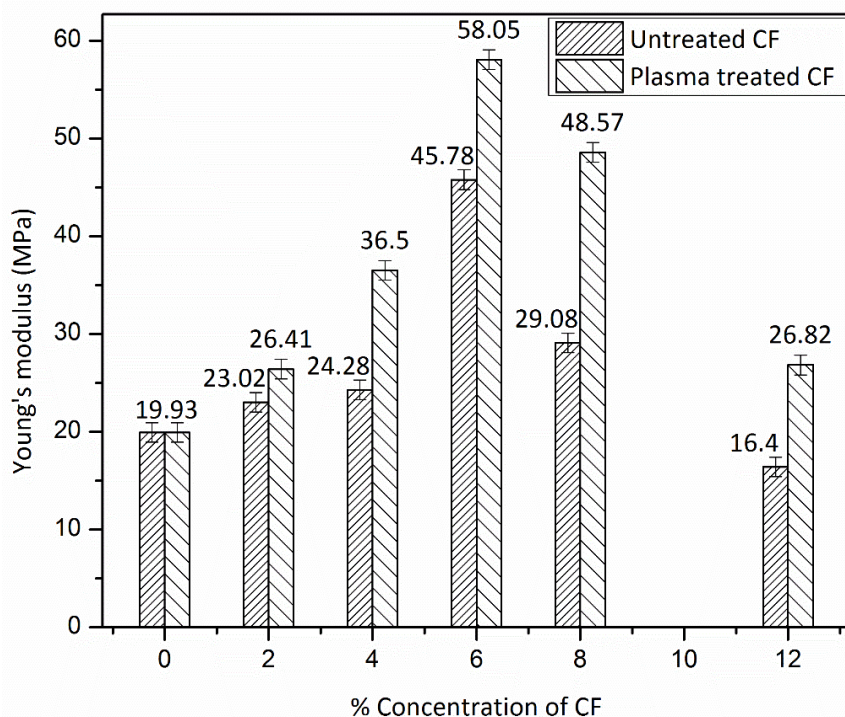


Figure 29. Young's modulus of TPS, TPS/UCF and TPS/PCF biocomposite films.

#### 5.1.6 SEM analysis of composites

Figure 30a demonstrates the fracture surface of the composite with untreated fibers as reinforcement. It is obvious in the image that there are no proper adhesions among fibers and matrix. The red arrows show the created track of the fibers because of weak adhesions among fibers and thermoplastic starch matrix. Hence, this weakness in adhesion between reinforcement and matrix dues to poor mechanical properties of the composite. Figure 30b shows the adhesion of air plasma treated fiber to TPS matrix. As can be seen, the melted polymer cover the surface of fiber completely and this phenomenon makes a strong composite and perfect adhesion between fiber and matrix which causes to acceptable mechanical properties. Therefore, the fracture in composite occurs because of yielding in fibers not the lack of good adhesion between fiber and matrix. Figure 30c also illustrates the fracture surface of the composite with untreated cellulose fibers as reinforcement. As seen clearly, there is a gap between the surface of fiber and matrix which is the main reason for poor adhesion among cellulose fibers and TPS and it results in the poor mechanical properties. Figure 30d demonstrates the agglomerated regions of the plasma-treated cellulose fibers in TPS/PCF 12 wt%. These agglomerated cellulose fibers diminish the cohesion of the fibers to the matrix. It may be the most possible reason

for the deterioration of mechanical properties above 6 wt% CF for TPS/CF biocomposite films.

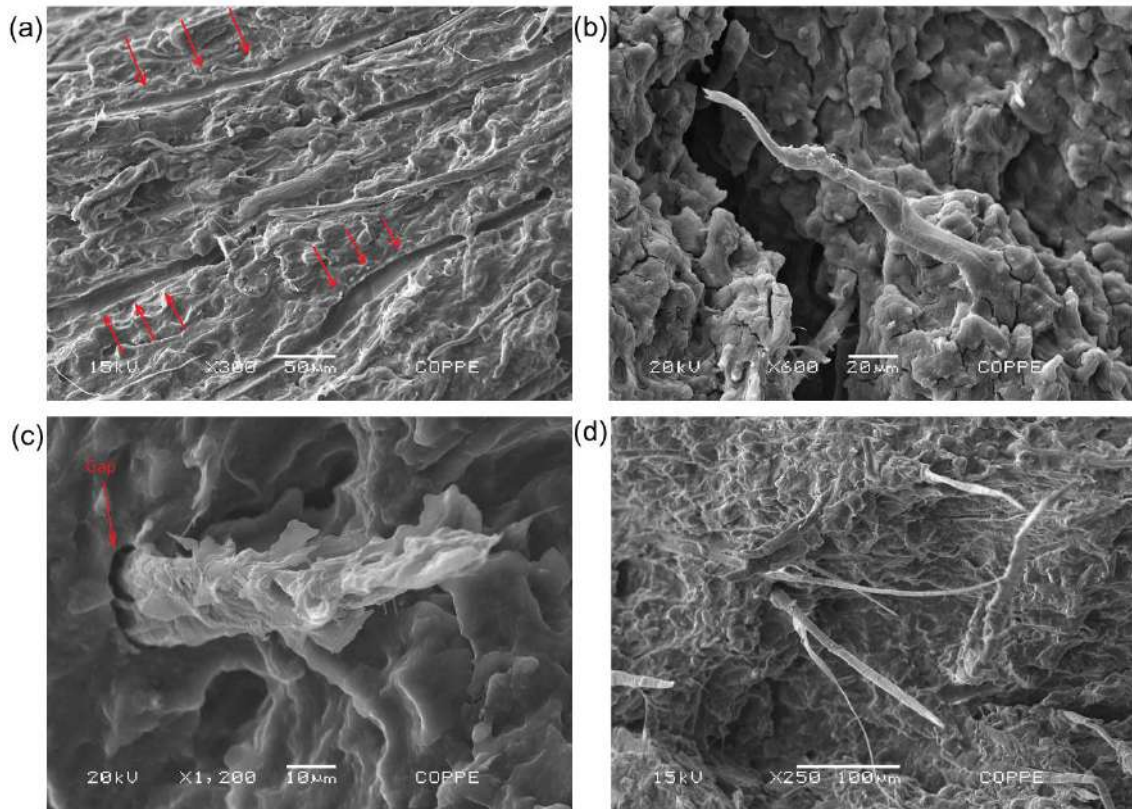


Figure 30. Microstructure of fracture surfaces of TPS/UCF 6 wt% (a, c), TPS/PCF 6 wt% (b), and TPS/PCF 12 wt% (d).

## 5.2 Thermoplastic Starch reinforced by starch nanoparticles

### 5.2.1 Dynamic mechanical analysis (DMA) of SNP films

Figure 31, 32 and 33 show the  $\tan \delta$ , the storage modulus ( $E'$ ) and loss modulus ( $E''$ ), respectively as function of the temperature of the prepared materials. Most of the polymeric samples do not exhibit the same property at different temperatures. Therefore, this test was carried out to understand the mechanical behavior of the polymer composites while they are subjected to different temperatures rather than room temperature. Storage modulus is a measure of stiffness of a polymeric composite (GHANBARI *et al.*, 2018). Figure 32 shows the storage modulus versus temperature of different SNP films at a frequency of 1 Hz. From the graph, it is clear that SNP1 shows the minimum storage modulus values, as SNP1 offers low degree of stiffness. However, considerable enhancements of storage modulus are noticed for all SNPs under probed temperature

range. Improvements in stiffness of all SNP films were observed, ascribed to high stiffness behavior of starch nanoparticles which can effectively constrain movement of TPS polymeric chains.

Loss modulus is regarded as a viscous response of the materials and can be measured as energy loss under stress or deformation as heat/cycle (JAWAID *et al.*, 2015, JIANG *et al.*, 2012). From Figure 32, it is apparent that the loss modulus also displays very similar trend with the storage modulus having variation of starch nanoparticles in prepared films. The loss modulus of the films increased with increasing glycerol content and duration of gelatinization across the entire temperature range investigated. Among all samples, SNP2 film showed the highest value of loss modulus as compared to others. The synergic increases in loss modulus for SNP2 resemble perfect homogeneous distribution, dispersion and good physical interaction between starch nanoparticles and the TPS matrix. The results could be ascribed to the formation of the films after evaporation of the water and ethanol and the formation of sufficient starch nanoparticles in the film (BABAEE *et al.*, 2015). As mentioned earlier, the formed nanoparticles restricted the molecular chains movement of the TPS, thereby improving its thermal stability (PETERSSON & OKSMAN, 2006).

The variation of damping factor ( $\tan \delta$ ) with the variation of temperature for different composite systems is shown in Figure 31. The damping factor specifies the elastic or viscous properties of a system and its peak height is related to the internal energy dissipation of the film (JAWAID *et al.*, 2015). The plasticized SNP films show relatively higher  $\tan \delta$  peak height, as the incorporation of nanoparticles considerably increases the viscoelastic damping factor of the TPS. An increase in the  $\tan \delta$  value with temperature indicates that the films were becoming more viscous after raising the temperature. The results confirmed an improvement in dynamic mechanical properties of the SNP films compared to neat TPS. The increase in storage modulus, together with a positive shift in the  $\tan \delta$  peak for the SNP film could be due to the strong chemical interaction between the matrix and the nanoparticles that restricted the segmental mobility of the polymer chains in the vicinity of the nano-reinforcements (BONDESON *et al.*, 2007).

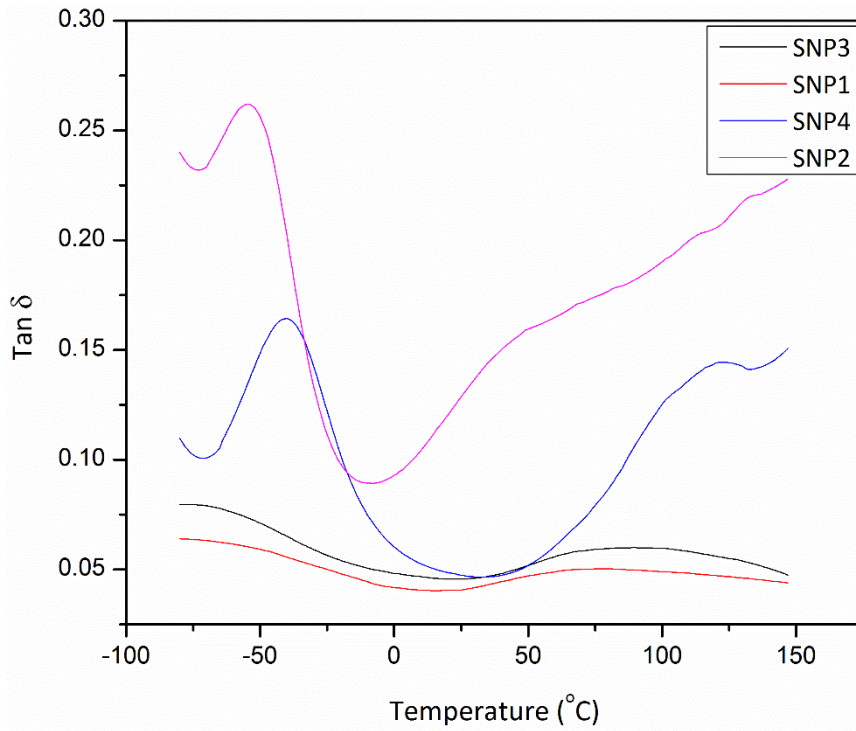


Figure 31. Loss factor ( $\tan \delta$ ) – temperature curves of SNP films.

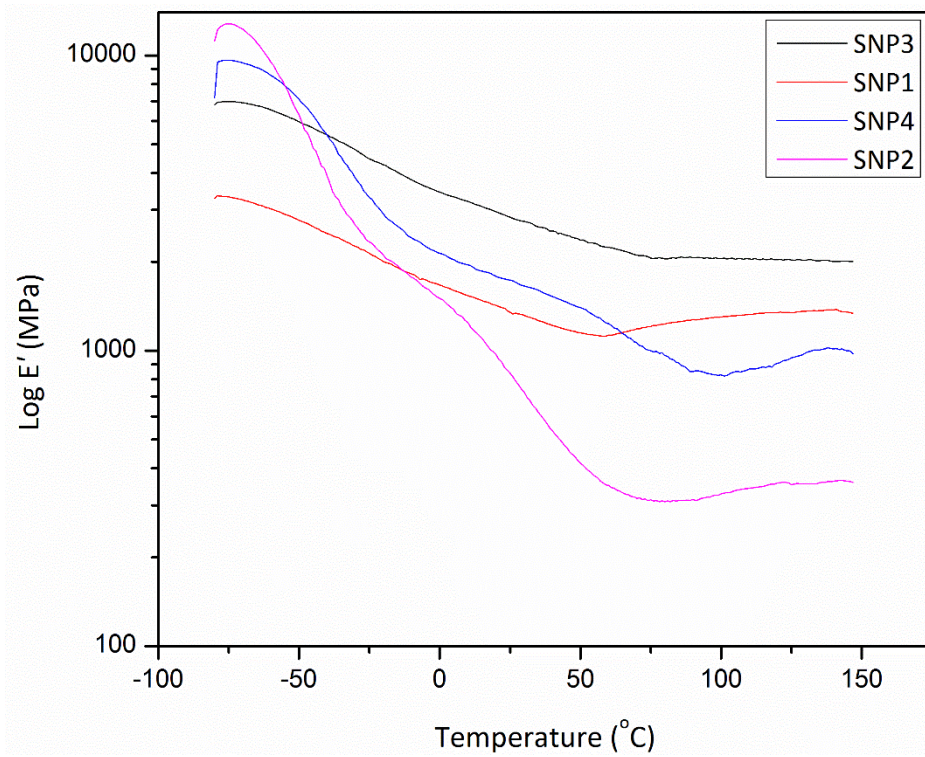


Figure 32. Storage modulus of SNP films.

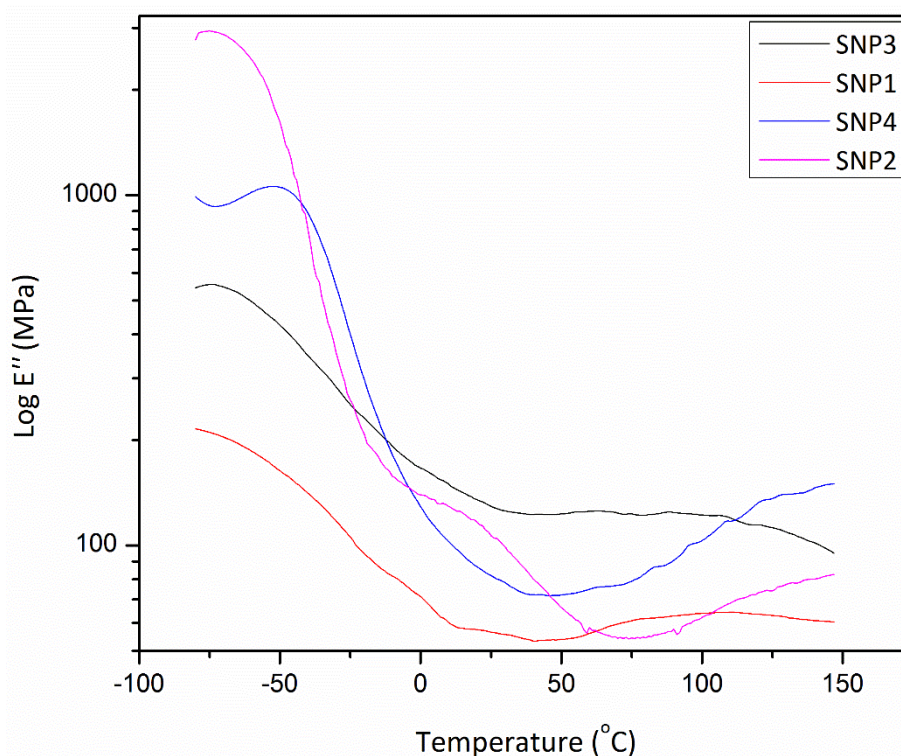


Figure 33. Loss modulus of SNP films.

### 5.2.2 Fourier transform infrared spectroscopy (FT-IR) of SNP films

The miscibility of the components in the prepared films can be assessed by verifying the displacements of the absorption peaks in the infrared in relation to the wavenumber due to the interactions between functional groups. Figure 34 showed the FTIR spectra of the SNP films. The characteristic peak occurred at  $1650\text{ cm}^{-1}$ , which Ma et al. (MA *et al.*, 2008) believed to be a feature of tightly bound water present in the starch. The absorption bands between  $1000$  and  $1200\text{ cm}^{-1}$  were characteristic of the  $\text{-C-O-}$  stretching on polysaccharide skeleton. The peak at  $2920\text{ cm}^{-1}$  is associated with asymmetric C-H stretching. The spectra presents a similarity to the study illustrated by Akrami et al. (AKRAMI *et al.*, 2016), which describes a broad peak in the region of  $3000$  and  $3500\text{ cm}^{-1}$  corresponding to the vibration of the hydroxyl groups deformations associated to intermolecular hydrogen bonds. At  $1641\text{ cm}^{-1}$ , the peak is attributed to the angular deformation of O-H ( $\text{H}_2\text{O}$ ). The peaks  $1415$  and  $1338\text{ cm}^{-1}$  refer to the angular deformation of the C-H bond. The set of peaks between  $900$  and  $1150\text{ cm}^{-1}$  are attributed to the stretching of C-O bonds with C-C (C-O-C glycosidic bonds) contributions. REIS et al. (REIS *et al.*, 2008) also confirmed the main peaks observed for the starch sample.

Generally, an increase in the intensity of the peaks with the increase of the glycerol is observed, being able to be attributed to the interactions of the glycerol with the starch. The plasticizer has a low molecular weight and enters the starch helices by de-structuring the intermolecular bonds. The main differences of the peaks between plasticized starch samples (TPS) with different glycerol contents are in  $3276\text{ cm}^{-1}$  peak indicating changes in the hydrogen bond pattern of the TPS (starch/Glycerol) polymer. Another difference between the samples is the intensity of the peak at  $990\text{ cm}^{-1}$ , related to the angular deformation of the C-O-C glycosidic bonds.

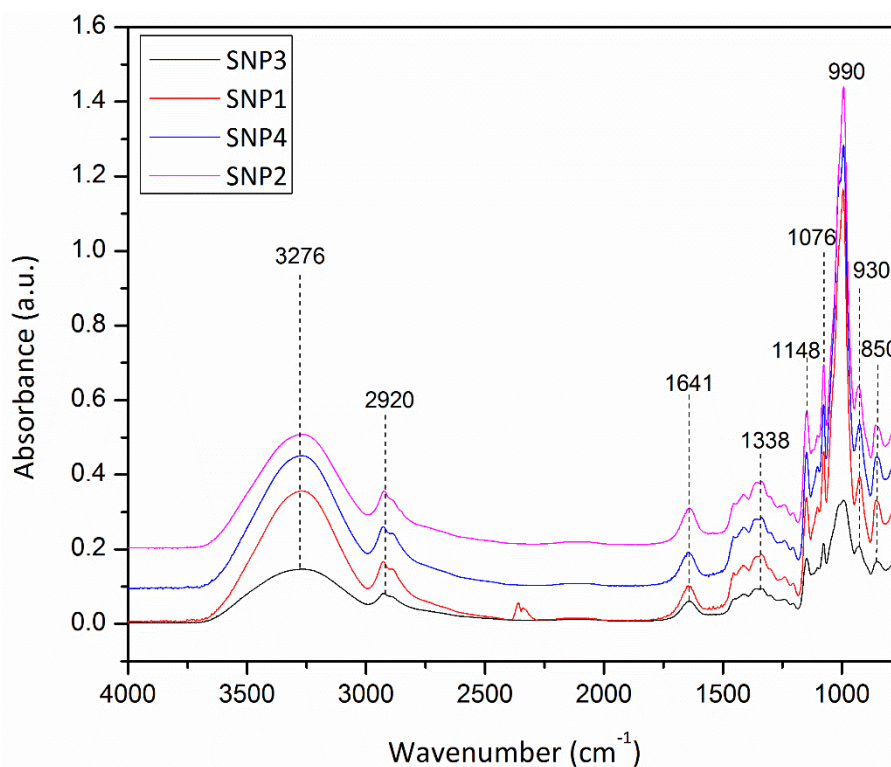


Figure 34. FT-IR curves of SNP films.

### 5.2.3 Crystalline properties of SNP films

Figure 35 illustrates the XRD diffraction pattern of the prepared films. As we know, native corn starch possessed the A-style crystallinity. In SNP, the  $V_H$ -style crystallinity (Figure 35), which was different from A-style crystallinity in corn starch, could originate from a single-helical structure “inclusion complex” made up of amylose and plasticizer. The similar  $V_H$ -style crystallinity also appeared in the plasticized corn starch. When ethanol was delivered dropwise to starch-paste solution, gelatinized starch nanoparticles

were precipitated. Therefore, the gelatinization destroyed A-style crystallinity of corn starch, and starch nanoparticles exhibited the V<sub>H</sub>-style crystallinity.

The crystallinity of the starch nanoparticles significantly reduced relative to native starch granules. These results suggest that the homogenization possibly impacted the arrangement of the double helical strands of the starch chains in the starch nanoparticles, because XRD analysis can detect the long-range order crystalline structure of starch granules such as the ordered packing of double helices (SEVENOU *et al.*, 2002, WILSON *et al.*, 1987).

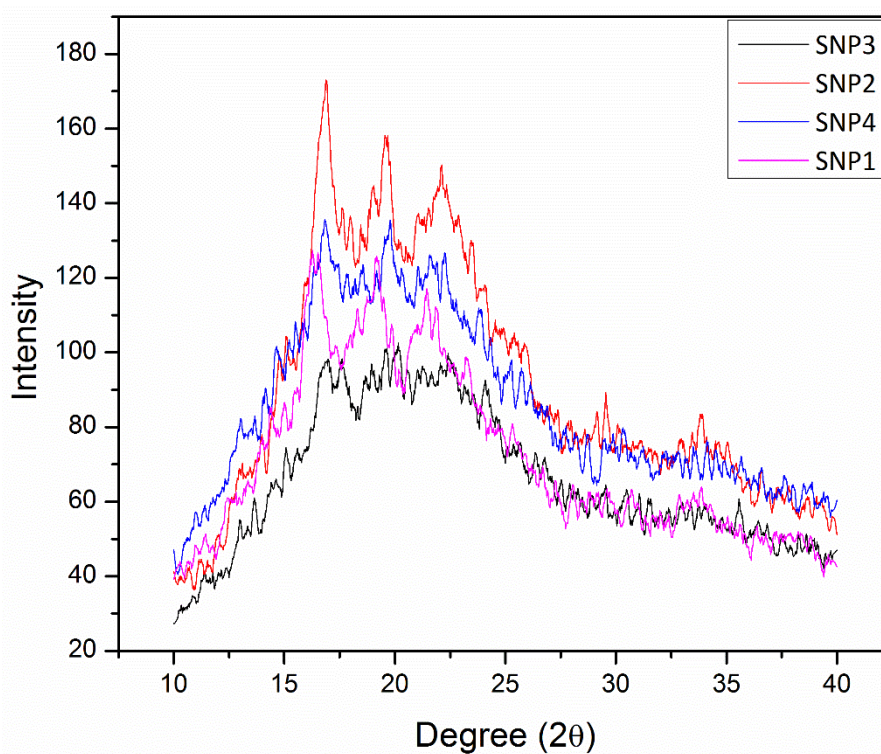


Figure 35. X-ray diffraction of SNP films.

#### 5.2.4 Thermogravimetric analysis (TGA) of SNP films

Figure 36 demonstrates thermogravimetric analysis curves of the SNP films. Also, figure 37 shows the first derivative thermogravimetric (DTG) curves of the same samples as well. The thermogravimetric analysis curves of the SNP films showed three degradation stages: 1) the mass loss attributed to the dehydration between 50 °C and 120 °C; 2) the degradation stage of the starch-rich phase of the film between 260 °C to 400 °C (MONTERO *et al.*, 2017). The starch nanoparticles increased thermal stability as is seen in figure 37. The thermal stability increases even more by elevating the percentage of the

nanoparticles from SNP1 to SNP2. The mass loss in the glycerol-rich phase area was also a little bit lower for the films with higher nanoparticles contents which indicates less free glycerol chains. The thermal stability increased significantly by increasing the glycerol content and gelatinization time.

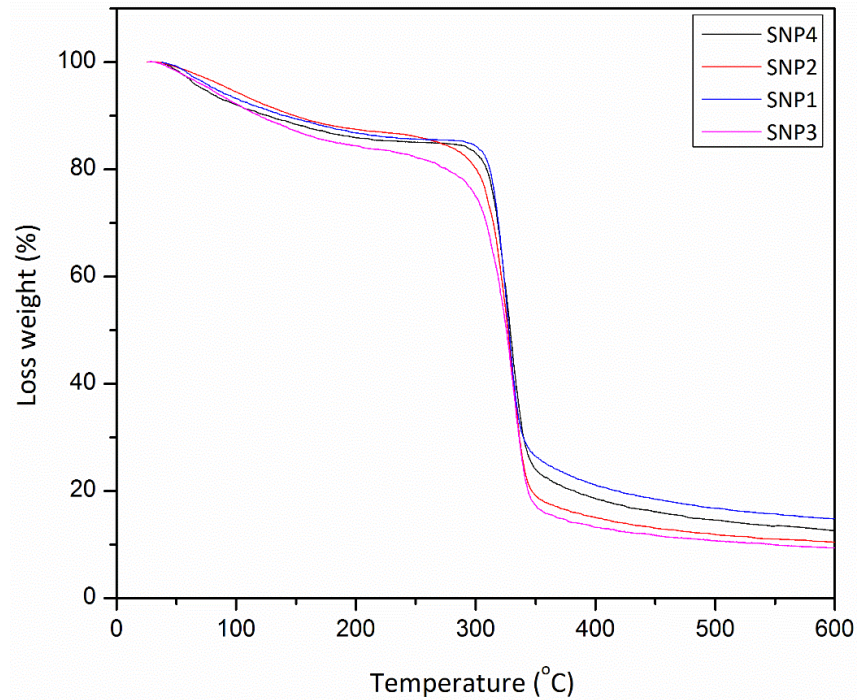


Figure 36. Thermogravimetric analysis (TGA) curves of SNP films.

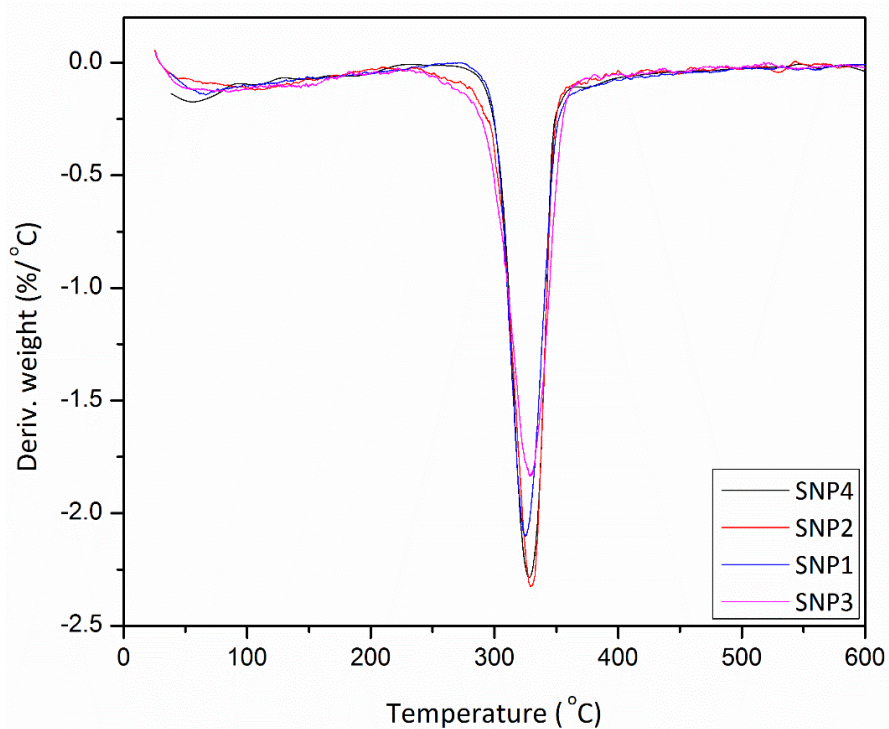


Figure 37. Derivative thermogravimetric (DTG) of SNP films.

### 5.2.5 Scanning electron microscopy (SEM) of SNP films

In the processing of SNP, native granular corn starch was gelatinized in water and formed starch paste. The preparation of SNP in water by dropwise addition of ethanol resulted in the nanoparticles (figure 38). Most of SNP possessed sizes in the range from 50 to 300 nm. It was known that the stability of the nanoparticle suspensions was important prerequisites for preparing these novel nanoparticles. The interaction of hydrogen bond between starch nanoparticles and starch paste played the important role on the stability of the precipitated nanoparticles in the suspension. The interaction of nanoparticles and ethanol seemed to decrease the aggregation of nanoparticles and large particles of starch reduced in Figure 38c. As shown in Figure 38d, no residual granular structure of corn starch was observed in the continuous phase. At the high temperature, water, and glycerol were known to physically break up the granules of corn starch and disrupt intermolecular and intramolecular hydrogen bonds and make the native starch plastic. The distribution of the nanoparticles in the polymer matrix is shown in Figure 38b. Starch nanoparticles was dispersed well in the film matrix and without obvious aggregation, which was attributed to the strong interaction because of chemical similarities between ethanol and cornstarch in film matrix. The quantity of nanoparticles for SNP3 sample decreased in comparison to the other prepared films (Figure 38). The reason might be the duration of gelatinization for SNP3 sample which was 30 min. As it can be seen, more nanoparticles can be found in the surface of SNP2 because of the long duration of gelatinization, glycerol content and addition of ethanol for 2 times in the process.

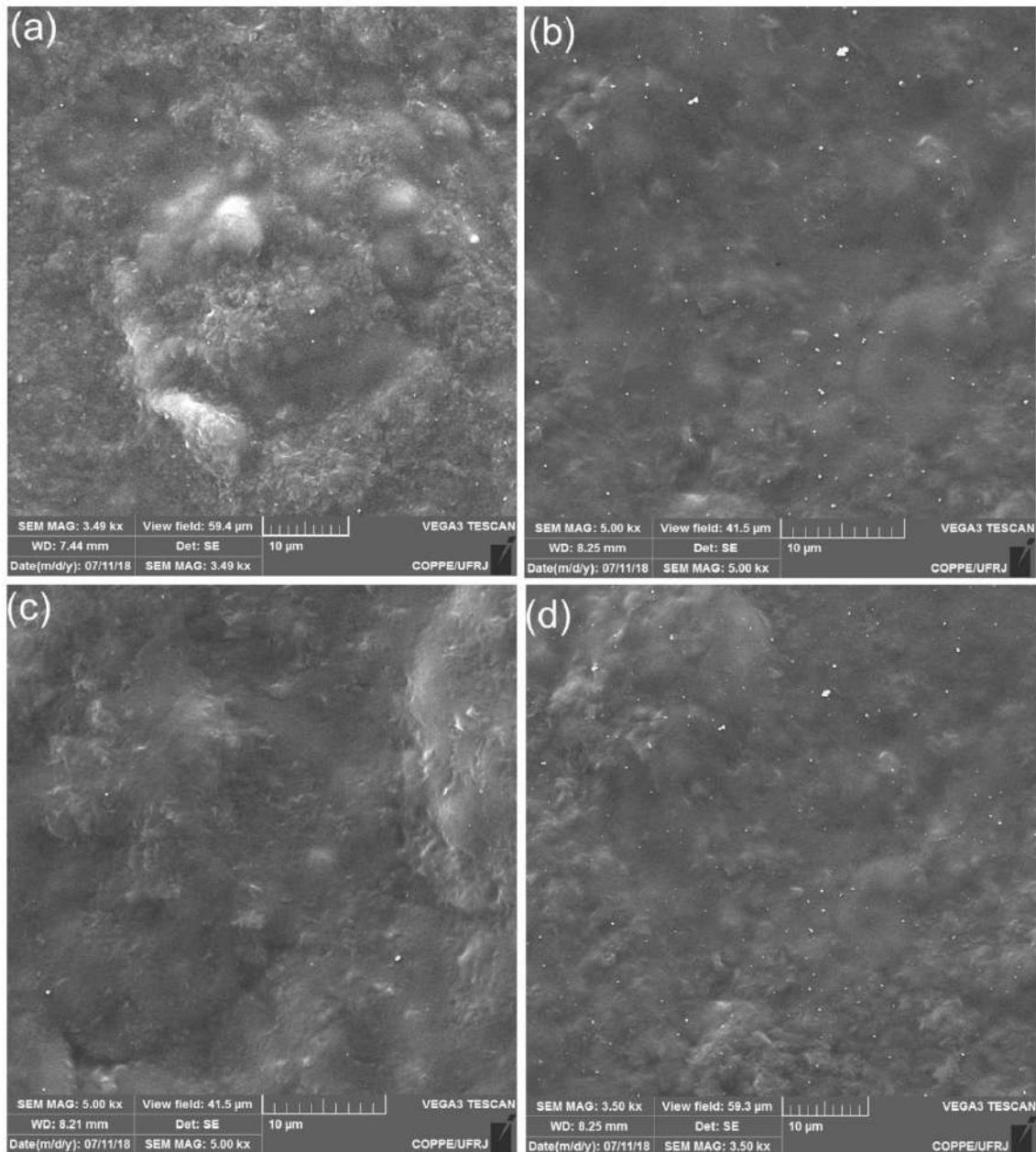


Figure 38. Scanning electron microscopy (SEM) of (a) SNP1, (b) SNP2, (c) SNP3, and (d) SNP4.

### 5.2.6 Topography of SNP films

The qualitative (morphology) and quantitative (roughness) parameters of the films were analyzed by AFM. It was used to examine the dispersion of SNPs in the starch matrix. As shown Figure 39, the dark zones are holes and rich in starch, whereas the brighter zones are protruded and rich in starch nanoparticles or aggregates. There is a relatively sharp contrast between starch and SNP phases. The control film presented a uniform and smoother surface across the area. The surface roughness increased and the uniformity of the nanocomposite films decreased as a result of SNP incorporation. This is in agreement

with the findings of Diaz-Visurraga et al. (DÍAZ-VISURRAGA *et al.*, 2010) and Zhou et al. (ZHOU *et al.*, 2009). Diaz-Visurraga et al. (DÍAZ-VISURRAGA *et al.*, 2010) who stated that the random dispersion of starch nanoparticles in the starch film matrix increased the film surface roughness. Furthermore, based on the results of the present study, it seems that low hydrophilicity of starch in comparison to the film components could be another probable reason for the tendency of starch nanoparticles to the external part of the starch film, giving rise to the surface roughness.

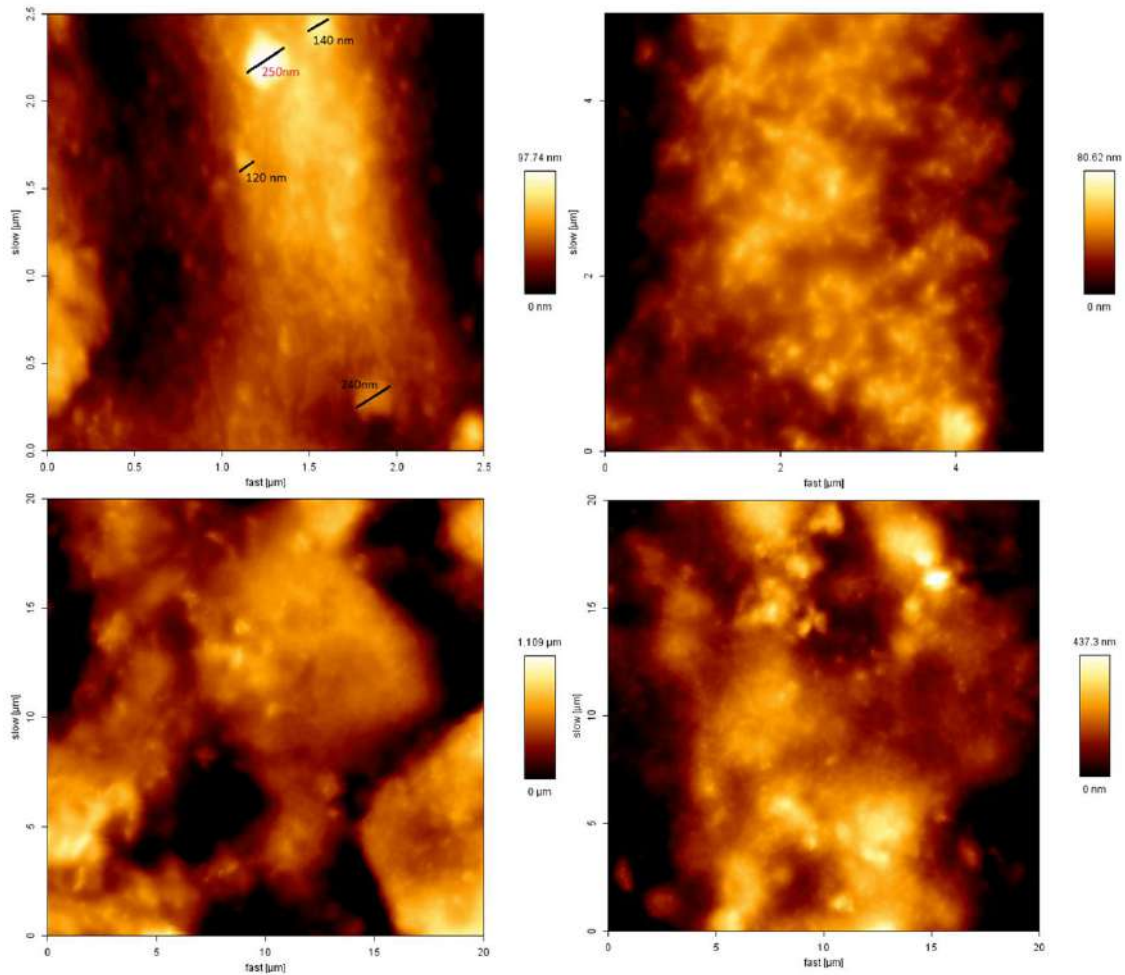


Figure 39. Atomic force microscopy (AFM) of (a) SNP1, (b) SNP2, (c) SNP3, and (d) SNP4.

### 5.2.7 Water contact angle of SNP films

Starch is a kind of polysaccharide which is formed by polymerization of glucose molecules, and it has good hydrophilicity. Thus, for the SNP films, the hydrophilic properties should be reduced to the utmost. One method to compare the hydrophilicity of starch films surfaces is the determination of the contact angle (CA) of

water droplet on the surfaces (NAFCHI *et al.*, 2012). A low contact angle indicates better hydrophilicity of the surface and vice versa. The CA value of SNP films are presented in Figure 40. As can be seen from Figure 40, the SNP films have significantly higher CA value compared to the starch-only films. These results indicate greater hydrophobicity of the SNP films compared to the starch-only films. Figure 40 also shows that increasing the time of gelatinization and glycerol content of the films leads to greater contact angle (the CA value were 90, 100, 71, and 85 responding to SNP1, SNP2, SNP3 and SNP4, respectively), indicating that the hydrophobicity of the SNP films significantly increased with the increase of gelatinization time and glycerol concentration. These results indicate that there is a strong interaction between starch and nanoparticles.

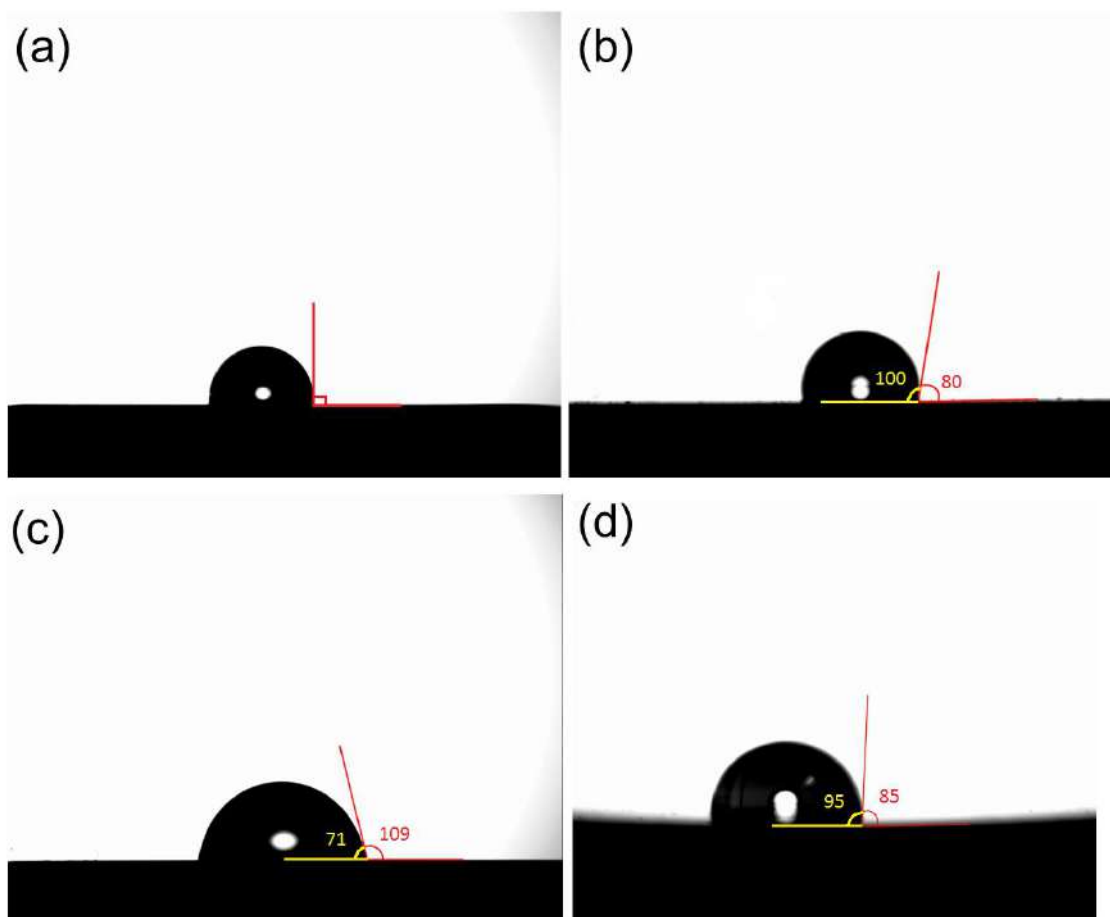


Figure 40. Contact angle images of (a) SNP1, (b) SNP2, (c) SNP3, and (d) SNP4.

Figure 41 demonstrates that the contact angle of SNP3 decreases by the time and it means that the water droplet is absorbing to the surface of the film. However, for the SNP1, SNP2, and SNP4, the reduction rate of contact angle decreased. This means that increase in gelatinization time and glycerol content leads to stabilization of the water droplet on

the surface of the mentioned film. So, the rate of the water absorption on the surface of SNP film decreased compared to neat starch.

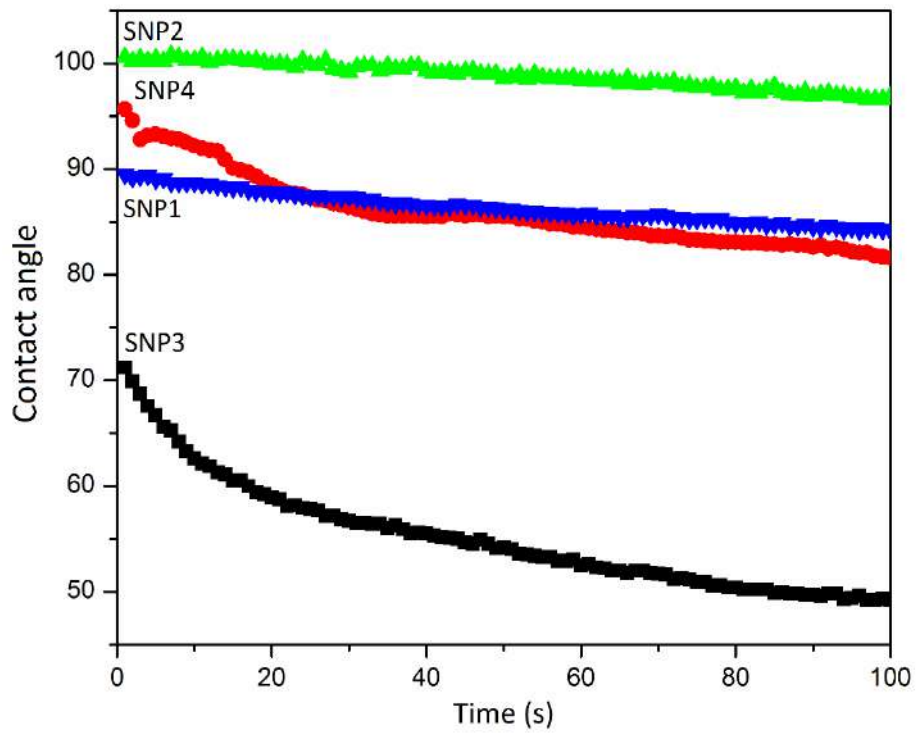


Figure 41. Contact angle measurements of (a) SNP1, (b) SNP2, (c) SNP3, and (d) SNP4.

## 6 CONCLUSION

The considerable plasma modification is carried out on the surface of the cellulose fibers successfully. The low-pressure air plasma treatment of the cellulose fibers has resulted in partially etching and ablation of the amorphous regions. The mentioned phenomena have enhanced the roughness of the surfaces and, also it has led to the growth of crystalline regions of the cellulose fibers. The results of SEM demonstrated the great interaction among fibers and TPS matrices after air plasma treatment. Also, it is obvious that after plasma treatment, the fibers have the stronger interaction with the matrix. By analyzing the neat TPS film and TPS/CF composites, it is clear that the mechanical properties of the composites are improved in comparison with TPS film. Thermogravimetric analysis demonstrated that an important decomposition has happened at almost 250-350 °C, showing the decomposition of glycerol and cellulose. FTIR proved that after air plasma treatment on the surface of cellulose fiber, there is a new peak at 1,540  $\text{cm}^{-1}$  which represented  $\text{COO}^-$  stretching vibrations, due to plasma surface oxidation and also, a shoulder at 1716  $\text{cm}^{-1}$  which is related to the ester groups interacting by H bonds.

On the other hand, for the SNP films, the addition of the glycerol and also alcohol for two times (once during the gelatinization and another after the process in room temperature), resulted in better mechanical behavior obtained by DMA. Also, the crystallinity of the SNP films increased for SNP2 film which is demonstrated by X-ray diffraction. Furthermore, AFM and SEM showed the enhancement of starch nanoparticles on the surface of SNP film for SNP2 sample, because the precipitation of nanoparticles during the addition of alcohol while the solution was gelatinizing. The distribution and the content of nanoparticles on the surface of the films decreases when the alcohol did not add to the solution during the gelatinization. FT-IR showed an increase in the intensity of the peaks with the increase of the glycerol, being able to be attributed to the interactions of the glycerol with the starch. The main differences of the peaks between plasticized starch samples (TPS) with different glycerol contents are in 3276  $\text{cm}^{-1}$  peak indicating changes in the hydrogen bond pattern of the TPS (starch/glycerol) polymer. Another difference between the samples is the intensity of the peak at 990  $\text{cm}^{-1}$ , related to the angular deformation of the C-O-C glycosidic bonds. TGA proved that the thermal stability increased significantly by increasing the glycerol content and gelatinization time. Water contact angle analysis showed significant results of the hydrophobicity of the surfaces of the films. It is demonstrated that the maximum contact angle obtained by

goniometer is  $100^\circ$  which is considerable for food packaging application. Also, the other measured contact angle resulted in  $90^\circ$ ,  $85^\circ$ , and  $71^\circ$  for SNP1, SNP4, and SNP3, respectively. These obtained results are so high in comparison with neat TPS films prepared so by simple gelatinization.

## 7 SUGGESTIONS FOR FUTURE WORKS

According to some results obtained for the plasma-treated fibers in the final of the project, the author suggests to other researchers who are interested in this area to characterize the prepared cellulose nanofibers by ultrasonic treatment. Actually, after the plasma treatment, we changed the surface characterization of modified fibers by ultrasonic treatment for 30 minutes in alcoholic solution. The obtained results were fantastic. We observed the cellulose nanofibers by SEM. Other researchers can continue this method to extract cellulose nanofibers from neat cellulose and fabricate the mentioned biocomposite in the text. The SEM images of cellulose nanofibers extracted by this method is demonstrated in Figure 42.

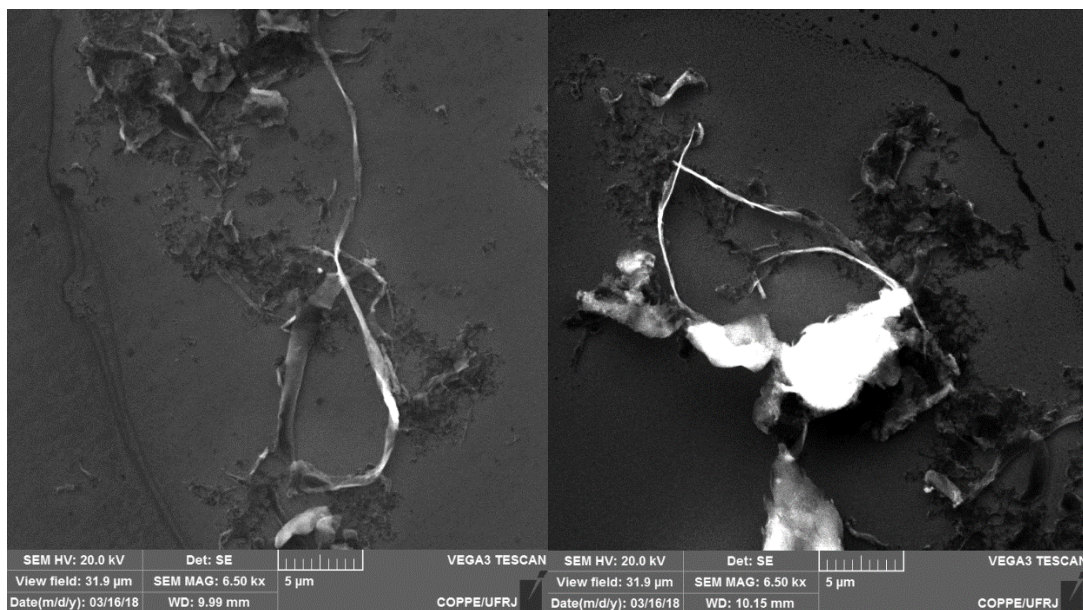


Figure 42. SEM images of the extracted cellulose nanofibers by plasma and ultrasonic treatments.

## 8 REFERENCES

- AGRAWALA, S., RAJAMANI, R.K., SONGFACK, P., et al., 1997, "Mechanics of media motion in tumbling mills with 3d discrete element method". In: *Minerals Engineering*. v. 10, pp. 215–227.
- AKRAMI, M., GHASEMI, I., AZIZI, H., et al., 2016, "A new approach in compatibilization of the poly(lactic acid)/thermoplastic starch (PLA/TPS) blends". In: *Carbohydrate Polymers*. v. 144, pp. 254–262.
- ALAIN, D., DANIELE, D., MICHEL, R.V., 2000, "Cellulose microfibrils from potato tuber cells: Processing and characterization of starch-cellulose microfibril composites". In: *Journal of Applied Polymer Science*. v. 76, pp. 2080–2092.
- ALILA, S., BOUFI, S., 2009, "Removal of organic pollutants from water by modified cellulose fibres". In: *Industrial Crops and Products*. v. 30, pp. 93–104.
- ANGELLIER, H., MOLINA-BOISSEAU, S., DOLE, P., et al., 2006, "Thermoplastic starch-waxy maize starch nanocrystals nanocomposites.". In: *Biomacromolecules*. v. 7, pp. 531–539.
- ANGLES, M.N., VIGNON, M.R., DUFRESNE, A., 2000a, "Plasticized starch and cellulose whiskers composites.". In: *Materiaux & Techniques (Paris)*. v. 88, pp. 59–61.
- ANGLES, M.N., VIGNON, M.R., DUFRESNE, A., 2000b. "Processing and characterization of plasticized starch/tunicin whiskers nanocomposite materials.". In: *Nat. Polym. Compos., [Proc. Third Int. Symp., Workshop Prog. Prod. Process. Cellul. Fibres Nat. Polym.]*. S.l.: s.n. 2000. pp. 206–211.
- ATICHOKUDOMCHAI, N., VARAVINIT, S., 2003, "Characterization and utilization of acid-modified cross-linked Tapioca starch in pharmaceutical tablets". In: *Carbohydrate Polymers*. v. 53, pp. 263–270.
- AYRILMIS, N., ASHORI, A., 2014, "LIGNOCELLULOSIC FIBERS AND NANOCELLULOSE AS REINFORCING FILLER IN THERMOPLASTIC COMPOSITES". In: *Eurasscience Journals Eurasian Journal of Forest Science*. v. 2, pp. 1–6.
- AZIZI SAMIR, M.A.S., ALLOIN, F., DUFRESNE, A., 2005. "Review of recent research into cellulosic whiskers, their properties and their application in nanocomposite field". . 2005. S.l.: s.n.

- BABAEI, M., JONOBI, M., HAMZEH, Y., et al., 2015, "Biodegradability and mechanical properties of reinforced starch nanocomposites using cellulose nanofibers". In: *Carbohydrate Polymers*. v. 132, pp. 1–8.
- BARARI, B., ELLINGHAM, T.K., GHAMHIA, I.I., et al., 2016, "Mechanical characterization of scalable cellulose nano-fiber based composites made using liquid composite molding process". In: *Composites Part B: Engineering*. v. 84, pp. 277–284.
- BASTIOLI, C., MAGISTRALI, P., GESTI GARCIA, S., 2012, "Starch in polymers technology". In: *ACS Symposium Series*. v. 1114, pp. 87–112.
- BASTOS, D.C., SANTOS, A.E.F., DA FONSECA, M.D., et al., 2013, "Inducing surface hydrophobization on cornstarch film by SF<sub>6</sub> and HMDSO plasma treatment". In: *Carbohydrate Polymers*. v. 91, pp. 675–681.
- BEL HAAJ, S., MAGNIN, A., PÉTRIER, C., et al., 2013, "Starch nanoparticles formation via high power ultrasonication". In: *Carbohydrate Polymers*. v. 92, pp. 1625–1632.
- BHATTACHARYA, D., GERMINARIO, L.T., WINTER, W.T., 2008, "Isolation, preparation and characterization of cellulose microfibrils obtained from bagasse". In: *Carbohydrate Polymers*. v. 73, pp. 371–377.
- BJORKMAN, A., SALMEN, L., 2000, "Studies on solid wood. II. The influence of chemical modifications on viscoelastic properties". In: *Cellulose Chemistry and Technology*. v. 34, pp. 7–20.
- BLEDZKI, A.K., FRANCISZCZAK, P., OSMAN, Z., et al., 2015, "Polypropylene biocomposites reinforced with softwood, abaca, jute, and kenaf fibers". In: *Industrial Crops and Products*. v. 70, pp. 91–99.
- BOGDANOWICZ, R., 2008, "Investigation of H<sub>2</sub>:CH<sub>4</sub> plasma composition by means of spatially resolved optical spectroscopy". In: *Acta Physica Polonica A*. v. 114.
- BONDESON, D., SYRE, P., NISKA, K.O., 2007, "All Cellulose Nanocomposites Produced by Extrusion". In: *Journal of Biobased Materials and Bioenergy*. v. 1, pp. 367–371.
- BRACCO, G., HOLST, B., 2013, "Surface science techniques". In: *Springer Series in Surface Sciences*. v. 51.
- CARROW, J.K., GAHARWAR, A.K., 2015, "Bioinspired polymeric nanocomposites for regenerative medicine". In: *Macromolecular Chemistry and Physics*. v. 216,

- pp. 248–264.
- CARVALHO, D.M. DE, QUEIROZ, J.H. DE, COLODETTE, J.L., 2016, "Assessment of alkaline pretreatment for the production of bioethanol from eucalyptus, sugarcane bagasse and sugarcane straw". In: *Industrial Crops and Products*. v. 94, pp. 932–941.
- CÉLINO, A., FRÉOUR, S., JACQUEMIN, F., et al., 2014, "The hygroscopic behavior of plant fibers: a review". In: *Frontiers in Chemistry*. v. 1.
- CHEN, F.F., 1984. "Introduction To Plasma Physics (I)". In: *Introduction to Plasma Physics and Controlled Fusion, Volume 1: Plasma Physics*. S.l.: s.n. pp. 1–4.
- CHIN, S.F., MOHD YAZID, S.N.A., PANG, S.C., 2014, "Preparation and characterization of starch nanoparticles for controlled release of curcumin". In: *International Journal of Polymer Science*. v. 2014.
- CHODAK, I., 2004, "Improving the properties of polyolefin waste by reactive processing". In: *Polymer - Plastics Technology and Engineering*. v. 43, pp. 1769–1777.
- DEBIAGI, F., MELLO, L.R.P.F., MALI, S., 2017. "Thermoplastic Starch-Based Blends: Processing, Structural, and Final Properties". In: *Starch-Based Materials in Food Packaging: Processing, Characterization and Applications*. S.l.: s.n. pp. 153–186.
- DEMIRBAS, A., 2010. "Political Impacts of Biorefinery". In: *Biorefineries: For Biomass Upgrading Facilities*. S.l.: s.n. pp. 221–226.
- DESMORAT, R., 2009, "Décomposition de Kelvin et concept de contraintes effectives multiples pour les matériaux anisotropes". In: *Comptes Rendus - Mécanique*. v. 337, pp. 733–738.
- DÍAZ-VISURRAGA, J., MELÉNDREZ, M.F., GARCÍA, A., et al., 2010, "Semitransparent chitosan-TiO<sub>2</sub> nanotubes composite film for food package applications". In: *Journal of Applied Polymer Science*. v. 116, pp. 3503–3515.
- DING, Y., KAN, J., 2016, "Characterization of nanoscale retrograded starch prepared by a sonochemical method". In: *Starch/Staerke*. v. 68, pp. 264–273.
- DUFRESNE, A., 2006, "Comparing the Mechanical Properties of High Performances Polymer Nanocomposites from Biological Sources". In: *Journal of Nanoscience and Nanotechnology*. v. 6, pp. 322–330.

- DUFRESNE, A., 2013, "Nanocellulose: A new ageless bionanomaterial". In: *Materials Today*. v. 16, pp. 220–227.
- DUNCAN, T. V., 2011, "Applications of nanotechnology in food packaging and food safety: Barrier materials, antimicrobials and sensors". In: *Journal of Colloid and Interface Science*. v. 363, pp. 1–24.
- EBELING, T., PAILLET, M., BORSALI, R., et al., 1999, "Shear-induced orientation phenomena in suspensions of cellulose microcrystals, revealed by small angle X-ray scattering". In: *Langmuir*. v. 15, pp. 6123–6126.
- FAHMA, F., HORI, N., IWAMOTO, S., et al., 2016, "Cellulose nanowhiskers from sugar palm fibers". In: *Emirates Journal of Food and Agriculture*. v. 28, pp. 566–571.
- FARUK, O., BLEDZKI, A.K., FINK, H.P., et al., 2012. "Biocomposites reinforced with natural fibers: 2000-2010". . 2012. S.l.: s.n.
- FELEKOGLU, B., TOSUN, K., BARADAN, B., 2009, "A comparative study on the flexural performance of plasma treated polypropylene fiber reinforced cementitious composites". In: *Journal of Materials Processing Technology*. v. 209, pp. 5133–5144.
- FILPPONEN, I., ARGYROPOULOS, D.S., 2010, "Regular linking of cellulose nanocrystals via click chemistry: Synthesis and formation of cellulose nanoplatelet gels". In: *Biomacromolecules*. v. 11, pp. 1060–1066.
- FORNES, T., YOON, P., KESKKULA, H., et al., 2013, "Polymer Layered-Silicate Nanocomposites from Thermally Stable Trialkyl- Imidazolium Treated Montmorillonite". In: *Polymer Degradation and Stability*. v. 44, pp. 1–24.
- GARCIA, N.L., RIBBA, L., DUFRESNE, A., et al., 2009, "Physico-Mechanical properties of biodegradable starch nanocomposites". In: *Macromolecular Materials and Engineering*. v. 294, pp. 169–177.
- GAUTAM, S.P., BUNDELA, P.S., PANDEY, A K., et al., 2010, "A review on systematic study of cellulose". In: *Journal of Applied and Natural Science*2. v. 2, pp. 330–343.
- GEJO, G., KURUVILLA, J., BOUDENNE, A., et al., 2010, "Recent Advances in Green Composites". In: *Key Engineering Materials*. v. 425, pp. 107–166.
- GEORGE, J., SABAPATHI, S.N., 2015, "Cellulose nanocrystals: Synthesis, functional properties, and applications". In: *Nanotechnology, Science and Applications*. v. 8, pp. 45–54.

- GHANBARI, A., TABARSA, T., ASHORI, A., et al., 2018, "Thermoplastic starch foamed composites reinforced with cellulose nanofibers: Thermal and mechanical properties". In: *Carbohydrate Polymers*. v. 197, pp. 305–311.
- GONÇALVES, P.M., NOREÑA, C.P.Z., DA SILVEIRA, N.P., et al., 2014, "Characterization of starch nanoparticles obtained from *Araucaria angustifolia* seeds by acid hydrolysis and ultrasound". In: *LWT - Food Science and Technology*. v. 58, pp. 21–27.
- GUPTA, A., KUMAR, A., 2012, "Chemical properties of natural fiber composites and mechanisms of chemical modifications". In: *Asian Journal of Chemistry*. v. 24, pp. 1831–1836.
- GURNETT, D. A., BHATTACHARJEE, A., 2005, "Introduction to Plasma Physics". In: *Introduction to Plasma Physics, by D. A. Gurnett and A. Bhattacharjee*, pp. 462. ISBN 0521364833. Cambridge, UK: Cambridge University Press, January 2005.
- GURUNATHAN, T., MOHANTY, S., NAYAK, S.K., 2015. "A review of the recent developments in biocomposites based on natural fibres and their application perspectives". . 2015. S.l.: s.n.
- H.-Y., K., S.S., P., S.-T., L., 2015, "Preparation, characterization and utilization of starch nanoparticles". In: *Colloids and Surfaces B: Biointerfaces*. v. 126, pp. 607–620.
- HABIBI, Y., LUCIA, L.A., ROJAS, O.J., 2010, "Cellulose nanocrystals: Chemistry, self-assembly, and applications". In: *Chemical Reviews*. v. 110, pp. 3479–3500.
- HEBEISH, A., EL-RAFIE, M.H., EL-SHEIKH, M.A., et al., 2014, "Ultra-Fine Characteristics of Starch Nanoparticles Prepared Using Native Starch With and Without Surfactant". In: *Journal of Inorganic and Organometallic Polymers and Materials*. v. 24, pp. 515–524.
- HENRIKSSON, M., HENRIKSSON, G., BERGLUND, L.A., et al., 2007, "An environmentally friendly method for enzyme-assisted preparation of microfibrillated cellulose (MFC) nanofibers". In: *European Polymer Journal*. v. 43, pp. 3434–3441.
- HEPWORTH, D.G., HOBSON, R.N., BRUCE, D.M., et al., 2000, "Use of unretted hemp fibre in composite manufacture". In: *Composites Part A: Applied Science and Manufacturing*. v. 31, pp. 1279–1283.

- HEREDIA-GUERRERO, J.A., BENÁ-TEZ, J.J., DOMÁ-NGUEZ, E., et al., 2014, "Infrared and Raman spectroscopic features of plant cuticles: a review". In: *Frontiers in Plant Science*. v. 5.
- HIRAI, A., INUI, O., HORII, F., et al., 2009, "Phase separation behavior in aqueous suspensions of bacterial cellulose nanocrystals prepared by sulfuric acid treatment". In: *Langmuir*. v. 25, pp. 497–502.
- HIROTA, M., TAMURA, N., SAITO, T., et al., 2010, "Water dispersion of cellulose II nanocrystals prepared by TEMPO-mediated oxidation of mercerized cellulose at pH 4.8". In: *Cellulose*. v. 17, pp. 279–288.
- HONG, Y., LIU, G., GU, Z., 2015, "Preparation and characterization of hydrophilic debranched starch modified by pullulanase on swollen granule starch". In: *Food Research International*. v. 67, pp. 212–218.
- IMAI, T., SUGIYAMA, J., 1998, "Nanodomains of I<sub>α</sub> and I<sub>β</sub> Cellulose in Algal Microfibrils". In: *Macromolecules*. v. 31, pp. 6275–6279.
- IOELOVICH, M., 2009, "Accessibility and crystallinity of cellulose". In: *BioResources*. v. 4, pp. 1168–1177.
- ISOGAI, A., SAITO, T., FUKUZUMI, H., 2011. "TEMPO-oxidized cellulose nanofibers". . 2011. S.l.: s.n.
- JAMALI, A., EVANS, P.D., 2011, "Etching of wood surfaces by glow discharge plasma". In: *Wood Science and Technology*. v. 45, pp. 169–182.
- JAWAID, M., ALOTHMAN, O.Y., SABA, N., et al., 2015, "Effect of fibers treatment on dynamic mechanical and thermal properties of epoxy hybrid composites". In: *Polymer Composites*. v. 36, pp. 1669–1674.
- JIANG, W., JIN, F.L., PARK, S.J., 2012, "Thermo-mechanical behaviors of epoxy resins reinforced with nano-Al<sub>2</sub>O<sub>3</sub> particles". In: *Journal of Industrial and Engineering Chemistry*. v. 18, pp. 594–596.
- JIUGAO, Y., NING, W., XIAOFEI, M., 2005, "The effects of citric acid on the properties of thermoplastic starch plasticized by glycerol". In: *Starch/Staerke*. v. 57, pp. 494–504.
- JOHANSSON, L.S., CAMPBELL, J.M., KOLJONEN, K., et al., 1999, "Evaluation of surface lignin on cellulose fibers with XPS". In: *Applied Surface Science*. v. 144–145, pp. 92–95.
- JOHN, M.J., FRANCIS, B., VARUGHESE, K.T., et al., 2008, "Effect of chemical modification on properties of hybrid fiber biocomposites". In: *Composites Part*

- A: *Applied Science and Manufacturing*. v. 39, pp. 352–363.
- JOHN, M.J., THOMAS, S., 2012, *Natural polymers. Volume 1, Composites*. . S.l., s.n.
- KARGARZADEH, H., JOHAR, N., AHMAD, I., 2017, "Starch biocomposite film reinforced by multiscale rice husk fiber". In: *Composites Science and Technology*. v. 151, pp. 147–155.
- KAUSHIK, A., SINGH, M., VERMA, G., 2010, "Green nanocomposites based on thermoplastic starch and steam exploded cellulose nanofibrils from wheat straw". In: *Carbohydrate Polymers*. v. 82, pp. 337–345.
- KAW, A.K., 2005, *Mechanics of Composite Materials, Second Edition*. . S.l., s.n.
- KIM, H.Y., LEE, J.H., KIM, J.Y., et al., 2012, "Characterization of nanoparticles prepared by acid hydrolysis of various starches". In: *Starch/Staerke*. v. 64, pp. 367–373.
- KIM, H.Y., PARK, D.J., KIM, J.Y., et al., 2013, "Preparation of crystalline starch nanoparticles using cold acid hydrolysis and ultrasonication". In: *Carbohydrate Polymers*. v. 98, pp. 295–301.
- KIM, J.Y., LIM, S.T., 2009, "Preparation of nano-sized starch particles by complex formation with n-butanol". In: *Carbohydrate Polymers*. v. 76, pp. 110–116.
- KLEMM, D., HEUBLEIN, B., FINK, H.P., et al., 2005. "Cellulose: Fascinating biopolymer and sustainable raw material". . 2005. S.l.: s.n.
- KO, J.K., KIM, Y., XIMENES, E., et al., 2015, "Effect of liquid hot water pretreatment severity on properties of hardwood lignin and enzymatic hydrolysis of cellulose". In: *Biotechnology and Bioengineering*. v. 112, pp. 252–262.
- KOHJIYA, S., IKEDA, Y., 2014, *Chemistry, manufacture and applications of natural rubber*. . S.l., s.n.
- KRÄSSIG, H.A., 1995, "Cellulose: structure, accessibility, and reactivity". In: *Carbohydrate Polymers*. v. 26, pp. 313–314.
- KRISTO, E., BILIADERIS, C., 2007, "Physical properties of starch nanocrystal-reinforced pullulan films". In: *Carbohydrate Polymers*. v. 68, pp. 146–158.
- KUMAR, A., SINGH NEGI, Y., CHOUDHARY, V., et al., 2014, "Characterization of Cellulose Nanocrystals Produced by Acid-Hydrolysis from Sugarcane Bagasse as Agro-Waste". In: *Journal of Materials Physics and Chemistry*. v. 2, pp. 1–8.
- KUSANO, Y., TEODORU, S., HANSEN, C.M., 2011, "The physical and chemical

- properties of plasma treated ultra-high-molecular-weight polyethylene fibers". In: *Surface and Coatings Technology*. v. 205, pp. 2793–2798.
- LAM, Y.L., KAN, C.W., YUEN, C.W.M., 2011, "Physical and chemical analysis of plasma-treated cotton fabric subjected to wrinkle-resistant finishing". In: *Cellulose*. v. 18, pp. 493–503.
- LAMANNA, M., MORALES, N.J., GARCIA, N.L., et al., 2013, "Development and characterization of starch nanoparticles by gamma radiation: Potential application as starch matrix filler". In: *Carbohydrate Polymers*. v. 97, pp. 90–97.
- LEE, S.Y., MOHAN, D.J., KANG, I.A., et al., 2009, "Nanocellulose reinforced PVA composite films: Effects of acid treatment and filler loading". In: *Fibers and Polymers*. v. 10, pp. 77–82.
- LEFEBVRE, J., GRAY, D.G., 2005. "AFM of adsorbed polyelectrolytes on cellulose I surfaces spin-coated on silicon wafers". . 2005. S.l.: s.n.
- LI, C., SUN, P., YANG, C., 2012, "Emulsion stabilized by starch nanocrystals". In: *Starch/Staerke*. v. 64, pp. 497–502.
- LI, H., RICHARDS, C., WATSON, J., 2014, "High-performance glass fiber development for composite applications". In: *International Journal of Applied Glass Science*. v. 5, pp. 65–81.
- LI, R., FEI, J., CAI, Y., et al., 2009, "Cellulose whiskers extracted from mulberry: A novel biomass production". In: *Carbohydrate Polymers*. v. 76, pp. 94–99.
- LI, R., YE, L., MAI, Y.W., 1997. "Application of plasma technologies in fibre-reinforced polymer composites: A review of recent developments". . 1997. S.l.: s.n.
- LI, X., TABIL, L.G., PANIGRAHI, S., 2007. "Chemical treatments of natural fiber for use in natural fiber-reinforced composites: A review". . 2007. S.l.: s.n.
- LI, Y., MAI, Y.W., YE, L., 2000. "Sisal fibre and its composites: A review of recent developments". . 2000. S.l.: s.n.
- LI, Y., MANOLACHE, S., QIU, Y., et al., 2016, "Effect of atmospheric pressure plasma treatment condition on adhesion of ramie fibers to polypropylene for composite". In: *Applied Surface Science*. v. 364, pp. 294–301.
- LIMBERT, G., TAYLOR, M., 2002, "On the constitutive modeling of biological soft connective tissues. A general theoretical framework and explicit forms of the tensors of elasticity for strongly anisotropic continuum fiber-reinforced composites at finite strain". In: *International Journal of Solids and Structures*. v.

- 39, pp. 2343–2358.
- LIU, C., QIN, Y., LI, X., et al., 2016, "Preparation and characterization of starch nanoparticles via self-assembly at moderate temperature". In: *International Journal of Biological Macromolecules*. v. 84, pp. 354–360.
- LIU, Y., LIU, M., YANG, S., et al., 2018, "Liquid Crystalline Behaviors of Chitin Nanocrystals and Their Reinforcing Effect on Natural Rubber". In: *ACS Sustainable Chemistry and Engineering*. v. 6, pp. 325–336.
- LUO, Q.Z., D'ANGELO, N., MERLINO, R.L., 1998, "Shock formation in a negative ion plasma". In: *Physics of Plasmas*. v. 5, pp. 2868–2870.
- MA, X., JIAN, R., CHANG, P.R., et al., 2008, "Fabrication and characterization of citric acid-modified starch nanoparticles/plasticized-starch composites". In: *Biomacromolecules*. v. 9, pp. 3314–3320.
- MA, Y., CAI, C., WANG, J., et al., 2006, "Enzymatic hydrolysis of corn starch for producing fat mimetics". In: *Journal of Food Engineering*. v. 73, pp. 297–303.
- MAHLBERG, R., NIEMI, H.E.M., DENES, F.S., et al., 1999, "Application of AFM on the adhesion studies of oxygen-plasma-treated polypropylene and lignocellulosics". In: *Langmuir*. v. 15, pp. 2985–2992.
- MALAININE, M.E., DUFRESNE, A., DUPEYRE, D., et al., 2003, "Structure and morphology of cladodes and spines of *Opuntia ficus-indica*. Cellulose extraction and characterisation". In: *Carbohydrate Polymers*. v. 51, pp. 77–83.
- MALEKI-MOGHADDAM, M., YAHYAEI, M., BANISI, S., 2013, "A method to predict shape and trajectory of charge in industrial mills". In: *Minerals Engineering*. v. 46–47, pp. 157–166.
- MAN, Z., MUHAMMAD, N., SARWONO, A., et al., 2011, "Preparation of Cellulose Nanocrystals Using an Ionic Liquid.". In: *Journal of Polymers Environment*. v. 19, pp. 726–731.
- MARTINS, I.M.G., MAGINA, S.P., OLIVEIRA, L., et al., 2009, "New biocomposites based on thermoplastic starch and bacterial cellulose". In: *Composites Science and Technology*. v. 69, pp. 2163–2168.
- MASINA, N., CHOONARA, Y.E., KUMAR, P., et al., 2017. "A review of the chemical modification techniques of starch". . 2017. S.l.: s.n.
- MATHEW, A.P., OKSMAN, K., SAIN, M., 2006, "The effect of morphology and chemical characteristics of cellulose reinforcements on the crystallinity of

- polylactic acid". In: *Journal of Applied Polymer Science*. v. 101, pp. 300–310.
- MERINO, D., GUTIÉRREZ, T.J., MANSILLA, A.Y., et al., 2018, "Critical evaluation of starch-based antibacterial nanocomposites as agricultural mulch films: Study on their interactions with water and light". In: *ACS Sustainable Chemistry & Engineering*. pp. acssuschemeng.8b04162.
- MEZEY, Z., DÁNYÁDI, L., CZIGÁNY, T., et al., 2003, "Investigation of sisal fiber reinforced polymer composites". In: *Muanyag Es Gumi/Plastics and Rubber*. v. 40.
- MIAO, M., JIANG, B., ZHANG, T., et al., 2011, "Impact of mild acid hydrolysis on structure and digestion properties of waxy maize starch". In: *Food Chemistry*. v. 126, pp. 506–513.
- MISHRA, B.K., RAJAMANI, R.K., 1992, "The discrete element method for the simulation of ball mills". In: *Applied Mathematical Modelling*. v. 16, pp. 598–604.
- MITRA, B.C., 2014, "Environment friendly composite materials: Biocomposites and green composites". In: *Defence Science Journal*. v. 64, pp. 244–261.
- MOHANTY, A.K., DRZAL, L.T., MISRA, M., 2005, *NATURAL FIBERS , BIOPOLYMERS , AND BIOCOMPOSITES*. . S.l., s.n.
- MOHANTY, A.K., MISRA, M., DRZAL, L.T., 2002, "Sustainable Bio-Composites from renewable resources: Opportunities and challenges in the green materials world". In: *Journal of Polymers and the Environment*. v. 10, pp. 19–26.
- MONTERO, B., RICO, M., RODRÍGUEZ-LLAMAZARES, S., et al., 2017, "Effect of nanocellulose as a filler on biodegradable thermoplastic starch films from tuber, cereal and legume". In: *Carbohydrate Polymers*. v. 157, pp. 1094–1104.
- MOON, R.J., MARTINI, A., NAIRN, J., et al., 2011. "Cellulose nanomaterials review: Structure, properties and nanocomposites". . 2011. S.l.: s.n.
- MUKHOPADHYAY, S., FANGUEIRO, R., 2009, "Physical modification of natural fibers and thermoplastic films for composites - A review". In: *Journal of Thermoplastic Composite Materials*. v. 22, pp. 135–162.
- MULINARI, D.R., SARON, C., CARVALHO, K.C.C., et al., 2011, "Thermoplastic and thermosetting composites with natural fibers". In: *Thermoplastic and Thermosetting Polymers and Composites*. pp. 85–122.
- MÜLLER, C.M.O., LAURINDO, J.B., YAMASHITA, F., 2009, "Effect of cellulose

- fibers on the crystallinity and mechanical properties of starch-based films at different relative humidity values". In: *Carbohydrate Polymers*. v. 77, pp. 293–299.
- MUÑOZ-VÉLEZ, M.F., VALADEZ-GONZÁLEZ, A., HERRERA-FRANCO, P.J., 2017, "Effect of fiber surface treatment on the incorporation of carbon nanotubes and on the micromechanical properties of a single-carbon fiber-epoxy matrix composite". In: *Express Polymer Letters*. v. 11, pp. 704–718.
- MURANO, E., TOFFANIN, R., 2017, "Introduction to the themed issue “Natural Polysaccharides”". In: *Natural Product Communications*. v. 12.
- NABI SAHEB, D., JOG, J.P., 1999, "Natural fiber polymer composites: A review". In: *Advances in Polymer Technology*. v. 18, pp. 351–363.
- NAFCHI, A.M., ALIAS, A.K., MAHMUD, S., et al., 2012, "Antimicrobial, rheological, and physicochemical properties of sago starch films filled with nanorod-rich zinc oxide". In: *Journal of Food Engineering*. v. 113, pp. 511–519.
- NAKAGAITO, A.N., YANO, H., 2004, "The effect of morphological changes from pulp fiber towards nano-scale fibrillated cellulose on the mechanical properties of high-strength plant fiber based composites". In: *Applied Physics A: Materials Science and Processing*. v. 78, pp. 547–552.
- NAM, S., FRENCH, A.D., CONDON, B.D., et al., 2016, "Segal crystallinity index revisited by the simulation of X-ray diffraction patterns of cotton cellulose I $\beta$  and cellulose II". In: *Carbohydrate Polymers*. v. 135, pp. 1–9.
- NOSONOVSKY, M., BHUSHAN, B., 2012, "Green Tribology: Biomimetics, Energy Conservation and Sustainability". In: *Green Energy and Technology*. v. 49.
- OKUMURA, T., 2010, "Inductively coupled plasma sources and applications". In: *Physics Research International*.
- OLAYIDE OYEYEMI FABUNMI, LOPE G TABIL, PETER R CHANG, et al., 2007. "Developing Biodegradable Plastics from starch". In: *ASABE/CSBE North Central Intersectional Meeting*. S.l.: s.n. 2007.
- ORTEGA-TORO, R., BONILLA, J., TALENS, P., et al., 2017. "Future of Starch-Based Materials in Food Packaging". In: *Starch-Based Materials in Food Packaging: Processing, Characterization and Applications*. S.l.: s.n. pp. 257–312.
- PAPADIMITRIOU, S., BIKIARIS, D., 2009, "Novel self-assembled core-shell nanoparticles based on crystalline amorphous moieties of aliphatic copolyesters for efficient controlled drug release". In: *Journal of Controlled Release*. v. 138,

- pp. 177–184.
- PAPPAS, D., BUJANDA, A., DEMAREE, J.D., et al., 2006, "Surface modification of polyamide fibers and films using atmospheric plasmas". In: *Surface and Coatings Technology*. v. 201, pp. 4384–4388.
- PARETA, R., EDIRISINGHE, M.J., 2006, "A novel method for the preparation of starch films and coatings". In: *Carbohydrate Polymers*. v. 63, pp. 425–431.
- PETERSSON, L., OKSMAN, K., 2006, "Biopolymer based nanocomposites: Comparing layered silicates and microcrystalline cellulose as nanoreinforcement". In: *Composites Science and Technology*. v. 66, pp. 2187–2196.
- PHILIP, S., KESHAVARZ, T., ROY, I., 2007. "Polyhydroxyalkanoates: Biodegradable polymers with a range of applications". . 2007. S.l.: s.n.
- PICKERING, K.L., 2008, *Properties and performance of natural-fibre composites*. . S.l., s.n.
- PICKERING, K.L., EFENDY, M.G.A., LE, T.M., 2016. "A review of recent developments in natural fibre composites and their mechanical performance". . 2016. S.l.: s.n.
- PREWO, K.M., BRENNAN, J.J., LAYDEN, G.K., 1986, "FIBER REINFORCED GLASSES AND GLASS-CERAMICS FOR HIGH PERFORMANCE APPLICATIONS.". In: *American Ceramic Society Bulletin*. v. 65, pp. 305–313, 322.
- RAFFAELE-ADDAMO, A., SELLI, E., BARNI, R., et al., 2006, "Cold plasma-induced modification of the dyeing properties of poly(ethylene terephthalate) fibers". In: *Applied Surface Science*. v. 252, pp. 2265–2275.
- RAMESH, M., MITCHELL, J.R., JUMEL, K., et al., 1999, "Amylose content of rice starch". In: *Starch/Staerke*. v. 51, pp. 311–313.
- RÅNBÏ, B.G., 1951, "III. Fibrous macromolecular systems. Cellulose and muscle. The colloidal properties of cellulose micelles". In: *Discussions of the Faraday Society*. v. 11, pp. 158–164.
- RAY, D., SARKAR, B.K., RANA, A.K., et al., 2001, "The mechanical properties of vinylester resin matrix composites reinforced with alkali-treated jute fibres". In: *Composites: Part A: Applied Science and Manufacturing*. v. 32, pp. 119–127.
- REIS, K.C., PEREIRA, J., SMITH, A.C., et al., 2008. "Characterization of

- polyhydroxybutyrate-hydroxyvalerate (PHB-HV)/maize starch blend films". . 2008. S.l.: s.n.
- ROMAN, M., WINTER, W.T., 2004, "Effect of sulfate groups from sulfuric acid hydrolysis on the thermal degradation behavior of bacterial cellulose". In: *Biomacromolecules*. v. 5, pp. 1671–1677.
- ROSA, M.F., CHIOU, B. SEN, MEDEIROS, E.S., et al., 2009, "Effect of fiber treatments on tensile and thermal properties of starch/ethylene vinyl alcohol copolymers/coir biocomposites". In: *Bioresource Technology*. v. 100, pp. 5196–5202.
- SAHARI, J., SAPUAN % \_ REV, S.M., 2011, "NATURAL FIBRE REINFORCED BIODEGRADABLE POLYMER COMPOSITES". In: *Adv. Mater. Sci*. v. 30, pp. 166–174.
- SANCHEZ-GARCIA, M.D., LAGARON, J.M., 2010, "On the use of plant cellulose nanowhiskers to enhance the barrier properties of polylactic acid". In: *Cellulose*. v. 17, pp. 987–1004.
- SANTOS, P.A., SPINACÉ, M.A.S., KAREN K. G. FERMOSELLI, et al., 2009, "Efeito da Forma de Processamento e do Tratamento da Fibra de Curauá nas Propriedades de Compósitos com Poliamida-6". In: *Polímeros: Ciência e Tecnologia*. v. 19, pp. 31–39.
- SATYANARAYANA, K.G., ARIZAGA, G.G.C., WYPYCH, F., 2009. "Biodegradable composites based on lignocellulosic fibers-An overview". . 2009. S.l.: s.n.
- SEVENOU, O., HILL, S.E., FARHAT, I.A., et al., 2002, "Organisation of the external region of the starch granule as determined by infrared spectroscopy". In: *International Journal of Biological Macromolecules*. v. 31, pp. 79–85.
- SHI, A.M., LI, D., WANG, L.J., et al., 2011, "Preparation of starch-based nanoparticles through high-pressure homogenization and miniemulsion cross-linking: Influence of various process parameters on particle size and stability". In: *Carbohydrate Polymers*. v. 83, pp. 1604–1610.
- SHUJUN, W., JIUGAO, Y., JINGLIN, Y., 2006, "Preparation and characterization of compatible and degradable thermoplastic starch/polyethylene film". In: *Journal of Polymers and the Environment*. v. 14, pp. 65–70.
- SIAUEIRA, G., BRAS, J., DUFRESNE, A., 2009, "Cellulose whiskers versus microfibrils: Influence of the nature of the nanoparticle and its surface functionalization on the thermal and mechanical properties of nanocomposites".

- In: *Biomacromolecules*. v. 10, pp. 425–432.
- SINHA, E., PANIGRAHI, S., 2009, "Effect of plasma treatment on structure, wettability of jute fiber and flexural strength of its composite". In: *Journal of Composite Materials*. v. 43, pp. 1791–1802.
- SIQUEIRA, G., ABDILLAHI, H., BRAS, J., et al., 2010a, "High reinforcing capability cellulose nanocrystals extracted from *Syngonanthus nitens* (Capim Dourado)". In: *Cellulose*. v. 17, pp. 289–298.
- SIQUEIRA, G., BRAS, J., DUFRESNE, A., 2010b. "Cellulosic bionanocomposites: A review of preparation, properties and applications". . 2010. S.l.: s.n.
- SIQUEIRA, G., TAPIN-LINGUA, S., BRAS, J., et al., 2011, "Mechanical properties of natural rubber nanocomposites reinforced with cellulosic nanoparticles obtained from combined mechanical shearing, and enzymatic and acid hydrolysis of sisal fibers". In: *Cellulose*. v. 18, pp. 57–65.
- VAN SOEST, J.J.G., HULLEMAN, S.H.D., DE WIT, D., et al., 1996, "Crystallinity in starch bioplastics". In: *Industrial Crops and Products*. v. 5, pp. 11–22.
- SONG, D., THIO, Y.S., DENG, Y., 2011, "Starch nanoparticle formation via reactive extrusion and related mechanism study". In: *Carbohydrate Polymers*. v. 85, pp. 208–214.
- DE SOUZA LIMA, M.M., BORSALI, R., 2004. "Rodlike cellulose microcrystals: Structure, properties, and applications". . 2004. S.l.: s.n.
- STAMBOULIS, A., BAILLIE, C.A., PEIJS, T., 2001, "Effects of environmental conditions on mechanical and physical properties of flax fibers". In: *Composites - Part A: Applied Science and Manufacturing*. v. 32, pp. 1105–1115.
- ŠTURCOVA, A., HIS, I., APPERLEY, D.C., et al., 2004, "Structural details of crystalline cellulose from higher plants". In: *Biomacromolecules*. v. 5, pp. 1333–1339.
- SU, Y., BURGER, C., MA, H., et al., 2015, "Exploring the Nature of Cellulose Microfibrils". In: *Biomacromolecules*. v. 16, pp. 1201–1209.
- SUANPOOT, P., KUESENG, K., ORTMANN, S., et al., 2008, "Surface analysis of hydrophobicity of Thai silk treated by SF6 plasma". In: *Surface and Coatings Technology*. v. 202, pp. 5543–5549.
- SUGIYAMA, J., VUONG, R., CHANZY, H., 1991, "Electron Diffraction Study on the Two Crystalline Phases Occurring in Native Cellulose from an Algal Cell Wall". In: *Macromolecules*. v. 24, pp. 4168–4175.

- SUN, Y., LIANG, Q., CHI, H., et al., 2014. "The application of gas plasma technologies in surface modification of aramid fiber". . 2014. S.l.: s.n.
- SZYMOŃSKA, J., TARGOSZ-KORECKA, M., KROK, F., 2009. "Characterization of starch nanoparticles". In: *Journal of Physics: Conference Series*. S.l.: s.n. 2009.
- TANG, X.Z., KUMAR, P., ALAVI, S., et al., 2012. "Recent Advances in Biopolymers and Biopolymer-Based Nanocomposites for Food Packaging Materials". . 2012. S.l.: s.n.
- TAO, J., CUI, Y.H., JI, X.L., et al., 2007, "Properties of Biodegradable Thermoplastic Starch/Ethyl Cellulose Composite". In: *Key Engineering Materials*. v. 334–335, pp. 345–348.
- THAKUR, V.K., THAKUR, M.K., RAGHAVAN, P., et al., 2014, "Progress in green polymer composites from lignin for multifunctional applications: A review". In: *ACS Sustainable Chemistry and Engineering*. v. 2, pp. 1072–1092.
- TING, Y.H., LIU, C.C., PARK, S.M., et al., 2010, "Surface roughening of polystyrene and poly(methyl methacrylate) in Ar/O<sub>2</sub> plasma etching". In: *Polymers*. v. 2, pp. 649–663.
- VERT, M., DOS SANTOS, I., PONSART, S., et al., 2002, "Degradable polymers in a living environment: Where do you end up?". In: *Polymer International*. v. 51, pp. 840–844.
- VILASECA, F., MENDEZ, J.A., PÈLACH, A., et al., 2007, "Composite materials derived from biodegradable starch polymer and jute strands". In: *Process Biochemistry*. v. 42, pp. 329–334.
- VISAKH, P.M., SABU, T., ARUP, K.C., et al., 2013, *Advances in Elastomers I: Blends and Interpenetrating Networks*. . S.l., s.n.
- WADA, M., HEUX, L., SUGIYAMA, J., 2004, "Polymorphism of cellulose I family: Reinvestigation of cellulose IV1". In: *Biomacromolecules*. v. 5, pp. 1385–1391.
- WÅGBERG, L., DECHER, G., NORGREN, M., et al., 2008, "The build-up of polyelectrolyte multilayers of microfibrillated cellulose and cationic polyelectrolytes". In: *Langmuir*. v. 24, pp. 784–795.
- WALLACE RA, SANDER GP, F.R., 1991, *Biology: The Science of Life*. . S.l., s.n.
- WANG, B., SAIN, M., 2007, "Isolation of nanofibers from soybean source and their

- reinforcing capability on synthetic polymers". In: *Composites Science and Technology*. v. 67, pp. 2521–2527.
- WANG, Z., QIAO, X., SUN, K., 2018, "Rice straw cellulose nanofibrils reinforced poly(vinyl alcohol) composite films". In: *Carbohydrate Polymers*. v. 197, pp. 442–450.
- WILSON, R.H., KALICHEVSKY, M.T., RING, S.G., et al., 1987, "A fourier-transform infrared study of the gelation and retrogradation of waxy-maize starch". In: *Carbohydrate Research*. v. 166, pp. 162–165.
- WINARTI, C., SUNARTI, T.C., MANGUNWIDJAJA, D., et al., 2014, "Preparation of arrowroot starch nanoparticles by butanol-complex precipitation, and its application as bioactive encapsulation matrix". In: *International Food Research Journal*. v. 21, pp. 2207–2213.
- WOLLBOLDT, R.P., ZUCKERSTÄTTER, G., WEBER, H.K., et al., 2010, "Accessibility, reactivity and supramolecular structure of E. globulus pulps with reduced xylan content". In: *Wood Science and Technology*. v. 44, pp. 533–546.
- WRÓBLEWSKA-KREPSZTUL, J., RYDZKOWSKI, T., BOROWSKI, G., et al., 2018, "Recent progress in biodegradable polymers and nanocomposite-based packaging materials for sustainable environment". In: *International Journal of Polymer Analysis and Characterization*. v. 23, pp. 383–395.
- YEH, W.Y., YOUNG, R.J., 1998, "Molecular deformation processes in aromatic high modulus polymer fibres". In: *Polymer*. v. 40, pp. 857–870.
- YOUNG, R.J., DAY, R.J., ZAKIKHANI, M., et al., 1988, *Micromechanics of deformation of high-modulus polymer fibres and composites*. . S.l., s.n.
- YU, D., XIAO, S., TONG, C., et al., 2007, "Dialdehyde starch nanoparticles: Preparation and application in drug carrier". In: *Chinese Science Bulletin*. v. 52, pp. 2913–2918.
- ZHANG, Z., SHAN, H., SUN, J., et al., 2013, "Facile preparation of corn starch nanoparticles by alkali-freezing treatment". In: *RSC Advances*. v. 3, pp. 13406–13411.
- ZHOU, J.J., WANG, S.Y., GUNASEKARAN, S., 2009, "Preparation and characterization of whey protein film incorporated with TiO<sub>2</sub> nanoparticles". In: *Journal of Food Science*. v. 74.
- ZHOU, Y.M., FU, S.Y., ZHENG, L.M., et al., 2012, "Effect of nanocellulose isolation

techniques on the formation of reinforced poly(vinyl alcohol) nanocomposite films". In: *Express Polymer Letters*. v. 6, pp. 794–804.

ZHOU, Z., LIU, X., HU, B., et al., 2011, "Hydrophobic surface modification of ramie fibers with ethanol pretreatment and atmospheric pressure plasma treatment". In: *Surface and Coatings Technology*. v. 205, pp. 4205–4210.



Contents lists available at ScienceDirect

Composites Part B

journal homepage: [www.elsevier.com/locate/compositesb](http://www.elsevier.com/locate/compositesb)

## Improvement in adhesion of cellulose fibers to the thermoplastic starch matrix by plasma treatment modification

Mahyar Fazeli<sup>a</sup>, Jennifer Paola Florez, Renata Antoun Simão

*Federal University of Rio de Janeiro, Department of Materials Science and Engineering, P.O. Box: 68505, 21945-970, Rio de Janeiro, Brazil*



### ARTICLE INFO

**Keywords:**  
Biocomposite  
Plasma treatment  
Cellulose fiber  
Starch biopolymer

### ABSTRACT

This work deals with provision and characterization of the biopolymer-based composites achieved by incorporation of cellulose fibers as the reinforcement within the glycerol plasticized matrix formed by thermoplastic cornstarch biopolymer. The function of starch-based polymers is limited due to poor mechanical properties. However, it is improved with forming a biocomposite of thermoplastic starch (TPS) as matrix and the cellulose fibers (CF) as reinforcement. The surface of cellulose fibers is successfully modified using the air plasma treatment with the aim of improving the matrix/fiber adhesion. The modified fibers are studied using X-ray diffraction (XRD), scanning electron microscopy (SEM) and Fourier transform infrared spectroscopy (FTIR). The TPS/CF composites are prepared using high friction and hot compression procedure. Tensile test results and SEM images of the fracture surfaces show significant improvement of adhesion between treated cellulose fibers and TPS matrix. Thermogravimetric analysis shows a considerable decomposition at approximately 250–350 °C. XRD proved the significant increase in crystallinity percentage of composites compared to TPS.

### 1. Introduction

The evolution of renewable and biodegradable materials is a growing tendency, given the increase in environmental consciousness from the population, companies, and governments. The effects of human on the planet are clear in many areas and with growing population and consumption, many issues must be addressed, including the final destination of our waste, the ever-increasing amount of plastic particles in the oceans and land, as well as the energy consumption and renewability of the materials we produce [1]. In this context, polymers reinforced with natural fibers are an interesting alternative and, research in this field has been growing continuously in the last two decades. These materials can be partially or fully renewable and biodegradable, while also consuming less energy during production and having adequate mechanical properties for many applications [2]. One of the most important applications of biodegradable polymers reinforced with natural fillers is food packaging, which is reported by many researchers and also this paper [3–5].

The use of composites reinforced with natural fibers is growing but, is still a small market due to many factors, including the poor adhesion between fibers and matrices [6,7]. The solution to the problem is still an open scientific discussion with different kinds of treatments being tested by different research groups such as chemical, mechanical or the

combination of these treatments. This situation is similar to what happened when glass fibers appeared as a reinforcement phase for polymers until the silanization treatment was developed and became the industrial standard [8]. Natural plant fibers, however, come from many different species, with varying chemical composition, morphological characteristics, and sizes, make the development of a single compatibilization treatment challenging. Between the different possibilities being studied, plasma modification of the fibers is considered very promising and the environmentally friendly, which is a desired characteristic, given the context of the development of these materials [9–11].

The influence and properties of natural fiber reinforced biocomposites rely on the properties of each component (matrix and fibers), and the adhesion between fibers and matrix. To prepare suitable interfacial interactions, the surface properties should be improved appropriately [12,13]. Physical treatments such as corona treatment [14], plasma treatments [15] and electron beam irradiation [16], chemical treatments like alkali treatment [17–19], silane treatment [20] and acetylation treatment [21], etc. and the surface modifications of the fibers have been performed to ameliorate the adaptability between polymer matrices and the surfaces of the natural fibers. In spite of the fact the chemical treatments of the natural fibers have been partly victorious in enhancing the interfacial bonding, there are some weaknesses such as



# The Effect of Cellulose Nanofibers on the Properties of Starch Biopolymer

Mahyar Fazeli\* and Renata A. Simão

The current study deals with the preparation and characterization of polysaccharide-based biocomposite films acquired by the incorporation of cellulose nanofiber within glycerol plasticized matrix formed by starch. The application of starch-based films is restricted owing to highly hydrophilic nature and poor mechanical properties. These problems are solved by forming a nanocomposite of thermoplastic starch (TPS) as matrix and cellulose nanofiber (CNF) as reinforcement. CNF is successfully synthesized from short pure cellulose fibers by a chemo-mechanical process. TPS/CNF composite films are prepared by the polymer solution casting method, and their characterizations are obtained by water vapor transmission rate, differential scanning calorimetry (DSC), atomic force microscopy (AFM), oxygen transmission rate, X-ray diffraction (XRD), light transmittance, and tensile test. Even at the low concentration of CNF filled TPS, the composite film shows improvement in properties. The 0.4 wt% CNF loaded TPS films show approximately the maximum improvement in tensile strength. Above 0.5 wt% CNF, tensile strength starts to deteriorate. Water vapor transmission rate (WVTR) and oxygen transmission rate (OTR) results show improvement in water vapor barrier properties of TPS matrix. The DSC thermograms of TPS and composite films do not show any significant effect on the melting point of the composite film compared with the base polymer TPS. The AFM analysis shows the topography of the surface of the nanocomposite. The morphology of nanofibers is studied by using the scanning electron microscopy (SEM) and the transmission electron microscopy (TEM).

## 1. Introduction

In order to preserve the environment, many researchers are developing biocomposites from renewable resources such as cellulosic materials and biopolymers.<sup>[1]</sup> After service life, the solid waste of polymer materials creates a significant problem for the environment.<sup>[2]</sup> In most parts of the world, there are special rules and regulations to dispose of plastic wastes and recycling polymers.<sup>[3]</sup> The outreach of biodegradable materials from natural resources, such as starch, has prepared an opportunity to decrease the affiliation with petroleum-derived materials.<sup>[4]</sup>

M. Fazeli, R. A. Simão  
PEMM/COPPE  
Universidade Federal do Rio de Janeiro  
PO Box 68505, 21945-970 Rio de Janeiro, RJ, Brazil  
E-mail: m.fazeli@metalmat.ufjr.br

DOI: 10.1002/masy.201800110

The mechanical properties of starch biopolymers may be improved with the addition of natural fibers.<sup>[5]</sup> Different types of fibers with different kinds of structures have been compounded with polymer matrices to enhance the mechanical properties of the biocomposites.<sup>[6]</sup> Cellulose fibers have widespread application as a filler with thermoplastic polymers to fabricate biocomposite.<sup>[7]</sup> Using cellulose fibers as filler in biocomposites can decrease the final cost of products since it is abundant and available in nature. Furthermore, cellulose fibers have specified properties such as high specific stiffness, low density, and biodegradability.<sup>[8]</sup> It is considered that the mechanical properties of biocomposites depend on the orientation of fibers in biocomposites.<sup>[9]</sup> A biocomposite of cellulose fiber and thermoplastic starch with appropriate plasticizer can demonstrate better mechanical properties which are generally required in food packaging.<sup>[10]</sup> Cellulose nanofibers (CNF) which can be extracted from the cellulose fibers has excellent mechanical properties like glass and carbon fibers.<sup>[11]</sup> There are various kinds of treatments to extract CNF from cellulose fibers such as chemical,<sup>[12]</sup> mechanical,<sup>[13]</sup> or the combination of these treatments.<sup>[14]</sup>

The extraction of cellulose nanofiber from natural fibers and their applications as reinforcement in starch-based biocomposites have been studied in the literature. During last few years, the cellulose nanofiber extracted from hemp,<sup>[15]</sup> *Helicteres isora* plant,<sup>[16]</sup> banana peels,<sup>[17]</sup> wheat straw,<sup>[18]</sup> sisal,<sup>[19]</sup> Aloe Vera rind,<sup>[20]</sup> bamboo,<sup>[21]</sup> cassava bagasse<sup>[22]</sup> have been used to improve the mechanical properties and water sensitivity of thermoplastic starch matrix. Actually, nanofibrillation and pretreatment are required procedures for the extraction of cellulose nanofibers from natural fibers. The pretreatment process such as acid or alkali treatment,<sup>[23]</sup> ionic liquids,<sup>[24]</sup> enzymatic pretreatment,<sup>[25]</sup> and steam explosion treatment<sup>[26]</sup> were first used to remove non-cellulosic materials in plants. Some nanofibrillation technologies such as high-pressure homogenizers,<sup>[27]</sup> grinders,<sup>[28]</sup> and ultrasonic method<sup>[29]</sup> were used to generate high shear forces to separate the fibrils from the purified cellulose fibers.

Less attention in the literature is given to the extraction of nanofibers from commercially pure cellulose fibers. Actually,